DOPPLER EFFECT ON ULTRASONIC SIGNALS FOR PREGNANCY DETERMINATION IN SHEEP

PIERRE E. HERTZOG

DOPPLER EFFECT ON ULTRASONIC SIGNALS FOR PREGNANCY DETERMINATION IN SHEEP

PIERRE E. HERTZOG

Central University of Technology, Free State

DOPPLER EFFECT ON ULTRASONIC SIGNALS FOR PREGNANCY DETERMINATION IN SHEEP

by

Pierre Eduard Hertzog

Thesis submitted in fulfillment of the requirements for the degree

Doctor: Technologiae: Engineering: Electrical

in the

Faculty of Engineering, Information and Communication Technology

at the

Central University of Technology

Promoter: Prof. G.D. Jordaan D.Tech. (Eng)

April 2004

Central University of Technology, Free State

DECLARATION OF INDEPENDENT WORK

I, PIERRE EDUARD HERTZOG, hereby declare that the research project which has been submitted to the Technikon Free State by me for obtaining the degree DOCTOR: TECHNOLOGIAE: ENGINEERING: ELECTRICAL, is my independent work and has not been submitted by me or any other person previously in view of attaining any qualification.

P.E. HERTZOG

2004-05-01

DATE

ACKNOWLEDGEMENTS

My wife, Sunette and my sons, Dirkie and Hansie for their support and encouragement.

My parents, for their unconditional love and guidance for as long as I can remember.

My parents-in-law, for their love, interest and encouragement.

Technikon Free State, for providing the opportunity to complete this project.

My promotor, Prof. G.D. Jordaan for his friendship, advice and support during the project.

Mr N. Luwes for his help during the experimental phase of the project.

Dr. M. Truscott and Mrs R. Saayman for philological assistance in preparing the text.

My Heavenly Father, the AUTHOR OF ALL THINGS.

SUMMARY

Knowing the reproductive status of an animal (sheep in the case of this project) is of utmost importance to the modern farmer. Decisions concerning the management of the flock are influenced by knowledge of the percentage of animals that are pregnant at that specific time. The aim of the project was to gain knowledge for the development of an instrument that is affordable and with which the farmer can do pregnancy determination himself and therefore enables him to make the correct management decisions.

Experimental data were obtained from pregnant Dorper ewes with the aid of a portable Doppler instrument.

In order to gain insight in the frequency spectrum of the Doppler signal, simulations of Wavelet transforms (WT), Fourier transforms (FT) and short time Fourier transforms (STFT) were done in MathCAD. By using real data as input, simulations of correlation, autocorrelation and a specifically developed filter method were done in MathCAD. In the simulations known levels of noise were added to the Doppler signals. Satisfactory results were obtained from the simulations of autocorrelation and the filter method, which led to a DSP implementation of the two methods.

In the DSP implementation of the autocorrelation method signals with a SNR of -6.5 dB was successfully identified and with the filter method the fetal heartbeat with a SNR of -8 dB was also identified successfully. It can thus be concluded that both the filter and the autocorrelation method can be used successfully for the detection of the fetal heartbeat in noisy ultrasonic Doppler signals.

OPSOMMING

Kennis in verband met die reproduktiewe status van diere (skape in hierdie studie) is van uiterste belang vir die moderne veeboer. Bestuursbesluite word beinvloed deur die persentasie dragtige diere op 'n gegewe moment. Die doel van die projek was om inligting te versamel vir die ontwikkeling van 'n instrument waarmee die boer self dragtigheidsondersoeke kan doen, en sodoende die bestuur van sy kudde kan verbeter.

Eksperimentele data is versamel vanaf dragtige Dorper ooie met behulp van 'n draagbare Doppler instrument.

Ten einde 'n beter begrip te vorm van die frekwensiespektrum van die sein is MathCAD simulasies van Wavelet transformasies (WT), Fourier transformasies (FT) en kort periode Fourier transformasies (STFT) gedoen. Deur van werklike data as inset gebruik te maak is simulasies van korrelasie, autokorrelasie en 'n spesifiek ontwikkelde filter metode gedoen. In die simulasies is bekende vlakke van ruis by die Doppler seine gevoeg. Bevredigende resultate is van die autokorrelasie en filtermetodes verkry, waarna beide hierdie stelsels in DSP geïmplementeer is.

In die DSP implementering van die autokorrelasie metode is seine met 'n seinruisverhouding van -6.5 dB suksesvol herken. Met die DSP implementering van die filter metode is seine met 'n sein ruis verhouding van -8 dB steeds suksesvol herken. Daar kan dus afgelei word dat beide die filter sowel as die autokorrelasie metodes suksesvol gebruik kan word vir die herkenning van ruisdeurdrenkte ultrasoniese Doppler seine.

LIST OF ACRONYMS

ADC	Analog to Digital Conversion
ALU	Arithmetic Logical Unit
CAD	Computer Aided Design
CWT	Continuous Wavelet Transform
dB	Decibel
DSP	Digital Signal Processing
DTE	Doppler Tissue Echocardiography
FFT	Fast Fourier Transformation
FIR	Finite Impulse Response
FT	Fourier Transform
IIR	Infinite Impulse Response
MFLOPS	Million Floating Point Operations per Second
SNR	Signal-to-Noise Ratio
STFT	Short Time Fourier Transform
TI	Texas Instruments
VAB	Visual Application Bulder
VLIW	Very Long Instruction Word
WT	Wavelet Transform

CONTENTS

LIST OF FIGURES

LIST OF TABLES

1 Introduction

1.1 Aim of project

Knowing the reproductive status of an animal is of utmost importance to the modern sheep farmer. Decisions concerning the management of the flock are influenced by the knowledge of the percentage of animals that are pregnant at that specific time. Presently ultrasonic scanning and different chemical methods are used for pregnancy determination. As a result of different reasons these methods are not used on big scale by commercial farmers. In this study the Ultrasonic Doppler signal obtained from a pregnant ewe would be analysed by using digital signal processing (DSP) techniques. Currently, pregnancy determination has to be done by a veterinarian with an ultrasonic scanning device. The aim of the project would be to gain knowledge for the development of an instrument that is affordable and with which the farmer would be able to do the pregnancy determination himself and therefore enable him to make the correct management decisions.

1.2 Hypothesis

The fetal heart beat as obtained by using ultrasonic Doppler can be successfully recognised by means of using filter and autocorrelation methods.

1.3 Brief overview of project

The research procedure of the project is outlined in Figure 1.1.

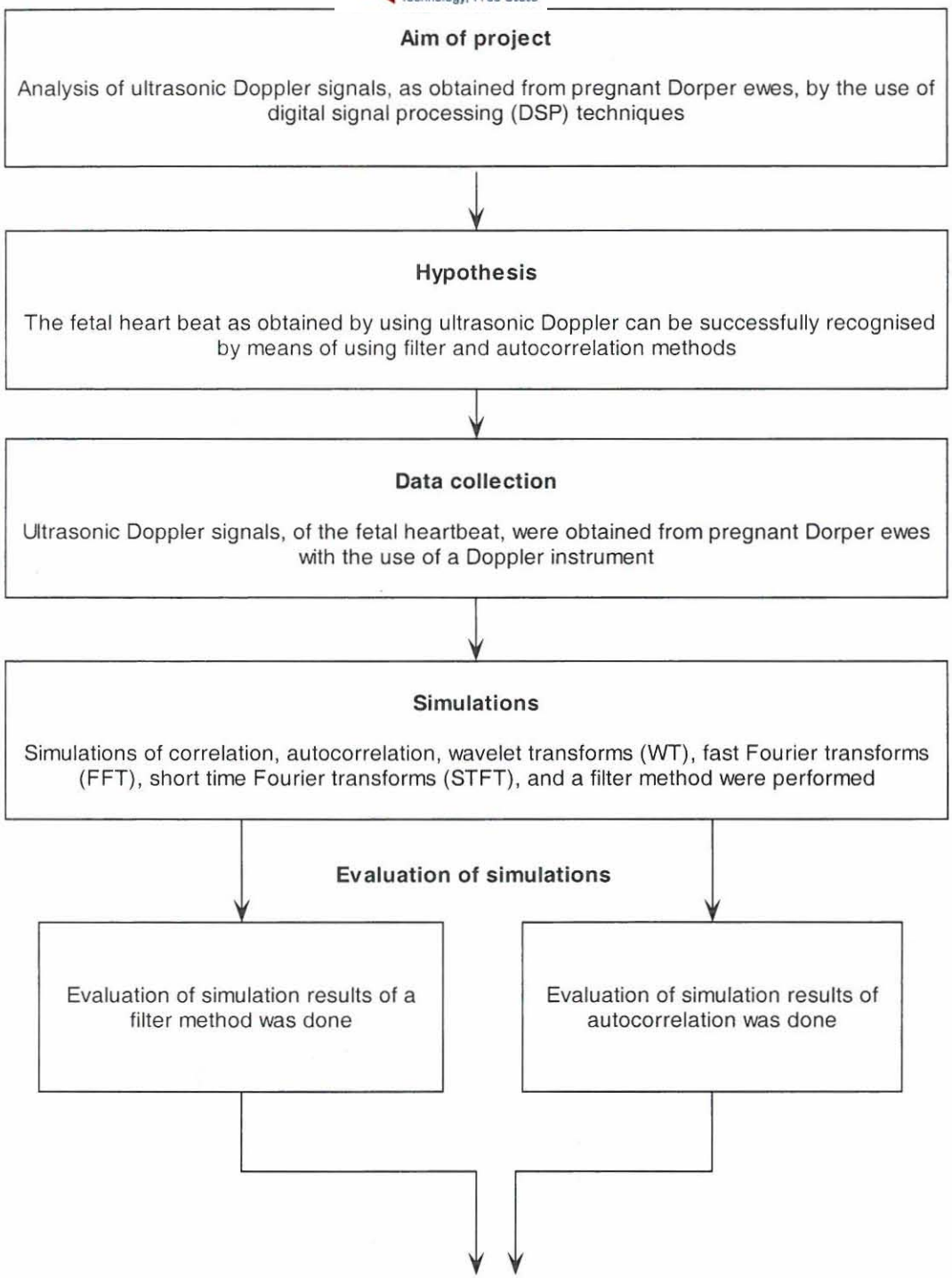

Figure 1.1: Flow of the project (continued on next page)

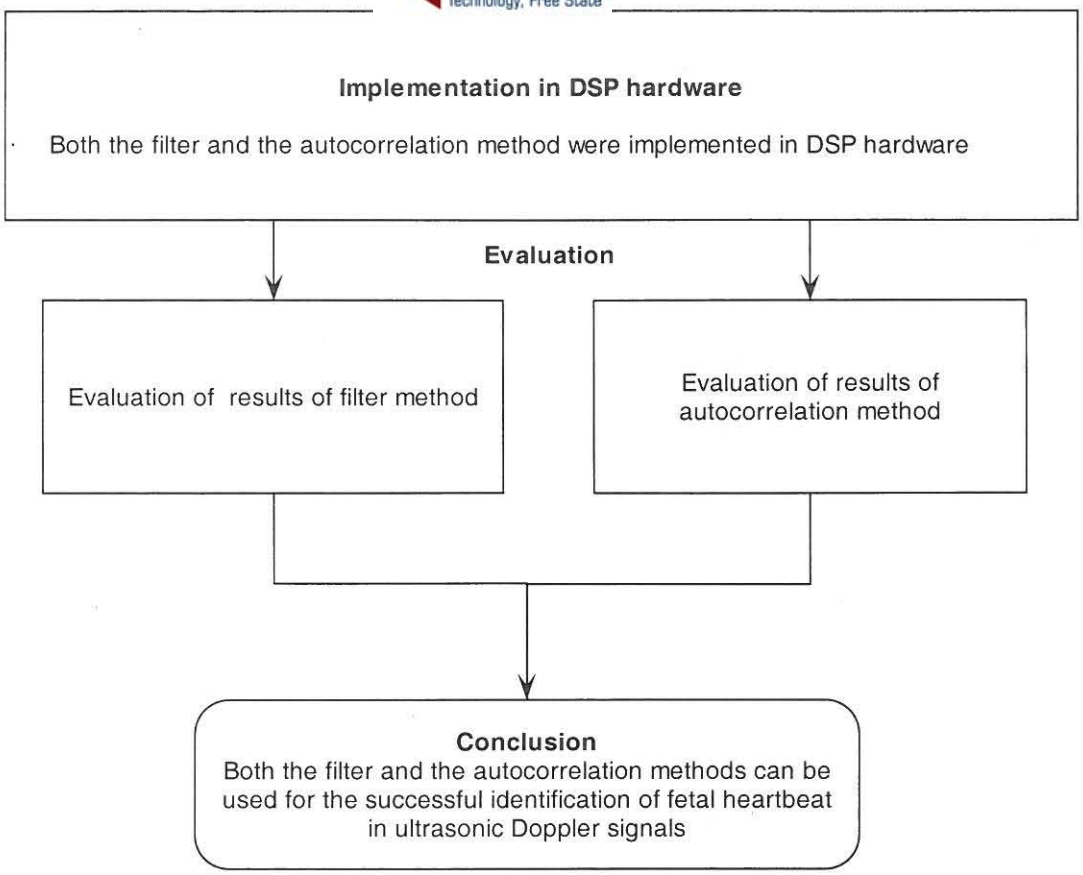

Figure 1.1: Flow of the project (continued)

1.4 General

The novel content of this thesis is as follows:

- A special filter method to detect the presence of the fetal heart beat was developed, simulated and implemented in DSP hardware;
- An autocorrelation method for the detection of fetal heart beat was simulated and implemented in DSP hardware and
- A unique decision-making process for the implementation of both the filter and the autocorrelation method in DSP hardware was developed.

2 Theory of ultrasound and Doppler

2.1 Introduction

The literary overview, in this chapter, consists of the following:

- The characteristics of ultrasound and its interaction with biomedical material;
- Doppler principles and instruments that are used for biomedical analysis and
- DSP techniques that are relevant to the recognition of repetitive patterns in the Doppler signals.

Table 2.1 gives an indication of the classification of the frequency spectrum of sound.

Table 2.1: The classification of the frequency spectrum of sound [14, p. 51]

Frequency	Type of Sound
Up to 20 Hz	Infrasound
117.1 Hz	Middle C
500 Hz	Used for underwater navigation
1.77 kHz	Upper soprano
16 kHz	Upper limit for normal hearing
20 kHz	Ultrasound
30 kHz	Early submarine detection
70 kHz	Upper limit of bats
>70 kHz	Sonar
500 kHz	Lower limit of nondestructive testing
500k Hz – 12 MHz	Medical imaging up to 12 MHz
	Doppler 2, 4, 6, 8 MHz
12 MHz - 100 MHz	Scanning Acoustic Microscope (SAM)

Ultrasound is defined as sound that is located above the human audible frequency. Generally, this is accepted as being above 20 kHz. However, it is only in exceptional circumstances that the human ear can detect frequencies greater than 16 kHz.

2.2 Physics of ultrasound

2.2.1 Characteristic acoustic impedance

Acoustic impedance of ultrasound can be seen as a complex quantity, similar to electrical impedance. Pressure and velocity of particles correspond to voltage and current respectively.

Acoustic impedance can be expressed by the following equation [14, p. 52]:

$$p = Zv \qquad \textbf{2-1}$$

Where:

p = particle pressure

Z = acoustic impedance

v = particle velocity

Acoustic impedance can also be described as the product of the density of the medium and speed of the sound in the medium:

$$Z = \rho c \qquad \textbf{2-2}$$

Where:

c = the speed of sound in the medium

ρ = the density in kgm^{-3}

This formula clearly proves that if the speed stays the same, material with a high density will have high acoustic impedance. For example, steel has higher acoustic impedance than Perspex.

The acoustic impedance of a number of materials is shown in Table 2.2.

Table 2.2: Acoustic impedance values for different materials [14, p. 53]

Material	Velocity ms^{-1}	Density kgm^{-3}	Acoustic Impedance $10^6 kgm^{-2}s^{-1}$
Steel	7900	5800	45.80
Bone	3760	1990	7.48
Skin	1537	1100	1.69
Muscle	1580	1041	1.64
Fat	1476	928	1.36
Blood	1584	1060	1.68
Water	993	1527	1.52
Air	330	1.2	0.0004

2.2.2 Reflection

If a longitudinal wave traveling through a medium meets an interface with a different density to that of the medium, reflection will occur. Geometric reflection laws determine that reflection will occur, when a wave (of a specific wavelength) arrives at the boundary of a differing medium, of which the size is greater in relation to the wavelength of the wave. However, the geometric laws will not be applicable, at times when the subject is smaller than the wavelength itself.

The practice of administering certain medications to patients can, for example, increase the reflection of blood flow. These medications consist of small “micro bubbles” which serve as “echo-enhancers”. The large difference between the acoustic resistance of the blood and that of the matter that makes up the bubbles, results in the reflection of a large portion of the ultrasonic signal [3, p. 159].

2.2.3 Attenuation

Most of the ultrasound power is concentrated in the middle of the ultrasound beam and disappears gradually as the distance from the beam axis increases [2, p. 1327]. An ultrasonic wave, traveling through a medium, will diminish with its passage. The reduction in intensity of the ultrasonic signal, as it travels through a medium, is called attenuation. The reduction of the wave can be attributed to a number of factors. These factors include reflection, change of the modus of the wave, spreading, scattering and absorption of the wave. The attenuation of the medium is expressed in terms of $dBcm^{-1}$ at specific frequencies. Table 2.3 gives an indication of the attenuation coefficient of different materials at 1 MHz.

Table 2.3: The attenuation coefficient of different materials at 1 MHz [20, p. 249]

Medium	Propagation velocity (ms^{-1})	Attenuation coefficient at 1 MHz ($dBcm^{-1}$)
Air	330	10
Bone	2700—4100	3—10
Fat	1500	1
Lung	650—1160	40
Muscle	1545—1630	1.5—2.5
Soft tissues	1460—1615	0.3—1.5

The intensity attenuation coefficient can be given as [14, p. 57]:

$$A_I = \frac{10}{x}\log\frac{I_1}{I_2} \qquad \textbf{2-3}$$

Where:

A_I = intensity attenuation coefficient

I_1 = intensity at position one

I_2 = intensity at position two

x = displacement between points one and two

2.2.4 Absorption

An ultrasonic wave is absorbed, when its energy is transformed to heat. Mechanical potential energy is transformed to other forms of energy, during the compression phase of the longitudinal cycle. Energy is transferred back to the wave, during the rarefaction phase. This energy transfer is referred to as the relaxation process. The specific time taken for this relaxation process is referred to as the relaxation time. When the wave occurs at a low frequency, there is enough time for the energy to be transformed. However, when the frequency of the wave is increased, the energy transfer goes out of phase and absorption occurs. The absorption increases with the frequency and peaks at the relaxation frequency. The absorption decreases at frequencies above the relaxation frequency, due to insufficient time available for the original energy transfer.

There are a large number of relaxation processes with different relaxation frequencies, present in the biomedical materials. It is for this reason that the absorption of tissue increases linearly with frequency and can be ascribed to a summation of absorption of a large number of relaxation processes (Figure 2.1) [14, p. 58].

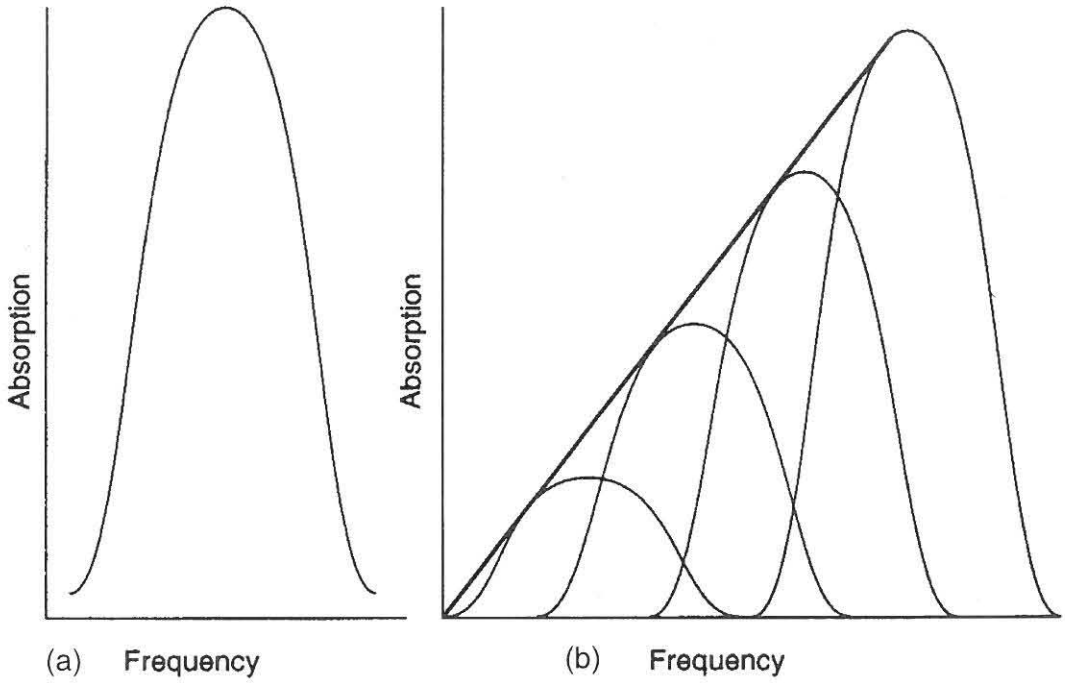

Figure 2.1: Single relaxation process (a) and the summation of many relaxation processes (b) [14, p. 58]

2.3 The Doppler effect

The sounds we hear are determined by their frequencies. When a moving body reflects sound, a slight variation in the frequency can be detected. This occurrence is referred to as the Doppler effect. For many years, the Doppler effect has been used to determine the speed and position of aircraft. One of the many uses of Doppler, in the medical field, includes the measurement of blood's speed, turbulence and flow-rate. Other applications include the recognition of fetal heartbeat and numerous other applications specific to the medical field [5, p. 1251] [22, p. 129].

2.3.1 Moving source and stationary detector

An example of a moving source and stationary detector is indicated in Figure 2.2. A reduction in the received frequency occurs, when the source moves away from the detector. An increase in frequency results, when the source moves towards the detector.

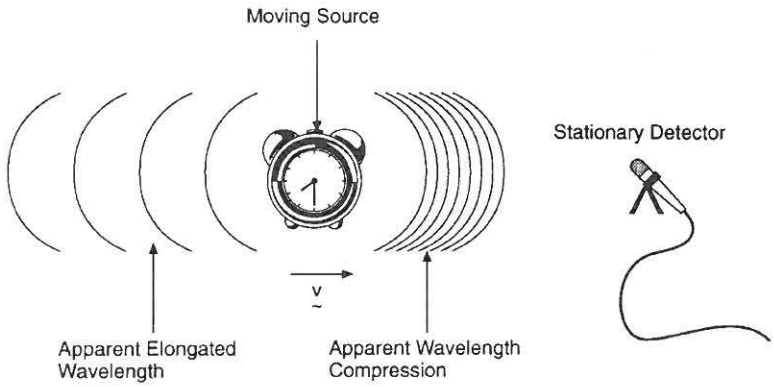

Figure 2.2: Moving source and stationary detector

The following is the expression for a moving source:

$$f_a = f_s \left(\frac{1}{1 + \frac{v}{c}} \right) \qquad \textbf{2-4}$$

Where:

fa = received frequency

fs = transmitted frequency

v = velocity of the source

c = velocity of sound in the medium

The sign of the velocity is positive for movement away from the detector and negative for movement towards the detector.

2.3.2 Stationary source and moving detector

In instances where the source is kept stationary whilst the detector is moved towards the source (such as the case indicated in Figure 2.3), it appears as if there is an increase in frequency. This can be ascribed to the fact that more waves cross over, at a given point in time.

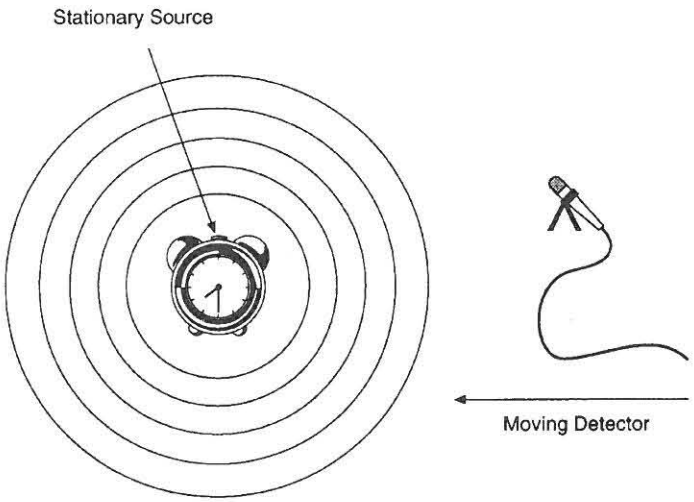

Figure 2.3: Stationary source and moving detector

The following is the equation for a moving detector:

$$f_a = f_s\left(1+\left(\frac{v}{c}\right)\right) \qquad \textbf{2-5}$$

Where:

fa = received frequency

fs = transmitted frequency

v = velocity of the source

c = velocity of sound in the medium

2.3.3 Doppler blood-flow analysis

In the analysis of blood-flow, ultrasound is reflected from the moving red blood cells back to the Doppler sensor [11, p. 420]. The first Doppler shift occurs as a result of the ultrasound making contact with the moving blood cells. This situation can be likened to the stationary source and moving detector. The second frequency shift occurs when the ultrasound is reflected back to the source. In this instance, this equates to a moving source and a stationary detector.

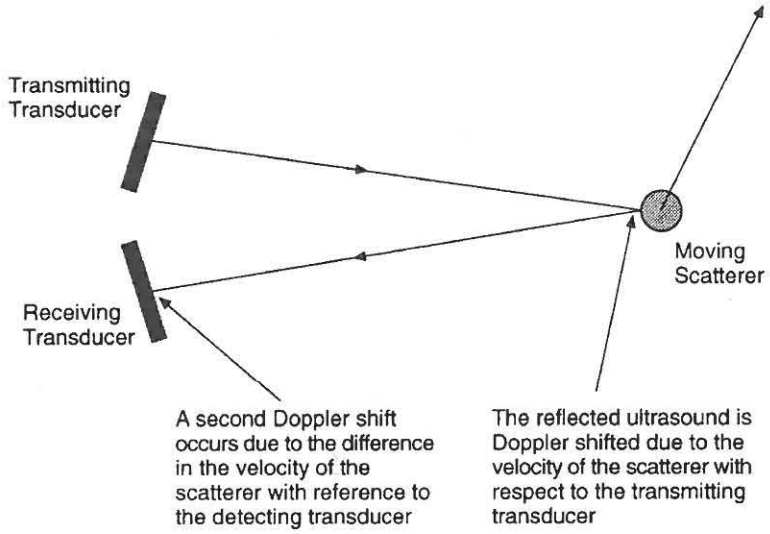

Figure 2.4: Doppler flow measurement [14, p. 64]

2.3.4 Continuous wave Doppler

Doppler ultrasound signals can be obtained by means of two methods, namely continuous wave Doppler and pulsed wave Doppler [20, p. 222] [16, p. 132].

Most human fetal monitors use continuous wave ultrasound [18, p. 47]. Figure 2.5 shows a block diagram of a continuous wave Doppler instrument.

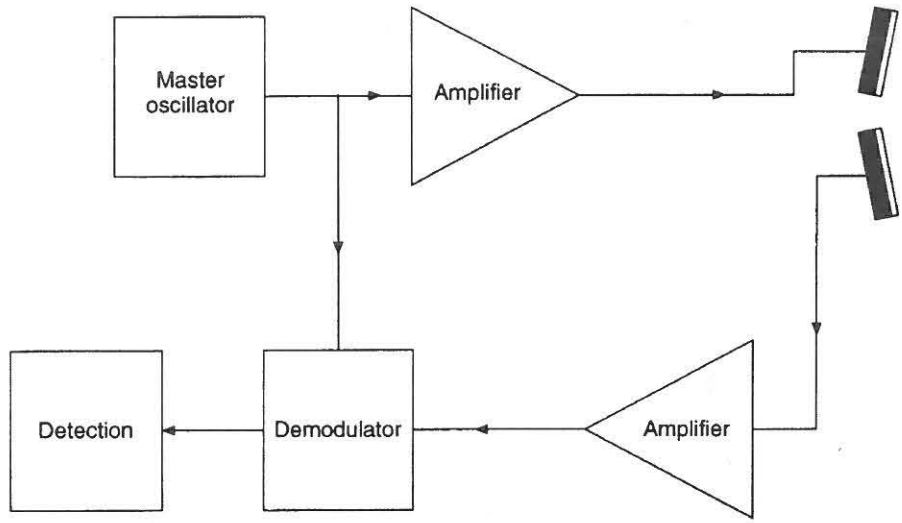

Figure 2.5: Block diagram of continuous wave Doppler instrument [14, p.163]

The main oscillator produces a sine wave, which is amplified and then connected to an ultrasonic transducer. A separate transducer is used to detect the received signal, as the transmitted signal is sent continuously. The received signal is amplified and then demodulated. Frequency shifts can occur as a result of, i) the movement of the sensor, ii) the movement of the patient, iii) the flow of blood or iv) the movement of certain organs.

2.3.5 Pulsed wave Doppler

The use of continuous wave Doppler measurement is problematic if the movement of organs, located at different depths is investigated. It is not possible to differentiate reflected signals at different depths with continuous wave Doppler measurement [32, p. 4].

With pulsed wave Doppler measurement, a short burst of pulses is transmitted. Due to the time lag present between the transmission and reception of the pulses, the depth of the investigation can be determined. Pulsed wave Doppler is

thus essential if, for example, blood-flow needs to be investigated in specific areas [1, p. 1550] [8, p. 337]. Doppler tissue echocardiography (DTE) is a modified pulsed Doppler technique which allows for the separation of the low velocities at the ventricular wall from the high velocity signals produced by the blood flow [24, p. 115]. Figure 2.6 indicates the block diagram of a pulsed wave Doppler instrument.

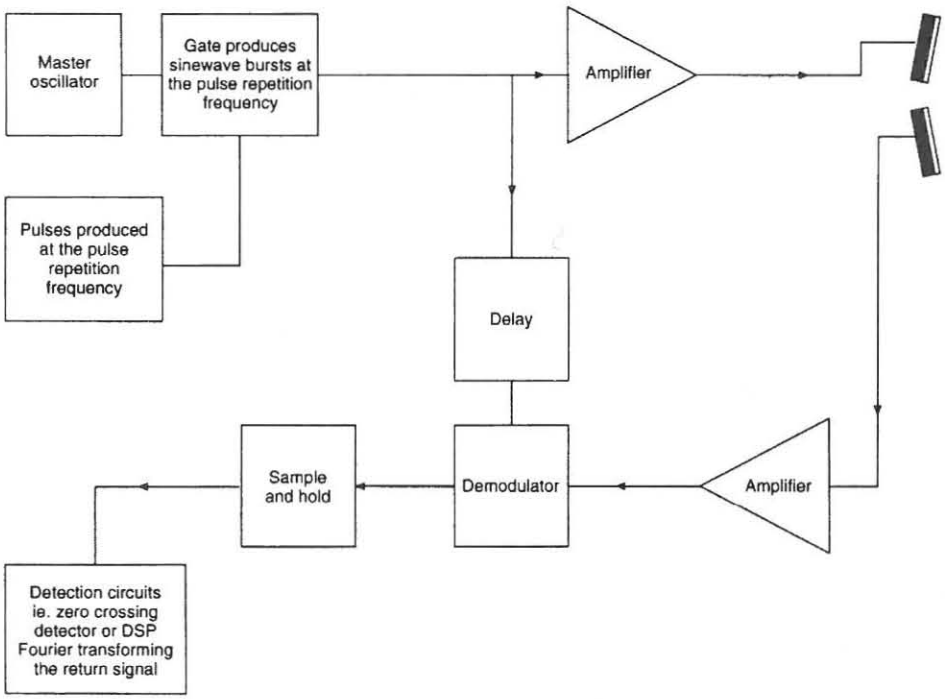

Figure 2.6: Block diagram of a pulsed wave Doppler instrument [14, p.163]

Short bursts of sine waves are sent to the amplifier and transmitted by the transducer. The burst of sine waves is delayed with a specific time delay. This delay is dependant on the penetration depth of the examination. The delayed signal now gets utilised for the demodulation of the reflected signal. In this way, penetration depth, as well as the Doppler signal from the specific depth, can be determined.

The demodulated signal, as obtained from a continuous wave Doppler instrument, forms the basis of the operational method in Chapter 3.

2.4 Summary

In Chapter 2 the relevant theory of ultrasonic signals as well as the principle of Doppler was discussed.

3 Processing the reflected Doppler signal

3.1 Wavelet and Fourier transforms

Any complex signal can be seen as the sum of a number of sine waves. This simple fact is the basis of the Fourier analysis [31]. In Doppler systems, spectral estimations were traditionally achieved with the Fast Fourier Transform (FFT) [9, p. 585] [17, p. 212] [21, p. 91]. Although the Fourier analysis functions satisfactorily if the frequency components that are present in the signal are constant over the total period of the signal, no information is available on exactly when specific frequency components appear. The Fourier analysis can determine which frequency components appear in the total signal, but not when the different components appear [4, p. 472]. The Fourier analysis is thus not ideally effective for non-stationary signals with a time dependent frequency spectrum [10, p. 452]. Since the FFT method inherently cannot offer a good spectral resolution at highly turbulent blood flows, it sometimes leads to wrong interpretation of cardiac Doppler signals [12, p. 436] [13, p. 231].

The discrete Fourier transform of a discrete time periodic signal is defined as [10, p. 447]:

$$X_k = \sum_{n=0}^{N-1} x(n) e^{(-jkn(2/N))} \qquad \textbf{3-1}$$

Where:

X_k = the discrete Fourier coefficients

N = the frame size

$x(n)$ = the input signal on time domain

n = sample

Figure 3.1 is an representation of a cosine signal that is described in equation 3-2.

$$x(t) = \cos(2\pi 10t) + \cos(2\pi 25t) + \cos(2\pi 50t) + \cos(2\pi 100t) \qquad \textbf{3-2}$$

Although the signals in Figure 3.1 and Figure 3.2 contain the same frequency components, the frequency components in Figure 3.2 occur at different times.

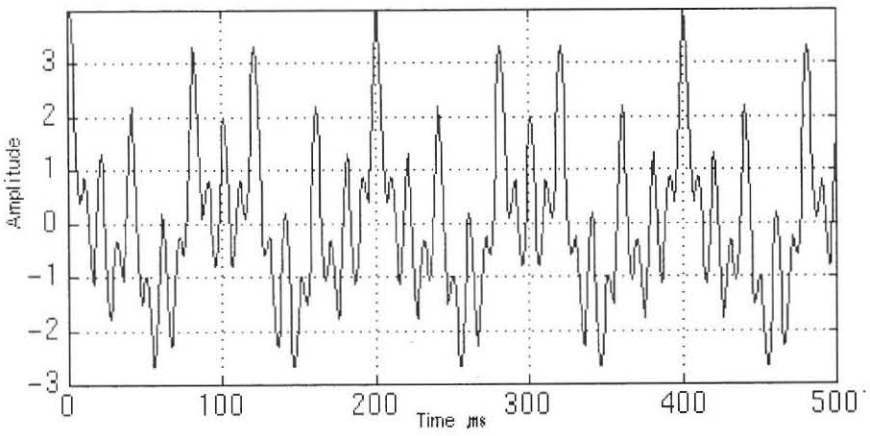

Figure 3.1: Cosine signal containing 10, 25, 50 and 100 Hz frequency components [25]

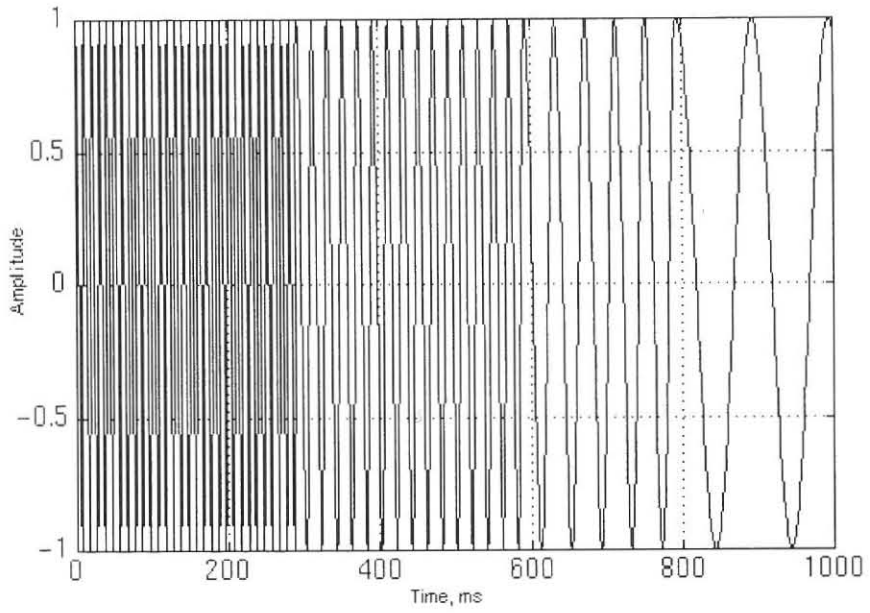

Figure 3.2: Signal containing 10, 25, 50 and 100 Hz frequency components [25]

The Short Time Fourier Transform (STFT) is a variation of the Fourier transformation (FT). With STFT the signal is broken up into specific constant periods [29, p. 231]. The FT can then individually be applied on each of these parts of the signal.

The problem with STFT is that if the signal is broken up over long periods, a good frequency resolution can exist, but a poor periodic resolution can be reflected. If the signal, however, is broken up into short periods and the FT applied on individual components, a better periodic resolution with a poor frequency resolution will be obtained [7, p. 87].

As an example the results of the STFT on the signal in Figure 3.3 are presented in Figure 3.4. The signal in Figure 3.3 was broken up into blocks of 50 samples and the FT applied to each block. Figure 3.4 is an indication of the frequency spectrum of each of the blocks. Each block gives an indication of a specific period of the total signal and the frequency changes with regard to the time can thus be observed.

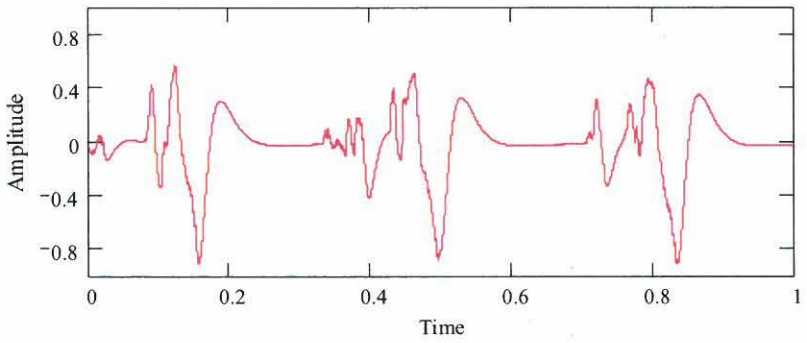

Figure 3.3: Time domain signal that was used for the STFT in Figure 3.4

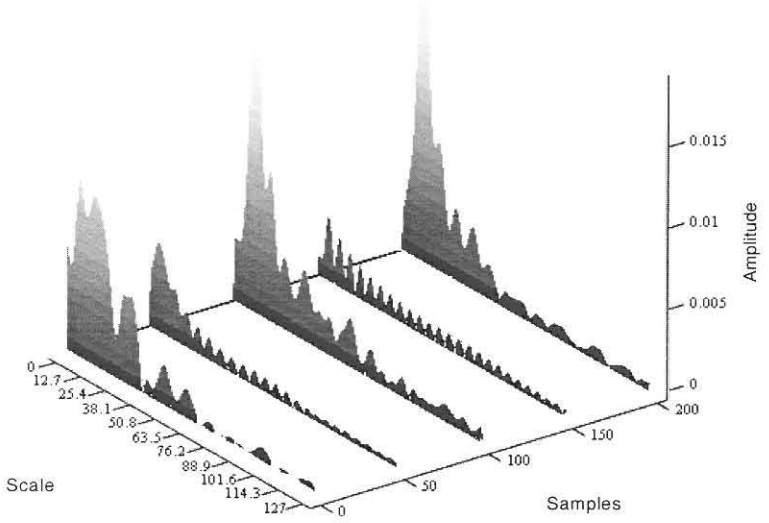

Figure 3.4: Three-dimensional representation of the signal in Figure 3.3 analysed with the use of STFT

Recently a new powerful method for the analysis of (non-stationary) signals, namely wavelet transformation (WT), was developed. In a wavelet transformation, linear combinations of the wavelet functions are used to represent the signal [30, p. 138]. In contrast with the lengthy duration of sine waves in the Fourier analysis, wavelets have limited periods and only appear in a few cycles. As in the Fourier analysis the wavelet analysis also has a fast algorithm to break the signal up into simple components.

$$CWT_{\chi}^{\psi} = \frac{1}{\sqrt{|s|}} \int \chi(t) \psi \left(\frac{t-\tau}{s} \right) dt \qquad \textbf{3-3}$$

Where:

Ψ (t) = the mother wavelet

τ = the translation parameter

s = the scale parameter

The term translation is related to the location of the window as the window is shifted through the signal.

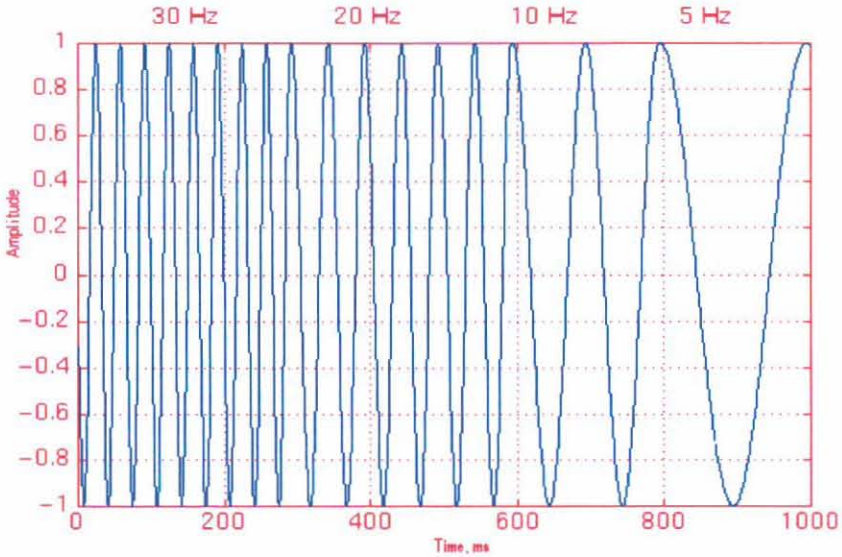

Figure 3.5: Signal with varying frequency in relation to time [25]

The translation axis gives an indication of time while the scale axis is an indication of the frequency. Please note that the low values on the scale axis in Figure 3.6 are an indication of high frequency components and the high values on the scale axis indicate the low frequency components. This is as a result of the fact that the scale parameter "s" in equation 3-3 is the inverse of the frequency.

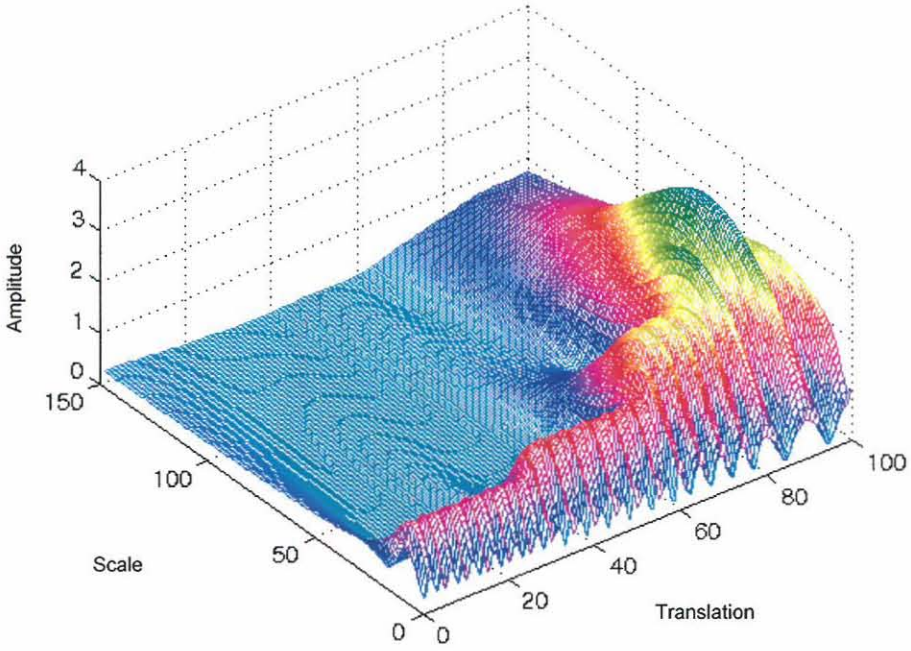

Figure 3.6: Wavelet transformation of time domain signal in Figure 3.5

Figure 3.7 is a continuous wavelet transformation (CWT) applied on the signal in Figure 3.3.

In order to investigate the influence of noise on the STFT and CWT, simulations with different levels of noise were carried out on the Doppler signal as obtained from the fetal heartbeat. In the simulations it was found that with the use of CWT and a signal-to-noise ratio of -6 dB, it was possible to recognise the heartbeat. The STFT simulation gave no clear indication of the presence of the heartbeat at the signal-to-noise ratio (SNR) of -6 dB. The results of the simulations of STFT and CWT at different signal-noise-ratios (SNR) are represented in Appendix B.

In Figure 3.7 the appearance of the frequency components, associated with the fetal heartbeat, can clearly be observed at specific time intervals.

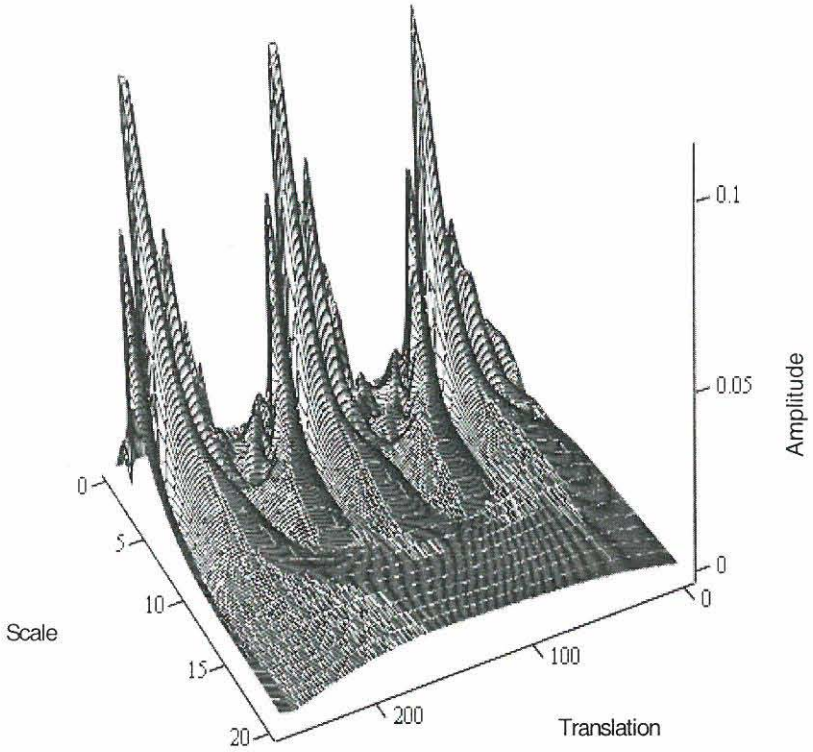

Figure 3.7: Wavelet transformation applied on measured Doppler signal in Figure 3.3

Characteristics of wavelet transformation (WT) are:

- Wavelets are localised in time and form good building blocks for a variety of signals. These signals sometimes consist of characteristics which change with time.
- Wavelets compact the energy functions of the signal into relative small quantities. This characteristic can especially be handy when using image compression.

Wavelet transformation (WT) can be applied in a wide area on a number of different fields, namely:

- Medical image processing;
- Pattern recognition;
- Numerical analysis and
- Flow dynamics studies [19, p. 5306].

Some people foresee wavelet compression as the future for both internet graphics and high resolution television graphics; this is because of its ability to compress signals more clearly than other methods [31].

Although the use of WT was investigated by means of simulations, it is not the final system to be implemented in this project. The reason being that with the implementation of the filter method, the appearance of certain frequencies in the signal was important and not the exact time when the frequencies appeared.

3.2 Correlation

There is a need to measure or specify the interdependence or association between signal values. Thus a quantitative indicator of correlation between signals is required [6, p. 317]. Correlation can be defined mathematically and can also be quantified [15, p. 243].

Typical applications of correlation are as follows:

- Image processing for robot sight where the observed image is compared with a stored image to determine the comparison between the two;
- Distance monitoring by means of satellite, where the data of different images can be compared;
- In radar and sonar systems the sent signal can be compared with the reflected signal and

- In the finding and recognising of noisy signals.

Suppose two signals with the same number of data points, which are sampled at the same time intervals, must be compared to each other. The correlation between the two signals can be obtained by determining the sum of the products of the sets of data points.

When the correlation between two random signals is calculated, it is found that the sum of the products tends to be zero. This is as a result of the probability that the products of the individual corresponding values of the two signals be either positive or negative. When the products are then added it tends to be zero, especially if the number of data points is increased. The cross-correlation between the two sets of data can be presented as [15, p. 245]:

$$r_{12} = \sum_{n=0}^{N-1} x_1(n) x_2(n) \qquad \textbf{3-4}$$

Where:

r_{12} = cross-correlation
$x_1(n)$ = data sequence one
$x_2(n)$ = data sequence two
N = the number of data points

The normalised value can be obtained by dividing the sum by the number of data points. The expression for normalised cross-correlation is thus:

$$r_{12} = \frac{1}{N} \sum_{n=0}^{N-1} x_1(n) x_2(n) \qquad \textbf{3-5}$$

Where:

r_{12} = normalised cross-correlation

$x_1(n)$ = data sequence one

$x_2(n)$ = data sequence two

N = the number of data points

Where two signals are correlated with each other, the phase difference between the signals is normally unknown. It can thus happen that the signals are the same, but as a result of the phase difference, no correlation is indicated between the signals. An example of this is presented in Figure 3.8.

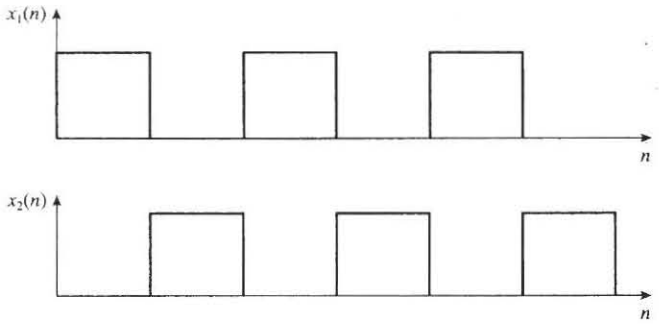

Figure 3.8: Out of phase, 100% correlated waveforms with zero correlation at time lag zero [15, p. 244]

The problem can be corrected by building in a changeable delay. This kind of delay can be interpreted as follows:

$$r_{12}(j) = \frac{1}{N}\sum_{n=0}^{N-1} x_1(n)x_2(n+j) \qquad \textbf{3-6}$$

Where:

r_{12} = cross-correlation

$x_1(n)$ = data sequence one

$x_2(n)$ = data sequence two

N = the number of data points

j = the delay

A further problem arises when numerous sets of data have to be compared to each other. When the end of the signal is reached there are no more sets of products. Certain values are zero and therefore the sum of the products is lower and over a period of time will tend towards zero. This is known as the end effect [15, p. 246]. Extending one signal can counteract the end effect.

3.3 Autocorrelation

The autocorrelation function is a means of measuring the correlation of a function with its own past, present, and future values [6, p. 319]. The autocorrelation function of a periodic waveform is itself a periodic waveform. It can be proved as follows [15, p. 255].

The periodic waveform $x(t)$ of period T satisfies:

$$x(t) = x(t + nT)$$

so,

$$r_{11}(\tau) = \lim_{T\to\infty} \frac{1}{T} \int_{-T/2}^{T/2} x(t)x(t+\tau)dt$$

$$= \lim_{T\to\infty} \frac{1}{T} \int_{-T/2}^{T/2} x(t)x(t+\tau+nT)dt$$

$$r_{11}(\tau) = r_{11}(\tau + nT)$$

Where:

r_{11} = autocorrelation

$x(t)$ = periodic waveform

T = period

τ = periodic in ı

Autocorrelating the signal tends to reduce the noise [15, p. 255].

For stationary random processes, the autocorrelation function tells us how rapidly we can expect the random signal to change as a function of time. If the autocorrelation function decays rapidly to zero it indicates that the process can be expected to change rapidly with time. A slow changing process will have an autocorrelation function that decays slowly [27, p. 142].

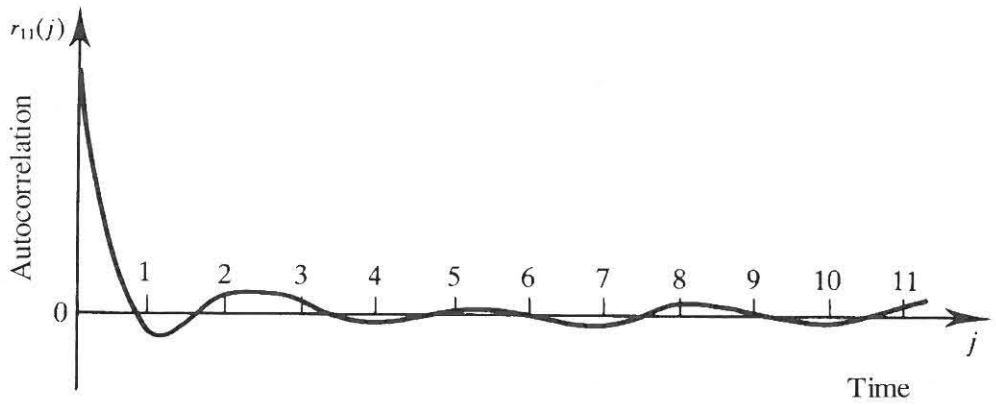

Figure 3.9: Autocorrelation function of a random signal [15, p. 249]

3.4 Summary

In Chapter 3 the aspects of the processing of the reflected Doppler signal is discussed. The advantage of WT in the analysis of non-stationary signals is highlighted. WT, FT and STFT were compared and discussed and correlation and autocorrelation were investigated.

4 Experimental design

4.1 Introduction

In order to obtain valid data for the analysis of the Doppler signal, the experimental design as shown in Figure 4.1 has been followed.

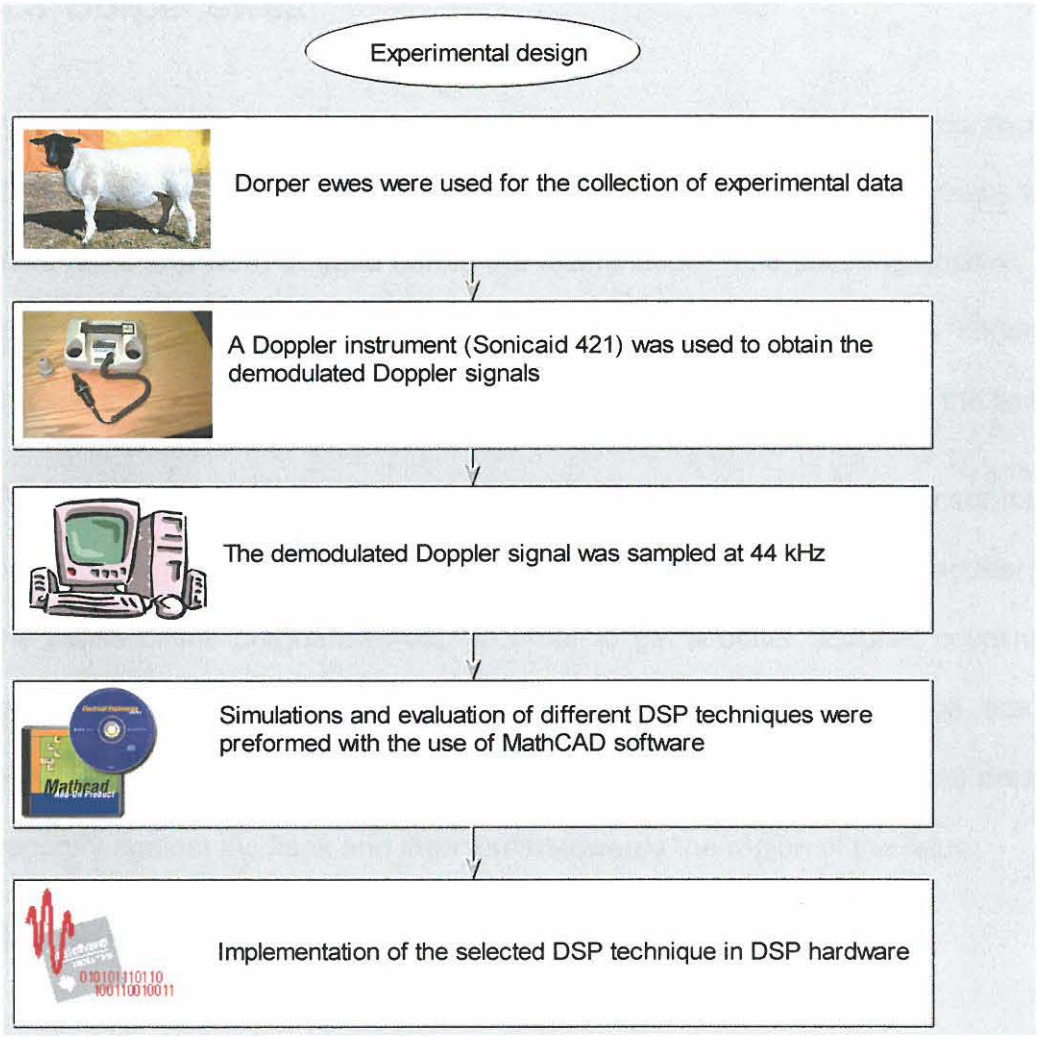

Figure 4.1: Experimental design

4.2 Doppler instrument

A Sonicaid 421 was used to collect the data. This instrument is manufactured by OXFORD Medical Limited [23, p. 6]. The Doppler instrument is designed to determine the heartbeat of a human fetus during pregnancy. One of the outputs of the instrument is a demodulated Doppler signal. The audio output level of the instrument is of such a level that a computer sound card can sample it.

4.3 Dorper ewes

A number of pregnant Dorper ewes were identified and within one month after data was obtained, they lambed. The ewes that were used in the sampling were quite tame and were at ease during the examination. The standing position was found to be the best position for the ewes during sampling. The ultrasonic transducer was placed next to the back left leg on a less hairy place of the flank.

Problems were experienced with the coupling where the ultrasonic sensor had to be placed against the skin of the sheep. This is due to the hair that appears on the flanks of the pregnant ewes. In order to get a better acoustic coupling, a suitable gel was used. The gel serves as an acoustic impedance adaptor between the skin of the sheep and the transducer. The transducer was pressed securely against the flank and then turned towards the region of the fetus.

4.4 Sound card

The output of the ultrasonic Doppler instrument was linked to a sound card for sampling. Goldwave software was used for the sampling of the signal.

4.5 Simulation

The files were converted to text files in order for the data to be analysed in MathCAD. In the analysis of the data the following methods were considered: Correlation, autocorrelation and a filter method. During the evaluation of the system the autocorrelation method was compared to the filter method.

4.6 DSP hardware

The DSP hardware which was used for the implementation of the system was the TMS320C6711 DSP development card of Texas Instruments (TI). The C6711 devices are based on the high-performance, advanced very-long-instruction-word (VLIW) architecture developed by Texas Instruments (TI), making these DSP's an excellent choice for multi-channel and multi-function applications.

The C6711 DSP devices can perform up to 900 million floating-point operations per second (MFLOPS) at a clock rate of 150 MHz. The C6711 DSP possesses the operational flexibility of high-speed controllers and the numerical capability of array processors. This processor has 32 general-purpose registers of 32-bit word length and eight highly independent functional units. The eight functional units provide four floating-/fixed-point ALU's, two fixed-point ALU's and two floating-/fixed-point multipliers.

4.7 Summary

In Chapter 4 the experimental design as well as the hardware and software that was used is discussed. The experimental data were obtained from the pregnant Dorper ewes with the aid of a portable Doppler instrument. The sampling of the

data was then done with the aid of a computer sound card. Simulations were completed with the aid of MathCAD software and the DSP hardware, used for the implementation of the system, was the TMS320C6711 DSP development card of Texas Instruments (TI).

5 Simulation and implementation of the filter method

5.1 Simulation of filter method

The signal in Figure 5.1 is a measured signal which was obtained with the aid of a Doppler instrument[1] from a pregnant Dorper ewe. The signal is viewed as noiseless. In order for the filter method to realise, the steps as presented in Figure 5.2 are applied on Figure 5.1. The complete MathCAD simulation of the filter method as presented in Figure 5.2 is presented in Appendix A.

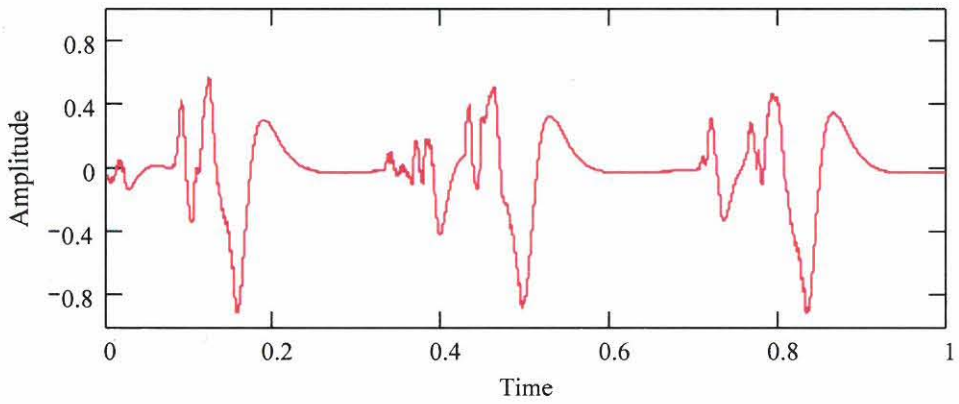

Figure 5.1: Experimentally obtained Doppler signal

[1] The Doppler instrument is discussed in more detail in paragraph 4.2 on page 29

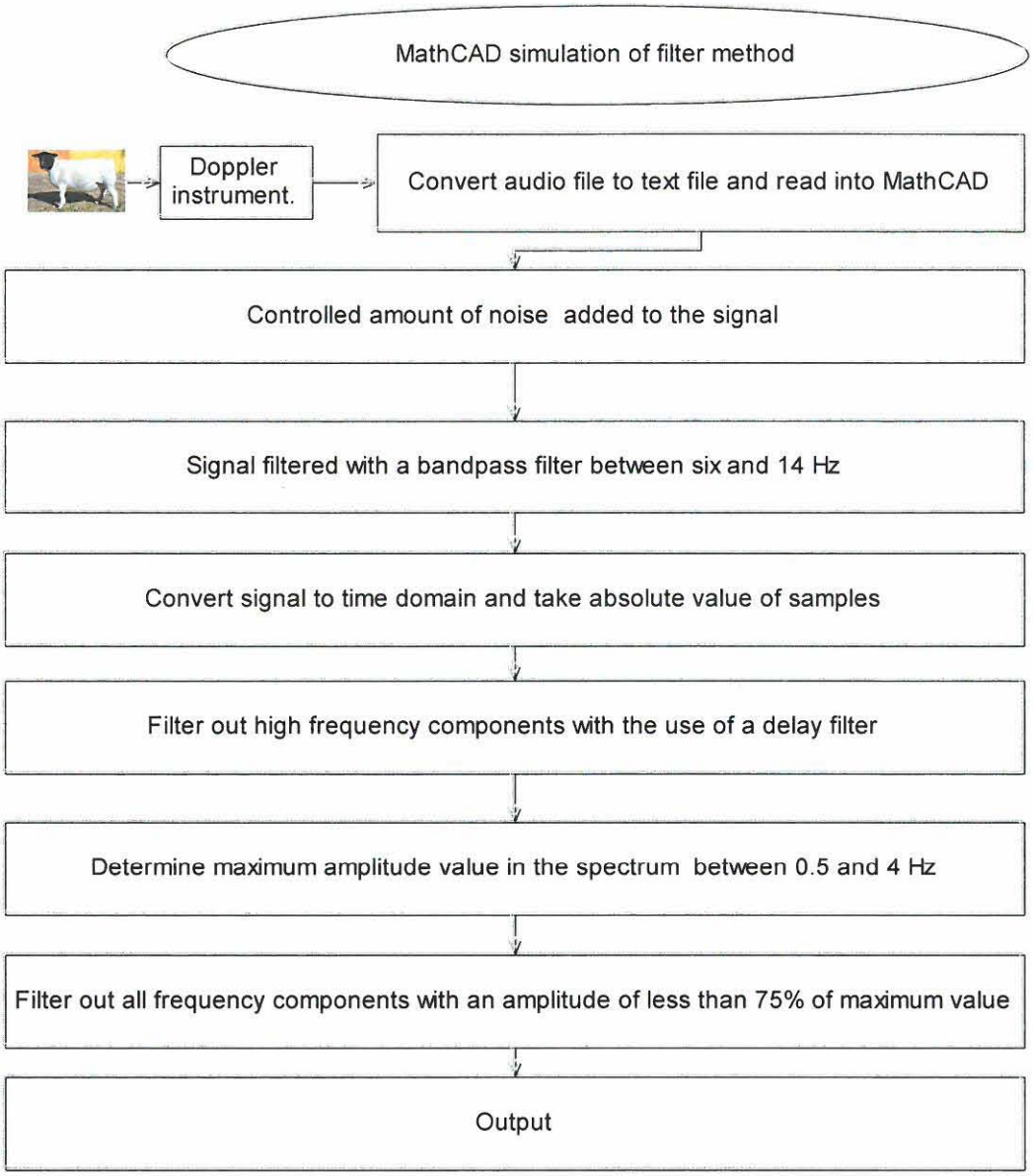

Figure 5.2: MathCAD simulation of filter method

In order to evaluate the operation of the system, a certain level of noise was added to the noiseless signal. In the explanation of the simulation a signal with a SNR of -3 dB was taken as a representative signal. Figure 5.3 indicates the signal after the noise was added to the signal at a SNR of -3 dB.

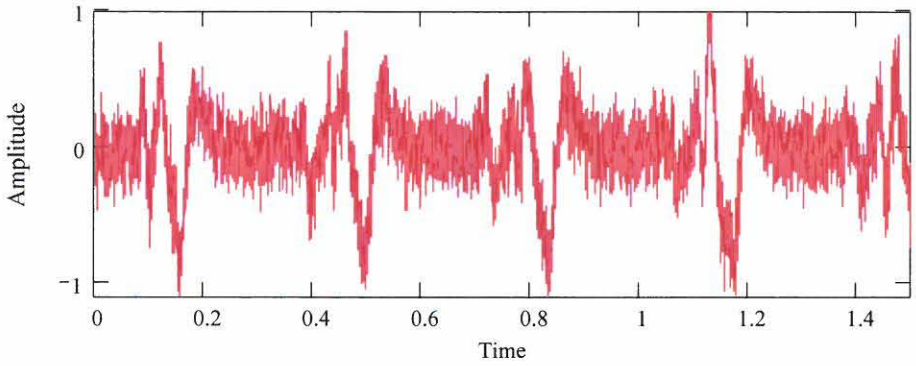

Figure 5.3: Measured signal with a SNR of -3 dB

The following step consists of a band pass filter with a pass band of between six and 14 Hz which is applied to the signal. Several simulations were done in order to determine the ideal filter bandwidth. The simulation results with different bandwidths are shown in Appendix B. The results in Table B.1 are an indication of the influence of the bandwidth of the first band pass filter on the simulation of the filter method. A pass band of between six and 14 Hz was chosen, based on the results in Appendix B. Figure 5.4 indicates the frequency spectrum of the Doppler signal, as well as the part of the frequency spectrum which is passed through by the six to 14 Hz band pass filter. In Figure 5.5 the signal is indicated after the six to 14 Hz band pass filter has been applied.

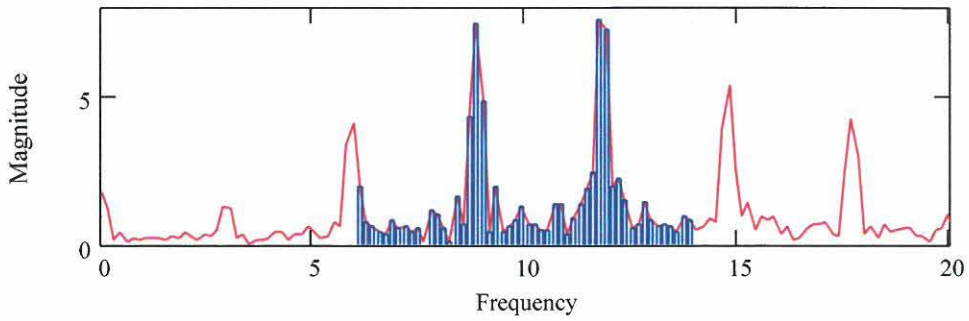

Figure 5.4: The frequency spectrum of the Doppler signal as well as the part of the band which was let through by the six to 14 Hz band pass filter

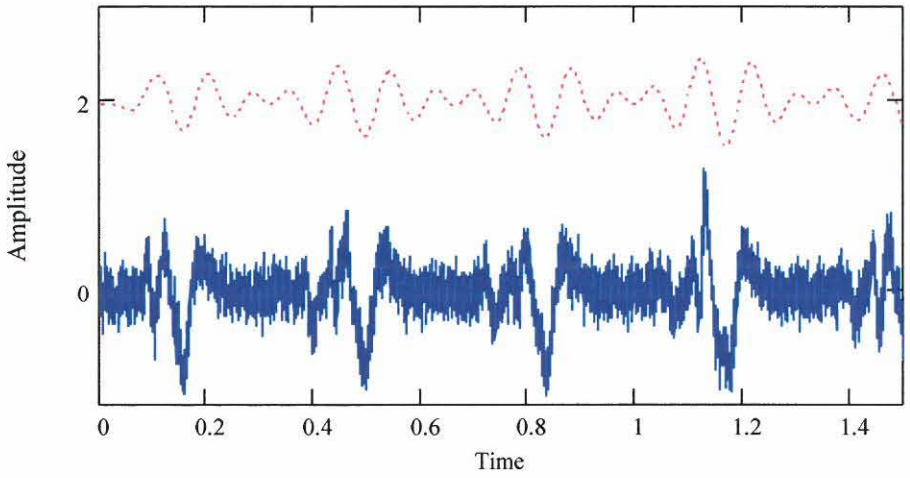

Figure 5.5: The original representative signal (bottom) and six to 14 Hz filtered signal (top)

The absolute value of the filtered signal is taken, after which a delay filter is applied to the signal. In the simulation the delayed signal is added to the non-delayed signal in order to realise a low pass filter.

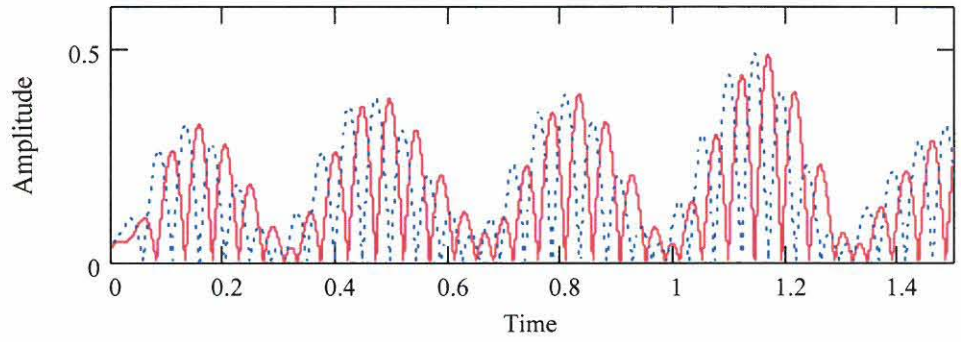

Figure 5.6: Absolute value of the filtered signal (—) and delayed absolute value of filtered signal (---)

The top signal in Figure 5.7 is the signal after the delay filter was applied. The noisy original measured signal is also indicated as the bottom signal in Figure 5.7.

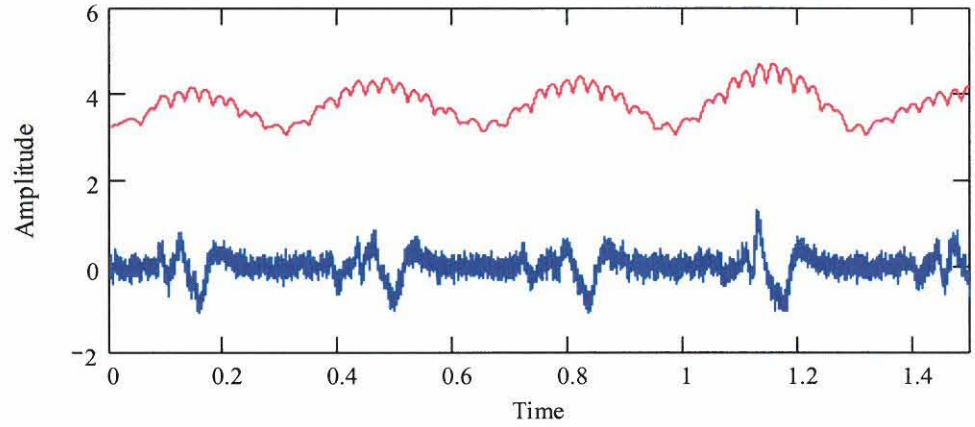

Figure 5.7: Signal after application of delay filter (top) and the original measured signal (bottom)

Figure 5.8 indicates the frequency spectrum of the filtered signal. A prominent frequency component between two and 4 Hz is observed. This frequency component is as a result of the presence of the fetus's heartbeat at the specific frequency.

Although the frequency component of between 0 and 6 Hz was filtered out early in the system, other frequency components appear in the band because a delay filter was applied on the absolute value of the high frequency components. The delay filter acts as a low pass filter and, because the bundles of high frequency components appear at the frequency of the fetal heartbeat, the frequency of the fetal heartbeat can be distinguished.

The next step is to determine the frequency of the fetal heartbeat. In the simulation the signal was switched to its frequency components by the use of a FFT. The frequency between 0.5 and 6 Hz was investigated and the component with the highest amplitude was selected.

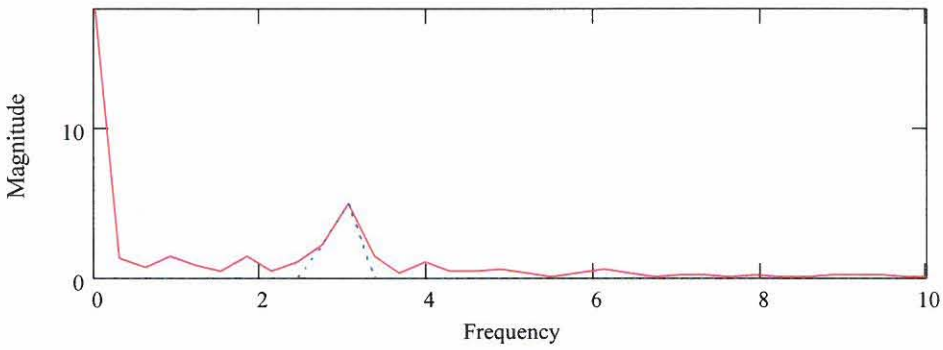

Figure 5.8: Frequency spectrum of the signal (—) and filtered spectrum (---)

Frequency components with amplitudes of less than 75% of the maximum component were eliminated. Thus only frequency components with amplitudes higher than 75% of the highest amplitude value between 0.5 and 6 Hz were left. This signal is retransformed back to the time axis and is indicated in Figure 5.9.

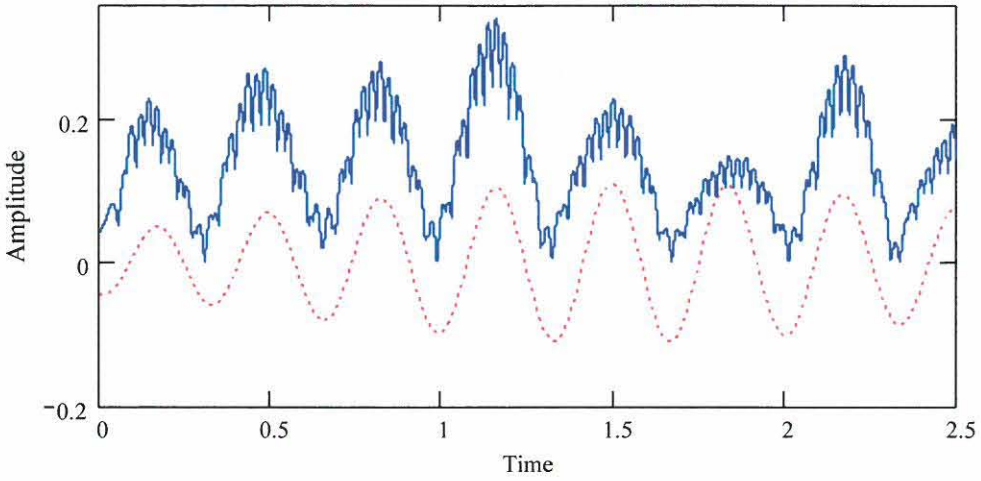

Figure 5.9: Signal before amplitude filter (—) and after application of amplitude filter (---)

The last step in the simulation was to change the isolated signal, with a frequency equal to the fetal heartbeat, into a square wave. The square wave is only a clearer indication of the appearance of the isolated frequency component which represents the fetal heartbeat. Figure 5.10 gives an indication of the original signal, the isolated frequency and the representative square wave.

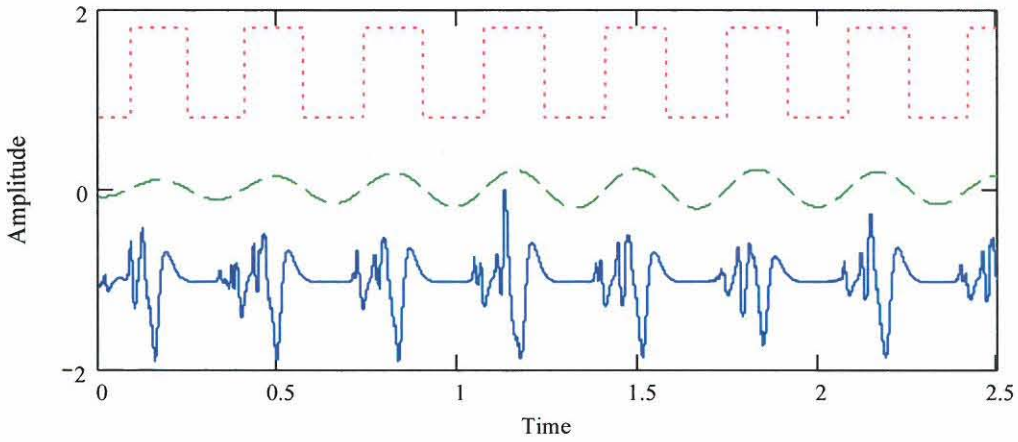

Figure 5.10: Original signal (bottom), isolated frequency (middle) and square wave (top)

5.2 Implementation of the filter method in DSP

Visual Application Builder (VAB) from Hyperception was used to develop the DSP software. This enabled the programmer to obtain a working system in DSP by means of applicable block components. The VAB software was developed and tested for use in the TMS320C6711 DSP development card of Texas Instruments (TI).

A few advantages when using the VAB software are [28]:

- The generation of DSP Object Code from a Block Diagram;
- Speeds up project development;
- Improves maintainability through modular and self-documenting design;
- Allows convenient migration across DSP platforms;
- Supports true component-based design and
- Compatibility with standard TI toolsets, including C compilers and assemblers. [28]

Figure 5.11 gives an indication of the flow of data in the DSP implementation process.

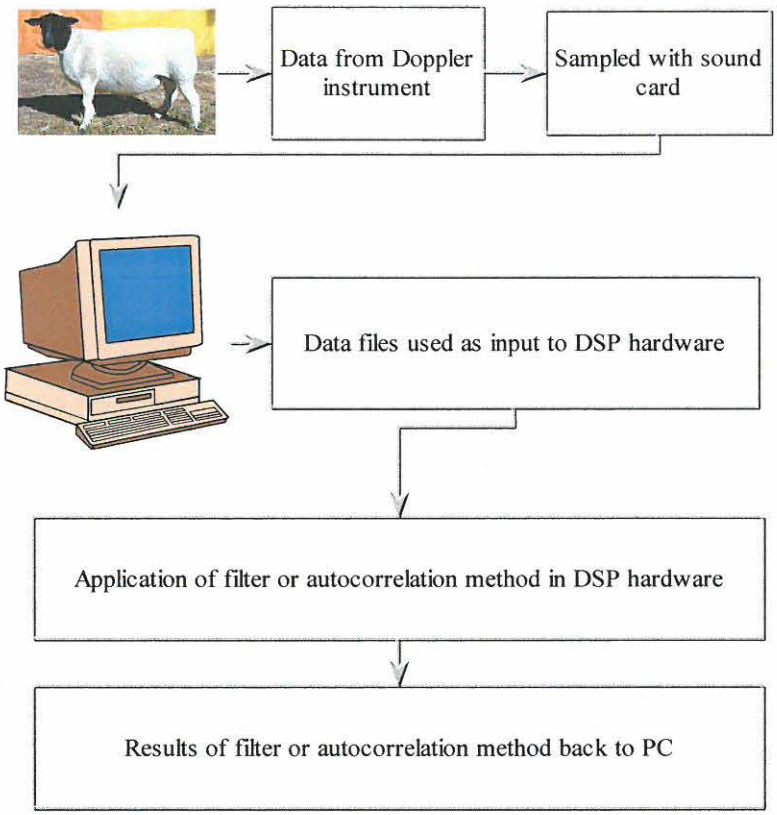

Figure 5.11: Flow of data in the DSP implementation process

Figure 5.12 represents the implementation of the filter method in the DSP hardware. The system in Figure 5.12 is applied to the measured Doppler signal to determine the presence or absence of the fetal heartbeat. The sampling frequency of 100 Hz is used for the implementation in DSP hardware. The block diagram presentation of the implementation is in accordance with the physical implementation which will henceforth be broadly discussed.

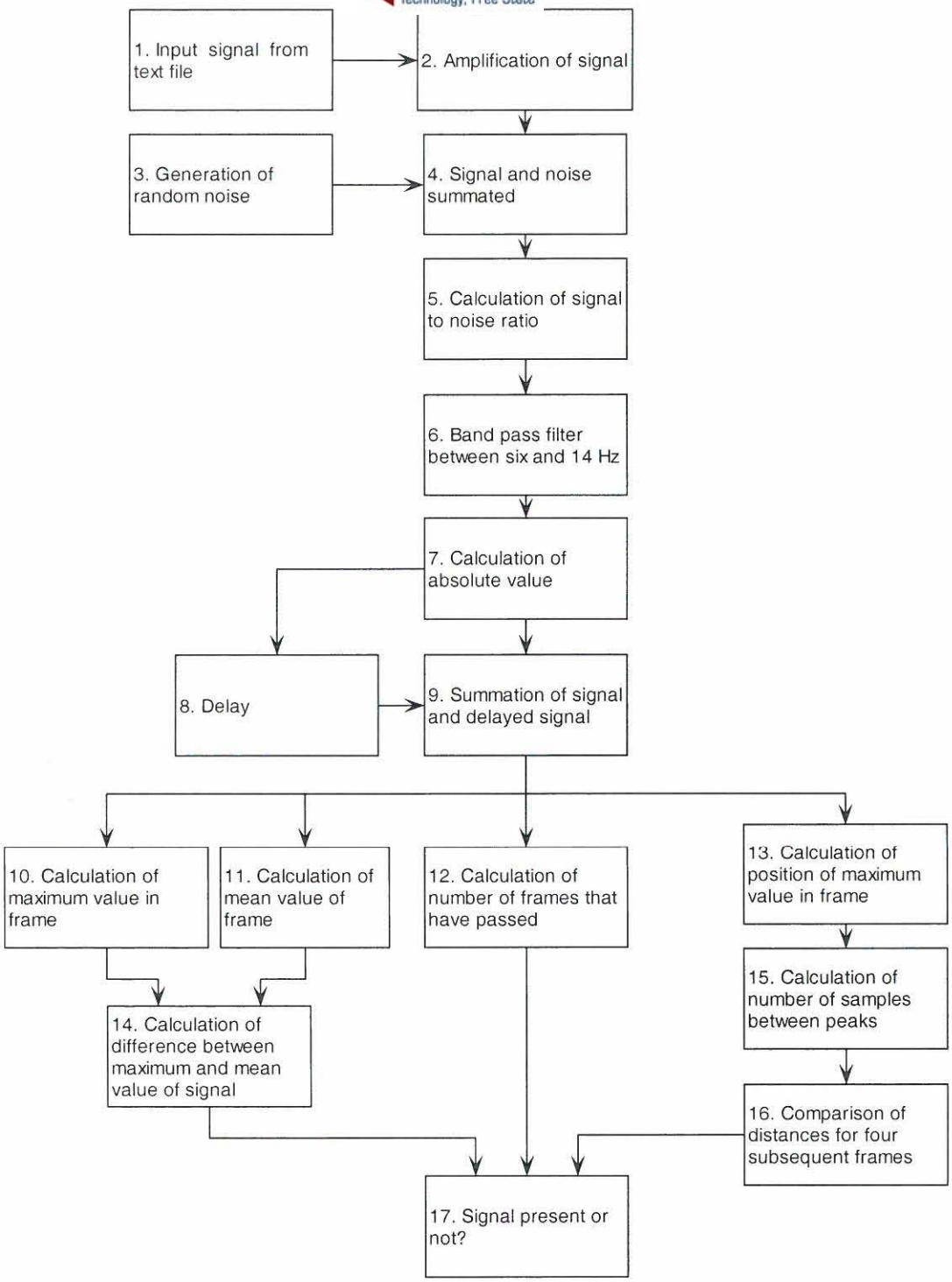

Figure 5.12: Implementation of the filter method in DSP hardware

As for the MathCAD simulations the pre-recorded signal in the text file was used as input in the implementation[2]. In order to evaluate the system at different SNR's the ideal signal was put through an adjustable amplifier before noise was added[3]. The noise was generated by the use of MathCAD and stored as a text file on the host computer, after which it was loaded onto the DSP hardware. In Figure 5.13 the heartbeat signal which has been amplified as well as the noise can be observed. In order to explain the implementation of the system, noise was added to obtain a SNR of 1.4 dB.

The buffers used in Figure 5.13, are used to collect data before displaying it on the display units.

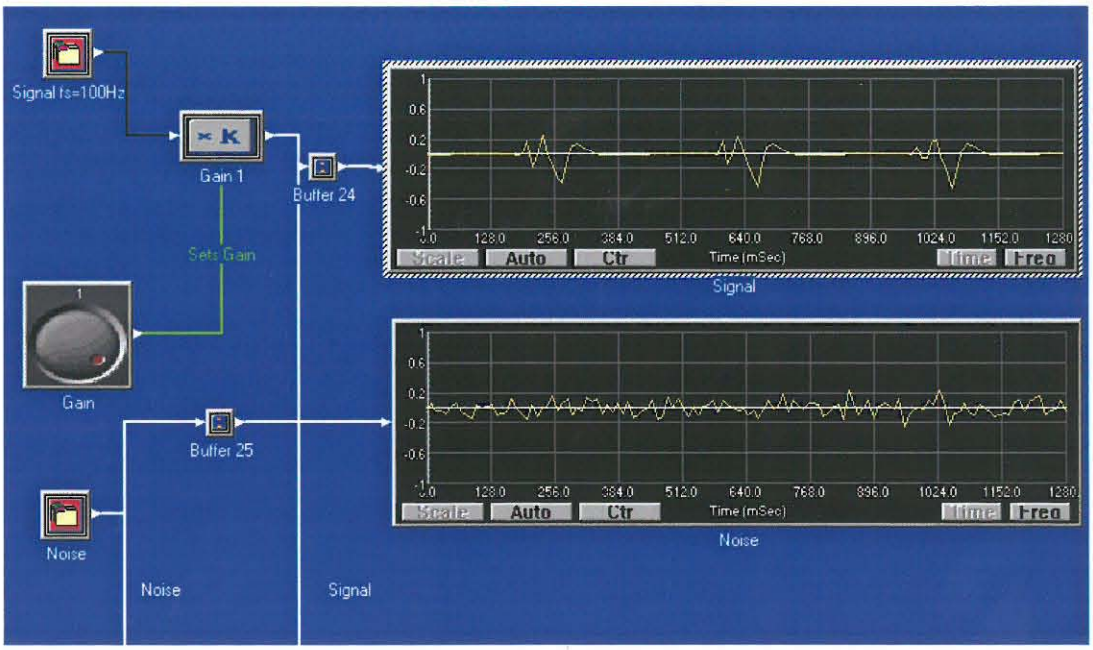

Figure 5.13: Noiseless signal and noise as read from the text file

[2] Block 1 of block diagram in Figure 5.12
[3] Block 2 of block diagram in Figure 5.12

Henceforth the SNR was calculated in dB[4]. This calculation was done in DSP hardware and the answer was loaded onto the host computer and displayed on the screen in dB.

The calculation of the SNR is indicated in Figure 5.14 and is executed as follows:

- The ideal signal, as well as the noise amplitude, is squared and;
- Thereafter the averages of the squared values of the complete signal is calculated;
- The average, squared, ideal signal is then divided by the average squared noise value;
- The result obtained is used as input for the dB amplitude block;
- The dB amplitude block realises the following equation $10\log(x)$ where x is the average of the squared signal values divided by the average of the squared noise values.
- The output of the dB amplitude block gives the SNR in dB, after which it is shown on the display unit

[4] Block 5 of block diagram in Figure 5.12

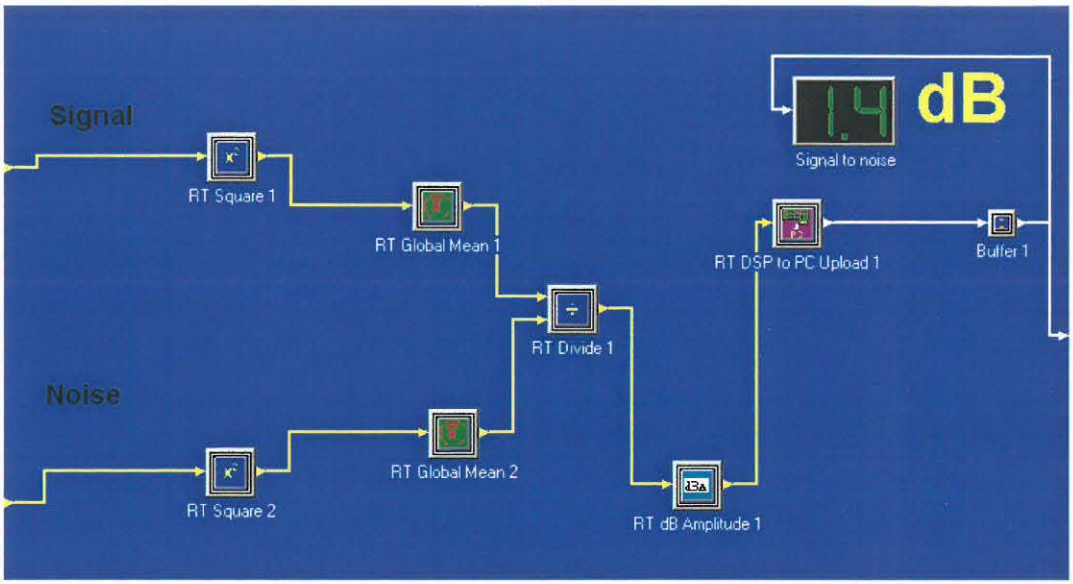

Figure 5.14: Calculation of SNR in dB

After calculation of the SNR, the noise is added to the signal. Figure 5.15 depicts the signal with an SNR of 1.4 dB. Note that the content of Figure 5.14 is actually the (S/N dB) block as indicated in Figure 5.15.

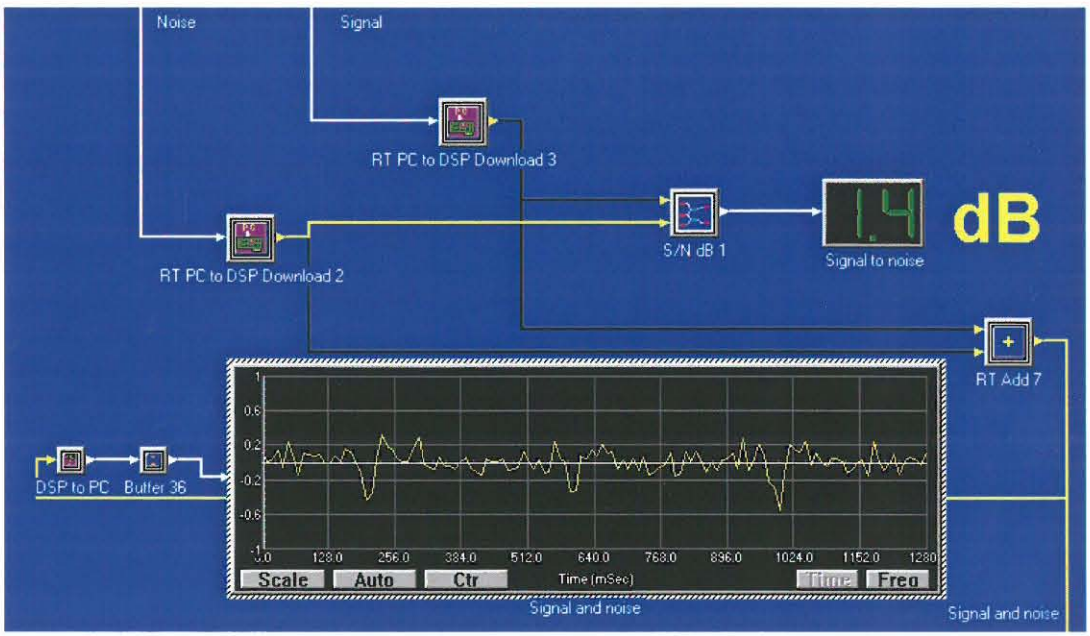

Figure 5.15: Signal containing noise

The following step in the implementation consists of a six to 14 Hz band pass filter[5]. These pass band values have bean determined experimentally as described in paragraph 5.1. The MathCAD function that was used to calculate the coefficients of the FIR filter is:

$$bandpass(f1, f2, N, w)$$

Where:

$f1$ = real valued lower cutoff frequency, given as fraction of the sampling frequency

$f2$ = real valued upper cutoff frequency, given as fraction of the sampling frequency

N = number of coefficients for the filter

w = windowing function index

The arguments for the windowing function index is:

1 rectangular windowing function

2 tapered rectangular windowing function

3 triangular windowing function

4 Hanning windowing function

5 Hamming windowing function

6 Blackman windowing function

The variables that was used for the calculation of the six to 14 Hz band pass FIR filter coefficients is:

$f1$ = 6 Hz

$f2$ = 14 Hz

N = 32

[5] Block 6 of block diagram in Figure 5.12

$w = 1$

The value of the y-axis in Figure 5.16 represents the calculated coefficients of the filter. The calculated coefficients are read into a text file, thereafter placed on the host computer and loaded onto the DSP hardware.

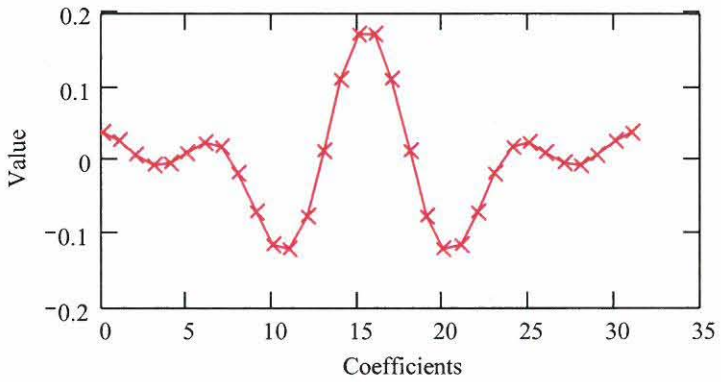

Figure 5.16: The 32 coefficients of the six to 14 Hz FIR filter

After the signal was filtered by means of the band pass filter, the absolute value was calculated[6]. In order to apply a simplified low pass filter on the signal, the signal[7] was delayed with two samples[8]. Hereafter the delayed signal was added to the original signal[9]. A MathCAD simulation of the system was used to determine the required delay experimentally. When studying the time domain of the signal, prominent peaks exist at intervals equal to the appearance of the fetal heartbeat. Above-mentioned process is depicted in Figure 5.17.

[6] Block 7 of block diagram in Figure 5.12
[7] The signal was sampled at 100 Hz
[8] Block 8 of block diagram in Figure 5.12
[9] Block 9 of block diagram in Figure 5.12

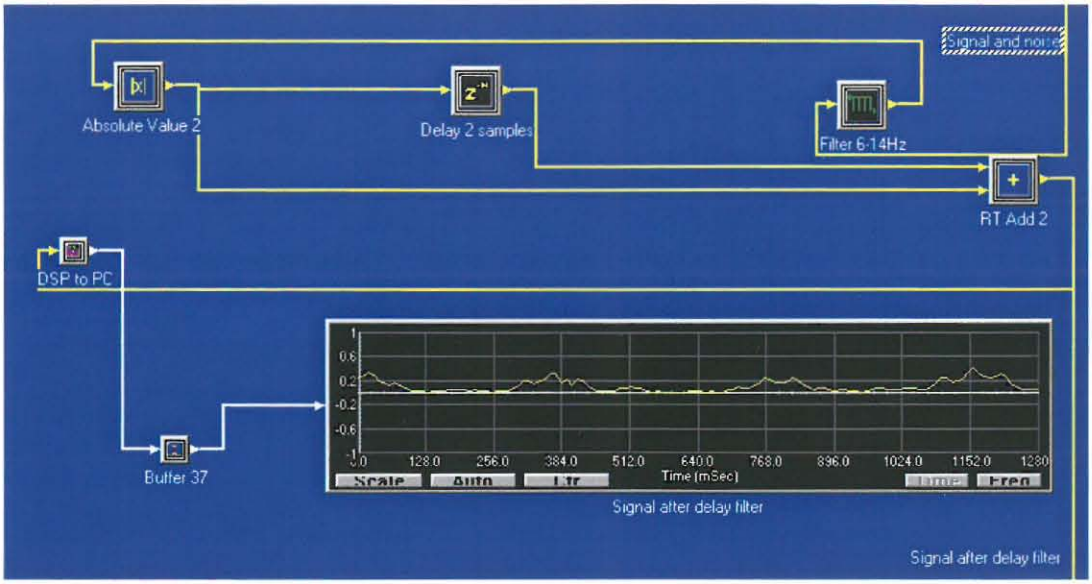

Figure 5.17: FIR band pass filter as well as the delay filter

5.2.1 Presence or absence of signal

In order to determine at which SNR the fetal heartbeat can be detected with certainty, the following system was developed.

The sampling frequency is 100 Hz and the fetal heartbeat occurs at 2.5 Hz. This means that there wil be at least one fetal heartbeat in every 40 samples. For this reason a frame sise of 40 samples was chosen and used in the implementation of the filter method. Because the output of the filter method produces a peak if the fetal heartbeat is present the maximum value of the data in each block of data could be determined. The time distance, or the number of samples between the maximum values of the consecutive blocks could then be calculated. The process is repeated for four blocks and every time the distance between the maximum values is calculated. The number of samples which appear between peaks of the consecutive blocks are then compared to determine the differences in the number

of samples. If the distances between the peaks fall within a certain value, it is an indication that the fetal heartbeat is present.

After a predetermined number of input data blocks a decision must be taken as to whether the fetal heartbeat is present or not[10] (Figure 5.18).

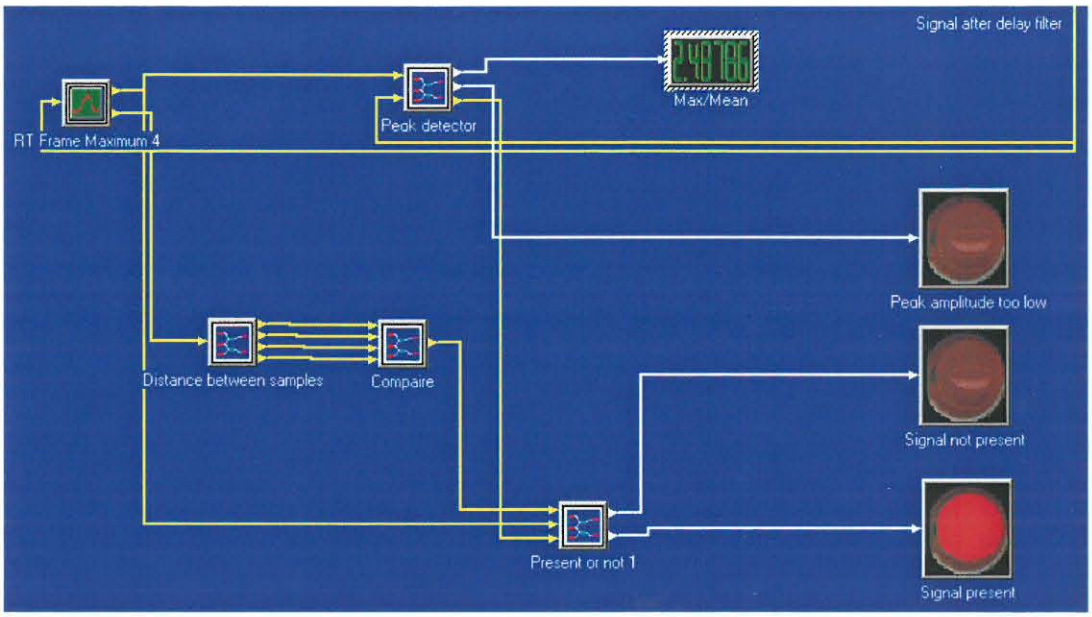

Figure 5.18: Presence or absence of fetal heartbeat

The maximum frame block in Figure 5.18 takes the signal after the delay filter as input. The block gathers all the data values in one frame. Thereafter the maximum value in the frame as well as the position of the maximum value is determined. The block has two outputs, namely one that indicates the maximum value and one that indicates the position of the maximum value.

The next block is the peak detector block. In this block the ratio between the average values of the signal and the peak values of the signal is determined[11]. The inside of the peak detector block is presented in Figure 5.19 and it has two

[10] Blocks 13,15 and 16 of block diagram in Figure 5.12
[11] Blocks 10,11 and 14 of block diagram in Figure 5.12

inputs. The first input is the maximum values as determined by the maximum frame block. The second input is the signal values. Thereafter the average of the maximum values of each block as well as the average signal value is calculated. The average of the maximum values is then divided by the average signal value, which then represents the ratio between the two.

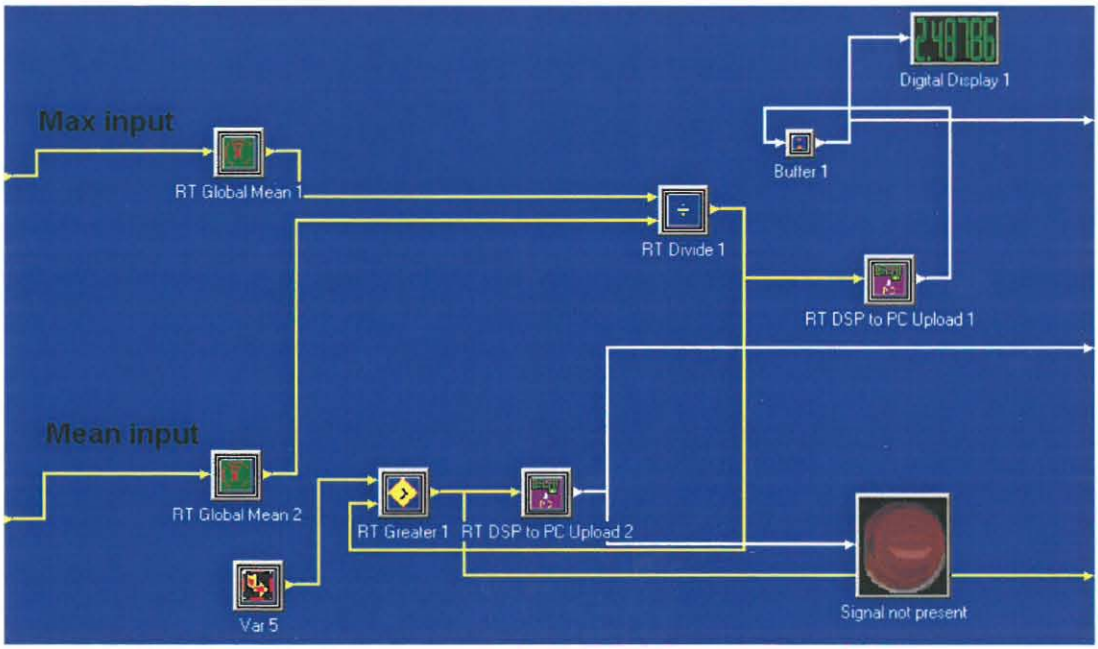

Figure 5.19: Peak detection block

In the second part of the peak detector block, the calculated ratio is compared with a predetermined value. As soon as the ratio between the average of the maximum and the average of the signal values are below the predetermined level an indication is given that the noise levels are too high and therefore the signal cannot successfully be identified.

In the "distance between samples" block, which is indicated in Figure 5.21, the sample distance between the maximum values of the four consecutive blocks of data are calculated. The input for the block is the position of the peak in a

specific frame. In Figure 5.21 the maximum value is at sample 30 for block 1 and sample 32 for block 2. The sample distance between the two maximum values can thus be calculated as, the number of samples in the block minus the number of the sample with the maximum value in block 1, plus the number of the sample with the maximum value in block 2. The distance between the samples with maximum values in Figure 5.21 is thus 42.

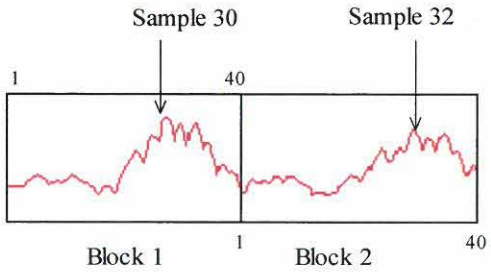

Figure 5.20: Example of calculation of distance between maximum values

The distance can thus be determined for four consecutive cycles. Because of the relative short data sequence and by experimentation with real data as input to the system, it was decided that the presence of four consecutive cycles is an indication of the presence of the fetal heartbeat.

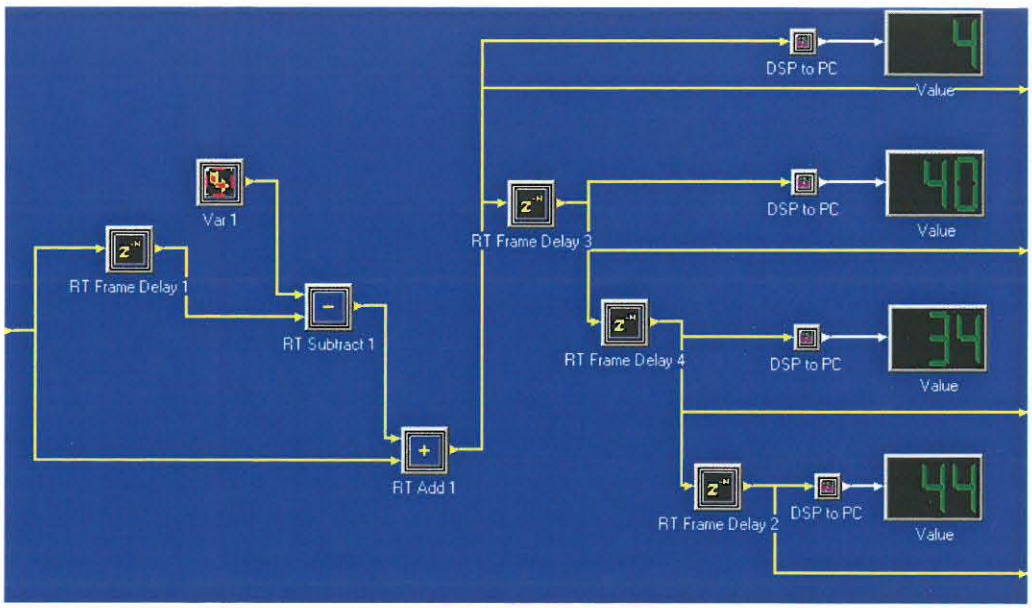

Figure 5.21: Distance between maximum values

In Figure 5.22 it shows how to determine whether the distances between the maximum values fall within the predetermined range. The average distance value of four consecutive maximum values can be determined. A specified value is then added and also subtracted from the average value. This predetermined value sets the range in which the four samples have to fall. The "in range" block limits are set within an upper and lower limit. If the average distance between the four peaks was for example 40 samples and the specified value that was added and subtracted, two, it would mean that the "in range" blocks limits would be set between 38 and 42. The block would give an output only if all four blocks had an input distance of between 38 and 42.

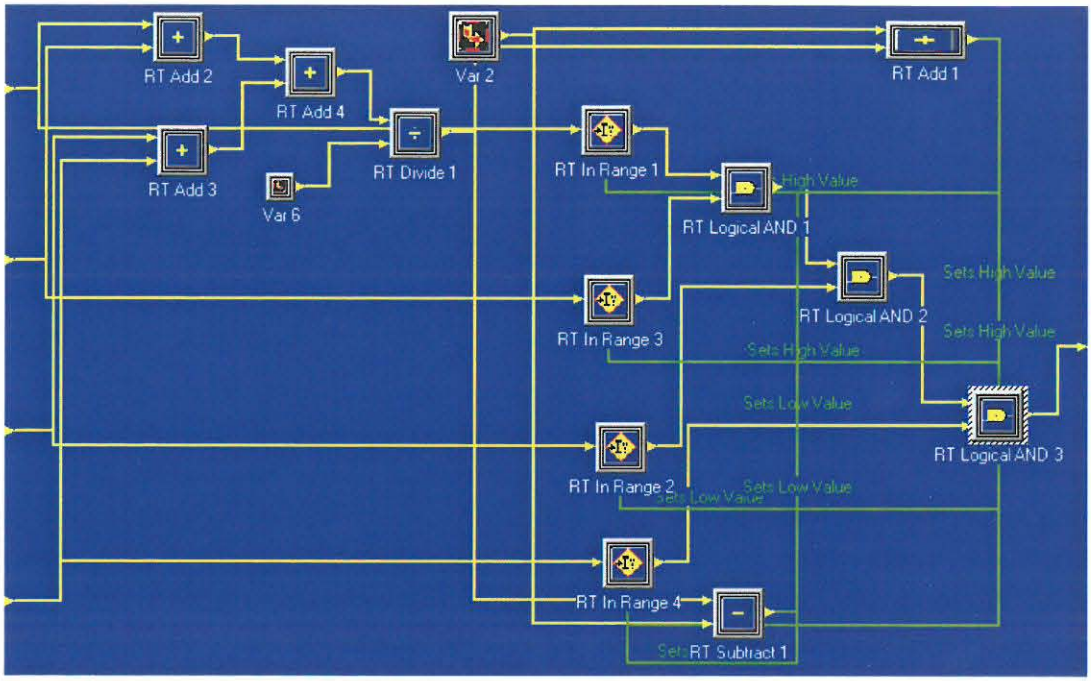

Figure 5.22: Distances in range or not?

The last block in Figure 5.18 is the "present or not" block[12]. The detail of this specific block is presented by the three inputs in Figure 5.23. The top input is the output of Figure 5.22 and is an indication that the maximum values of four consecutive frames of data occurred within a predetermined range. The middle input comes from the maximum value output in the maximum frame block. The bottom input in Figure 5.23 comes from the bottom output of Figure 5.19 and is an indication of whether the ratio between the average of the peak values and the average of the signal values were high enough.

[12] Block 17 of block diagram in Figure 5.12

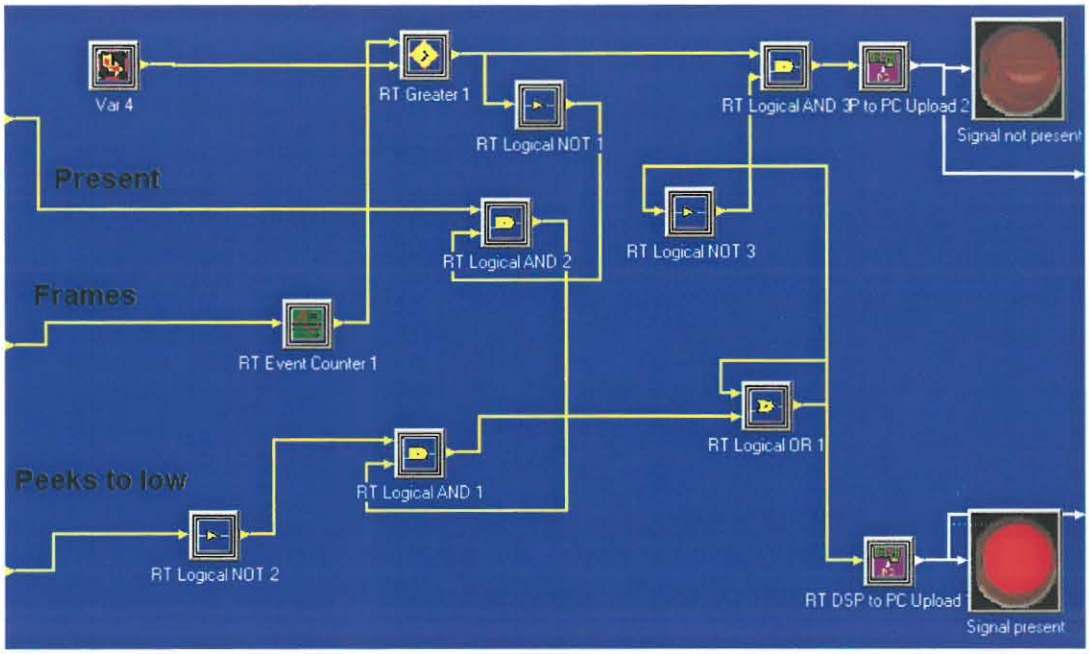

Figure 5.23: Logical decision-making process

The logical decision-making process is as follows:

The light which indicates that the signal is "*not present*" will switch on in the following circumstances:

- A number of frames have passed without the distances of the maximum values between four consecutive frames have appeared in a certain stretch or
- There is not a large enough variance between the average amplitude of the maximum values and the average amplitude of the signal values

The light which indicates that the signal is "*present*" will switch on in the following circumstances.

- A predetermined number of frames have not passed and

- The distance between the maximum values of four consecutive frames were in a specific range and

- The difference between the maximum values and the average of the signal values is sufficient.

5.3 Summary

In Chapter 5 the filter method was simulated with the aid of MathCAD and implemented in the DSP hardware. The DSP hardware which was used for the implementation of the filter method is the TMS320c6711 DSP development card of Texas Instruments (TI). The input data was obtained from pregnant Dorper ewes and a Doppler instrument was used to sample the data.

In the simulation a known level of noise was added to the signal. The signal is filtered with a six to 14 Hz band pass filter, of which the pass band has been determined experimentally. Thereafter the absolute value of the signal was determined and filtered with a delay filter. The maximum magnitude of the frequency components between 0.5 and 4 Hz was determined. Only frequency components with amplitudes of higher than 75% of the maximum values were selected. If present, the fetal heartbeat can then be observed in the selected frequency spectrum.

During the implementation of the DSP hardware noise was added to the system. A FIR band pass filter with a pass band of between six and 14 Hz was applied to the signal. Thereafter the absolute value of the filtered signal was determined. A delay filter, of which the delay was determined in the MathCAD simulation of the system, was implemented. In order to determine if the fetal heartbeat was

present or not, the distance between the different peaks of the filtered signal was determined. If this distance fell within a certain range then, with reasonable certainty, it could be assumed that the fetal heartbeat was present.

6 Autocorrelation method

6.1 Autocorrelation

Autocorrelation is generally used for identifying repeated patterns in noise filled signals[13]. The results which were obtained by means of the simulation of autocorrelation were compared to the results obtained from the filter method, as discussed in paragraph 5.1. A Doppler signal as obtained from a pregnant Dorper ewe, was used as input for both the simulations of the autocorrelation and the filter method. The simulation and implementation of autocorrelation as a method for identifying pregnancy in sheep is explained in this chapter.

6.2 Simulation of autocorrelation

In order to apply the principle of autocorrelation the following simulation was done. The signal $e(c)$ in Figure 6.1 obtained with the aid of a Doppler instrument[14] is a typical signal from a pregnant Dorper ewe.

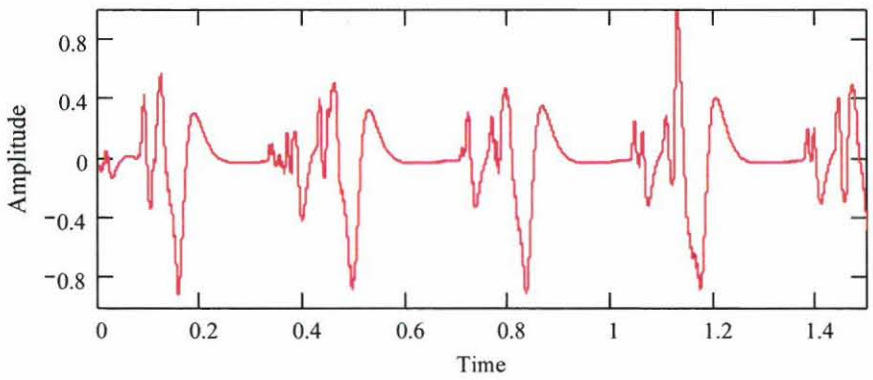

Figure 6.1: Doppler signal of the fetal heartbeat as obtained experimentally

[13] Autocorrelation is discussed in more detail in paragraph 3.3 on page 26
[14] The Doppler instrument is discussed in more detail in paragraph 4.2 on page 29

In autocorrelation a representative part of the signal is taken and then compared to the rest of the signal. Equation 6.1 shows the expression for correlation as used in this simulation:

$$d_c = \sum_w bl_w e(c+w) \qquad \textbf{6-1}$$

Where:

d_c = correlation between bl_w and $e(c)$

bl_w = part of the signal used for correlation

$e(c)$ = Doppler heartbeat signal

w = the amount of lag

As the correlation value determines the sum of the products, the places where the signals are similar will indicate the highest correlation value.

The first step in autocorrelation is to determine a suitable part of the signal to compare to the rest of the signal. As the calculation time is a function of the number of data points, care must be taken to avoid unnecessary long data sequences in the calculation of the correlation. The next step consists of taking the determined points of the signal and correlating them with the rest of the same signal.

The data points are then shifted on and again correlated with the signal. In Table 6.1 the correlation of different parts of the signal can be observed. The column on the left indicates which part of the signal is taken to correlate with the rest of the signal. In the column on the right of Table 6.1 the dotted line indicates the correlation value and the solid line indicates the signal. It can clearly be seen how the different parts of the signal's correlation varies.

In autocorrelation a representative part of the signal is taken and then compared to the rest of the signal. Equation 6.1 shows the expression for correlation as used in this simulation:

$$d_c = \sum_w b1_w e(c+w) \qquad \textbf{6-1}$$

Where:

d_c = correlation between $b1_w$ and $e(c)$

$b1_w$ = part of the signal used for correlation

$e(c)$ = Doppler heartbeat signal

w = the amount of lag

As the correlation value determines the sum of the products, the places where the signals are similar will indicate the highest correlation value.

The first step in autocorrelation is to determine a suitable part of the signal to compare to the rest of the signal. As the calculation time is a function of the number of data points, care must be taken to avoid unnecessary long data sequences in the calculation of the correlation. The next step consists of taking the determined points of the signal and correlating them with the rest of the same signal.

The data points are then shifted on and again correlated with the signal. In Table 6.1 the correlation of different parts of the signal can be observed. The column on the left indicates which part of the signal is taken to correlate with the rest of the signal. In the column on the right of Table 6.1 the dotted line indicates the correlation value and the solid line indicates the signal. It can clearly be seen how the different parts of the signal's correlation varies.

Table 6.1: Correlation of two different representative sections of the signal with the rest of the signal

Representative part of signal	Correlation with representative part of signal (top), original signal (bottom)
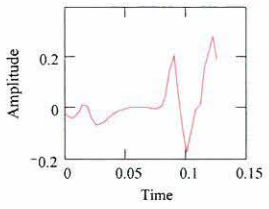	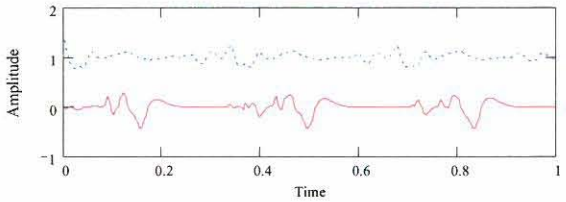
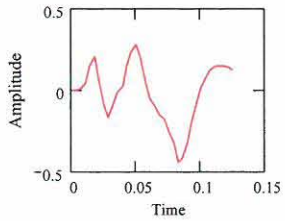	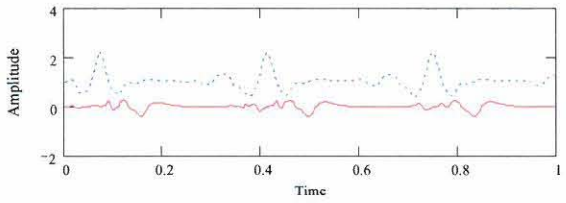

The correlation values can be written in a matrix and be presented three dimensional as in Figure 6.2. The peaks in Figure 6.2 indicate places of maximum correlation. Each point in the matrix has been set by the correlation between the original signal and part of the original signal. Thus the preferred reference signal with the largest correlation can be determined.

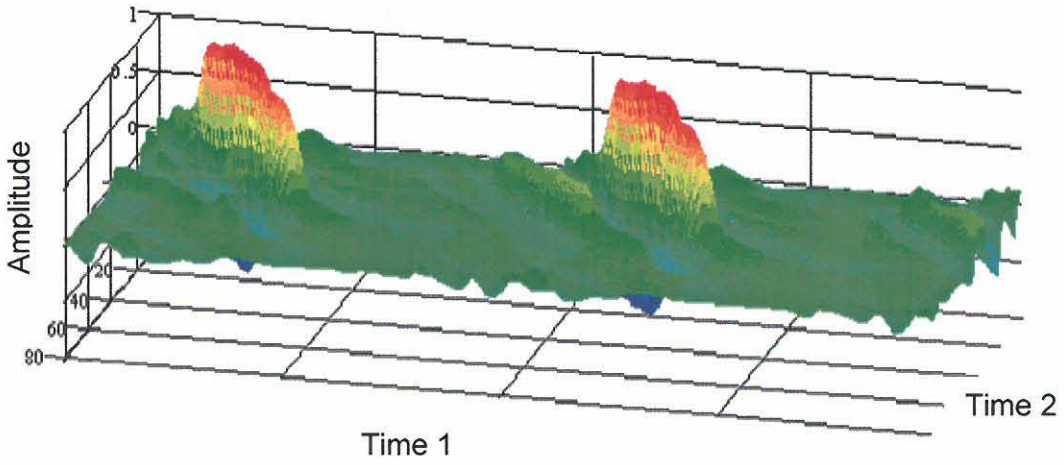

Figure 6.2: Correlation between different parts of the Doppler signal and the rest op the signal

Time 1 in Figure 6.2 indicates the position of the correlation of a specific part of the signal and time 2 indicates the number of the part of the signal that is correlated. The part of the signal indicating the highest correlation can be used to correlate with the rest of the signal. As an example the signal in Figure 6.4 is part of the Doppler signal in Figure 6.3 which best correlates with the original signal.

The original signal in Figure 6.3 is indicated by the solid line, while the correlation between the original signal and the signal in Figure 6.4 is indicated by the dotted line. The peaks which appear in the dotted line are an indication of the maximum correlation at a specific time in the signal. The correlation peaks appear at the frequency of the fetal heartbeat and it is an indication of the presence of the fetal heartbeat.

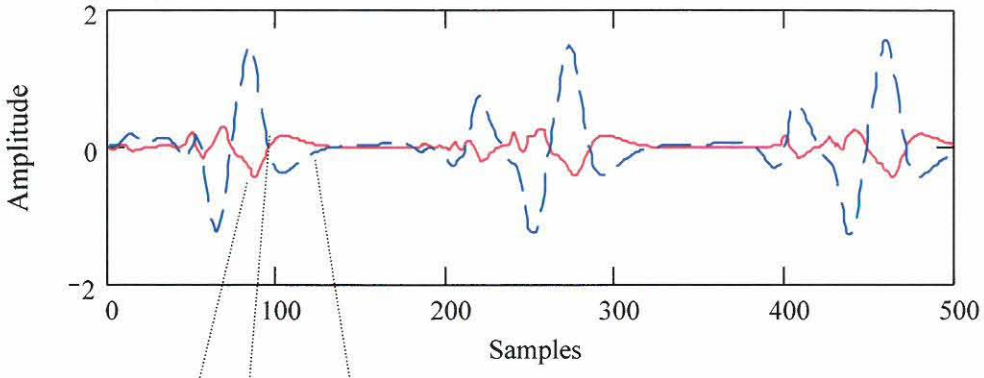

Figure 6.3: Original heartbeat signal (—) and correlation with Figure 6.4 (---)

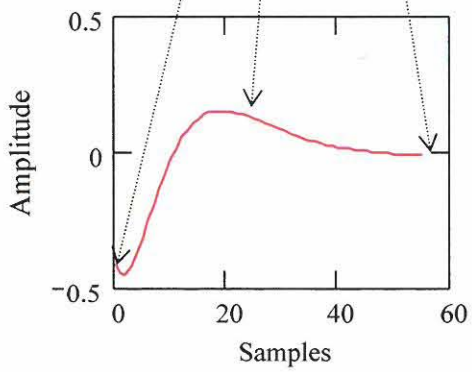

Figure 6.4 Part of the signal which is correlated with the rest of the signal

6.3 Implementation of autocorrelation in DSP hardware

Figure 6.5 indicates a block diagram presentation of the implementation of autocorrelation in DSP hardware. The prerecorded audio signal was converted to text format for the input of the DSP implementation[15]. The sampling frequency that was used for DSP implementation was 100 Hz and the data blocks[16] consisted of 40 samples each. In order to evaluate the system at different signal-

[15] Block 1 of block diagram in Figure 6.5
[16] The choice of block sizes is discussed in paragraaf 5.2

noise-ratios the ideal signal was taken through an adjustable amplifier before the noise was added[17].

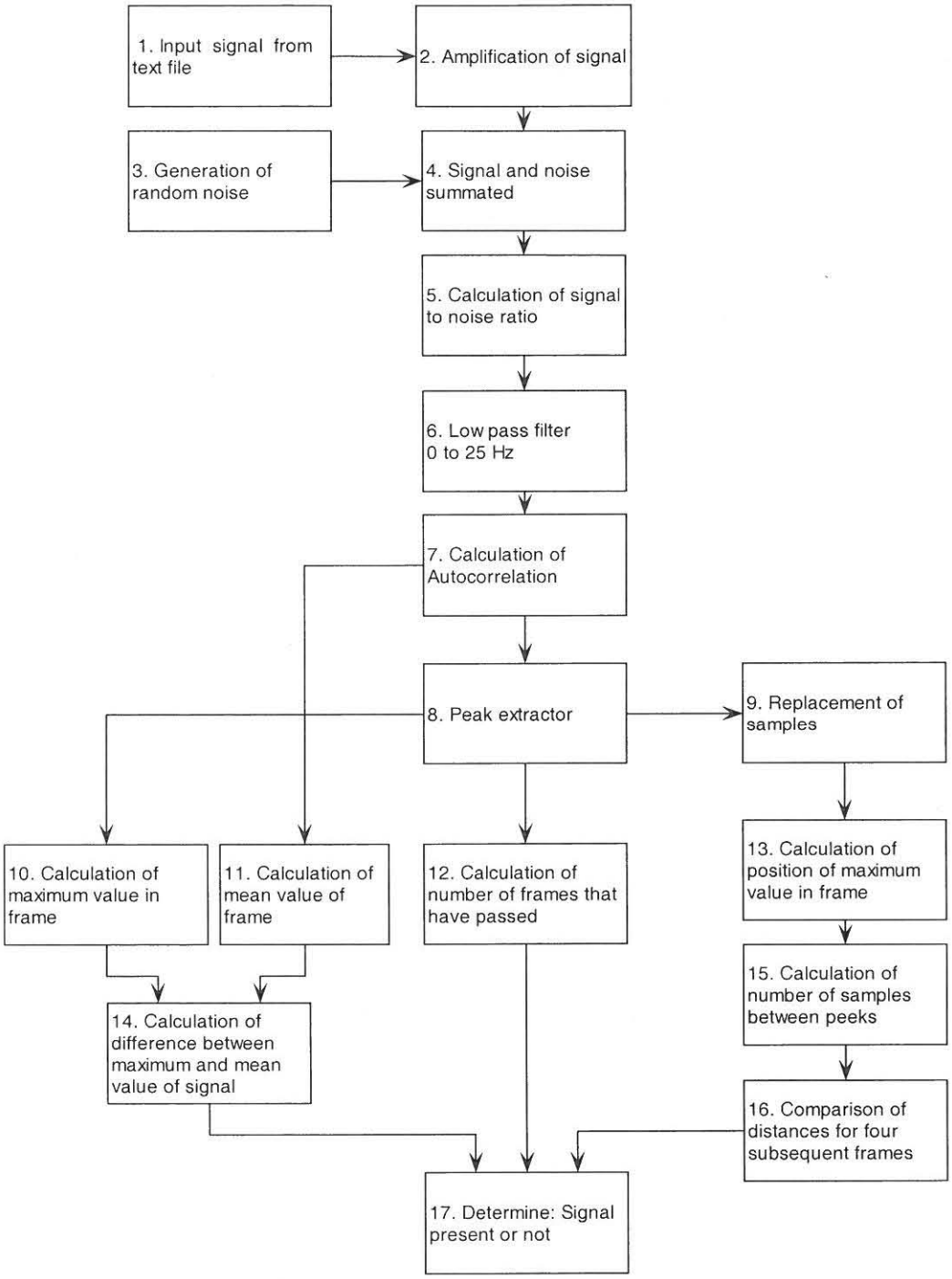

Figure 6.5: Implementation block diagram of autocorrelation in DSP hardware

[17] Block 2 of block diagram in Figure 6.5

In Figure 6.6 the heartbeat signal as well as the noise can be seen.

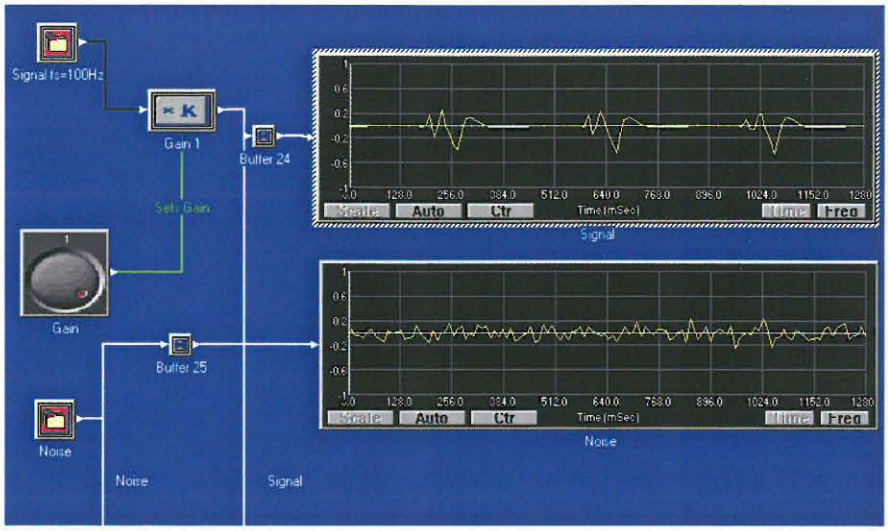

Figure 6.6: Input stage of DSP implementation

The calculation of the SNR was done in the DSP hardware and the result was uploaded to the host computer, where it was displayed in dB on the screen.[18]. The calculation of the SNR is as indicated in Figure 5.14 and discussed in paragraph 5.2.

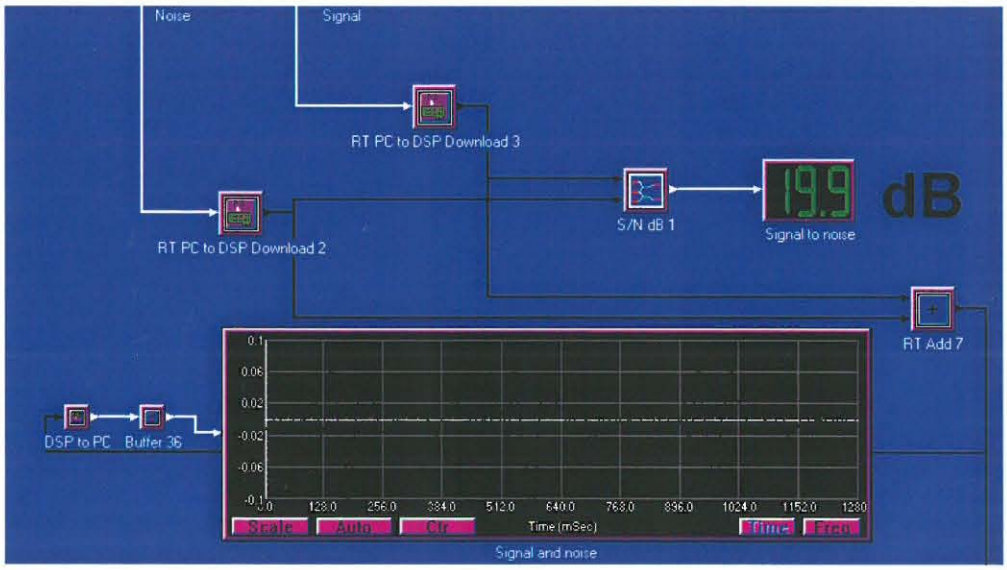

Figure 6.7: Summated signal and noise values

[18] Block 5 of block diagram in Figure 6.5

The next step in the implementation consists of a 25 Hz low pass filter[19]. An FIR filter, of which the 32 coefficients were calculated in MathCAD, was used. The coefficients of the FIR filter are indicated in Figure 6.8. The determined coefficients were taken and stored as a text file on the host computer, after which it was loaded onto the DSP hardware.

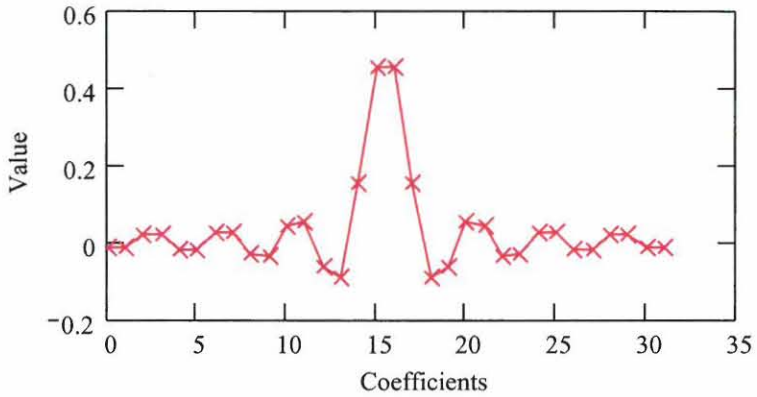

Figure 6.8: The 32 coefficients of the 25 Hz low pass finite impulse response (FIR) filter

After the signal was filtered through the 25 Hz low pass filter the following autocorrelation function was applied[20].

$$R(d) = \sum_{i=0..framesize} x(i) \cdot x(i-d) \qquad \textbf{6-2}$$

Where:

R = auto correlation

i = 0 to frame size

d = lag or time shift

In order to observe the maximum correlation points more clearly, a signal was fed into the peak detector block[21]. The function of the peak detector block was to

[19] Block 6 of block diagram in Figure 6.5
[20] Block 7 of block diagram in Figure 6.5

determine the maximum correlation value which appeared in a specific frame. The output of the block is the maximum value of the concerned block as well as the position where the maximum value appears in the frame. The position of the maximum value is the input for the replace sample block[22]. The function of the replace sample block is to replace a specific sample in the input data block with a specific value.

The input of the replace sample block which is shown in Figure 6.9 is as follows:

- The top input of the signal of which a certain sample must be replaced;
- The middle input is the determined value with which the specified sample has to be replaced and
- The bottom input is the position of the sample which has to be replaced.

The position of the maximum value[23] in a certain frame is determined and is replaced with a relative high value (Figure 6.9). The point of maximum correlation can thus be observed in Figure 6.9.

[21] Block 8 of block diagram in Figure 6.5
[22] Block 9 of block diagram in Figure 6.5
[23] The maximum value is the point in the frame where the correlation is at its peak

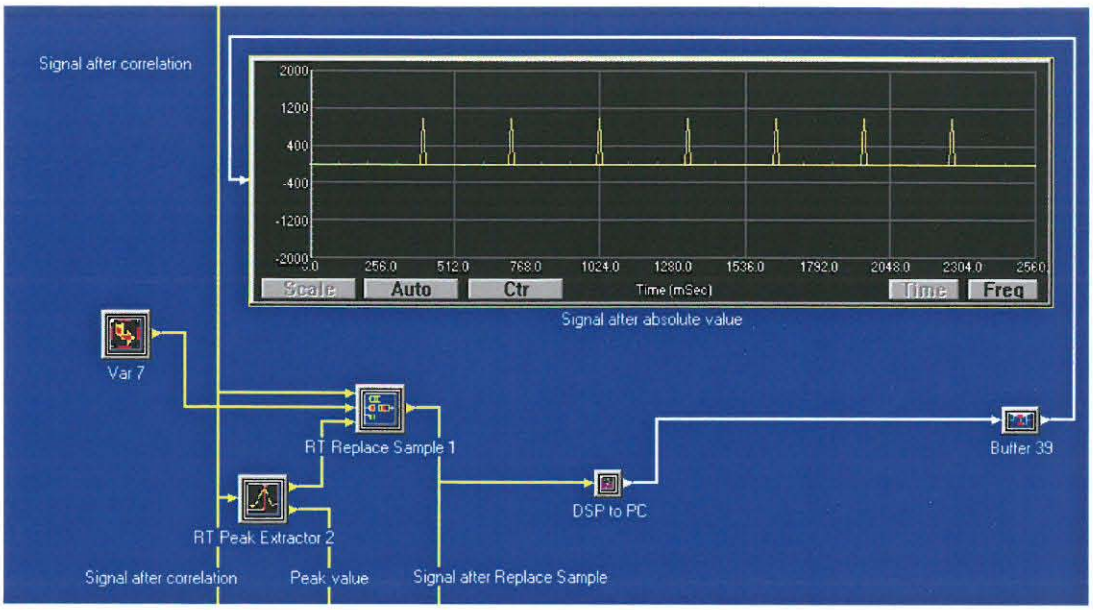

Figure 6.9: Points of maximum correlation

After autocorrelation was applied, the data was broken up into blocks. Each block consists of 40 samples[24]. The maximum value in the block of data as well as the distance or the number of samples between the maximum values of the consecutive blocks was calculated. The process is repeated for four blocks and in every case the distance between the maximum values is determined. The number of samples which appear between the consecutive blocks are now compared to determine what the difference in distance is between the maximum values.

As soon as the distance between peaks falls within a certain frame, it is an indication that the fetal heartbeat is present.

[24] The number of samples per block is discussed in paragraph 5.2

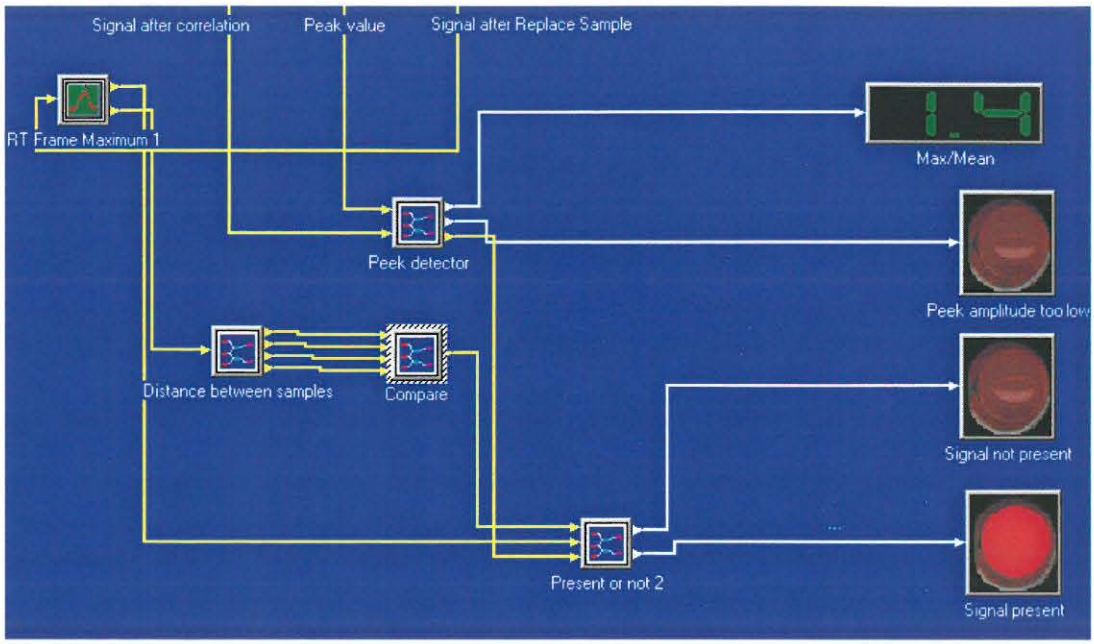

Figure 6.10: Decision-taking on whether the heartbeat is present or not

These comparisons, of where the positions of the peaks appear in the consecutive data blocks which indicate maximum correlation, is only done for a specified number of input blocks. Thereafter a decision has to be taken as to whether the fetal heartbeat is present or not.

The operation of the different blocks in Figure 6.10 is discussed in paragraph 5.2.1.

6.4 Summary

In Chapter 6 autocorrelation is simulated with the aid of MathCAD and implemented in the DSP hardware. The DSP hardware which was used for the development of the autocorrelation system is the TMS320c6711 DSP development card of Texas Instruments (TI).

The input data was obtained from pregnant Dorper ewes and a Doppler instrument was used to sample the data.

In the simulation parts of the signal which correlated best with the rest of the signal were determined. The correlation values between the chosen parts and the rest of the signal were then determined.

With the implementation in the DSP hardware different levels of noise was added to the system. The autocorrelation function was applied to the signal and the point of maximum correlation was determined. In order to determine as to whether the fetal heartbeat was present or not, the distance between the points of maximum correlation was determined. If the distance fell within a certain range it could with reasonable certainty be assumed that the fetal heartbeat was present.

7 Results

7.1 Introduction

In this chapter the results that were obtained from the simulations of the different methods on which the ultrasonic Doppler signal was analysed, are discussed. These results lead to the implementation of the filter as well as the autocorrelation methods in DSP hardware. Simulations of both methods were done with real data as input in MathCAD after which the systems were implemented in DSP hardware. The evaluation of the DSP implemented systems is also discussed in this chapter.

The evaluation consisted of the following:

- Identifying and constructing an ideal signal;
- The evaluation of simulations of the autocorrelation and the filter method and
- The evaluation of the DSP implementation of autocorrelation and the filter method.

In Figure 7.1 the different stages of the evaluation process are indicated.

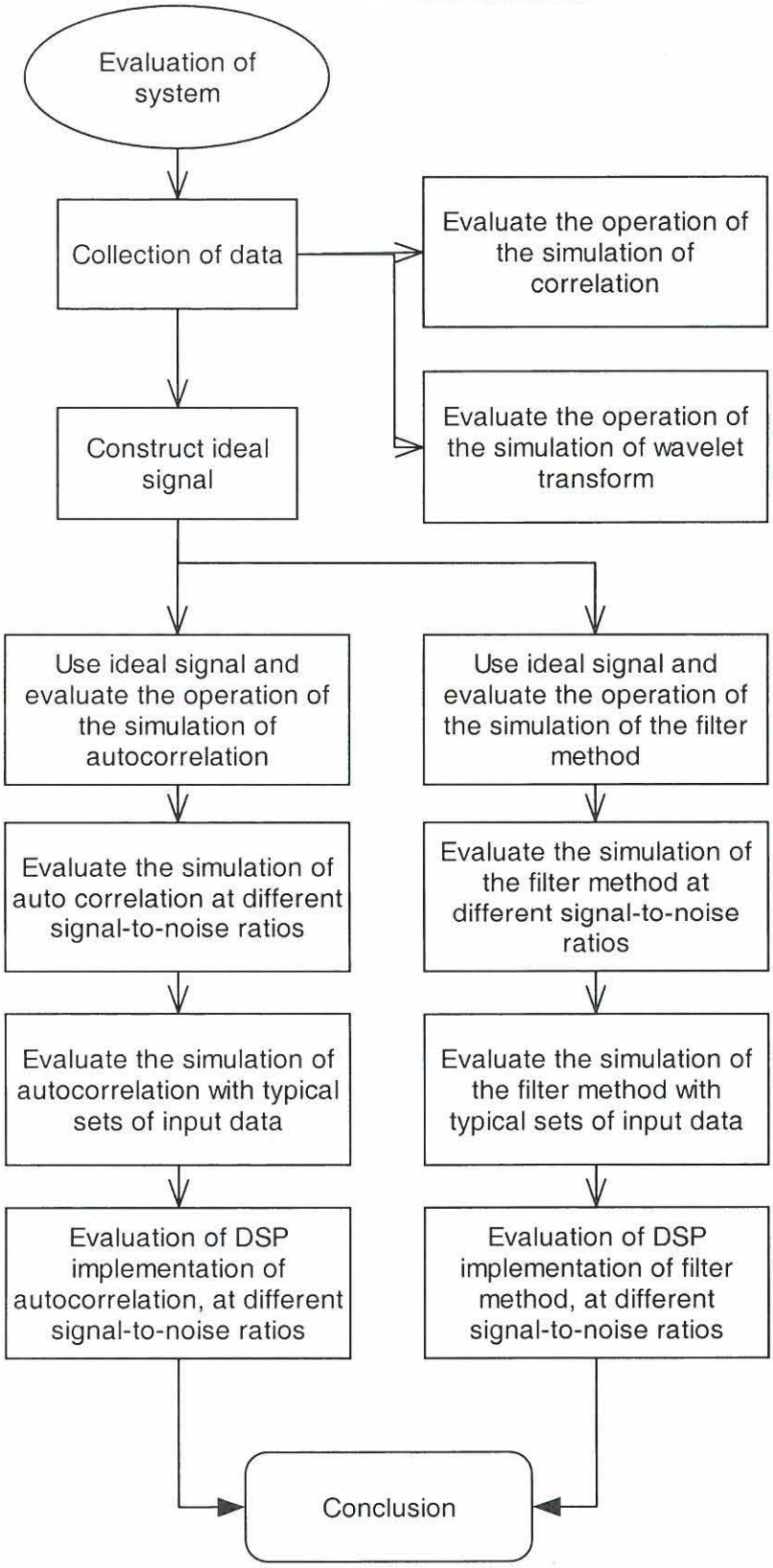

Figure 7.1: Stages of the evaluation process

7.2 Evaluation of the simulations with an ideal signal as input

The first step in the evaluation of the simulations was to take only the ideal signal without any noise as input for the simulations. An ideal signal was generated by taking all the measured data and identifying a single fetal heart beat which was the least influenced by the noise and contained all the characteristics of a heart beat[25]. The heart beat was then taken and duplicated to form an ideal signal.

7.3 Evaluation of the simulation of autocorrelation

During the evaluation of the autocorrelation method the ideal signal was taken as input and afterwards polluted by different levels of noise. The noise was added in order to determine at which SNR the autocorrelation method could still function satisfactorily. In Table 7.1 the output of the simulation of the autocorrelation method is indicated at different SNR's.

[25] The identification of the ideal signal is discussed in more detail in paragraph 8.2 on page 79.

Table 7.1: Output of simulation of autocorrelation method at different SNR's

SNR in dB	Output of autocorrelation method (top), ideal signal (middle) and ideal signal with noise (bottom)
No noise	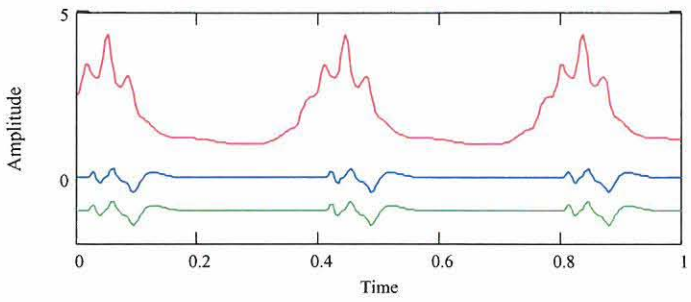
-3 dB	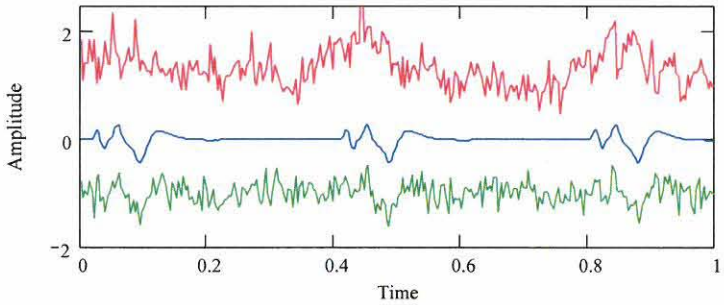
-6 dB	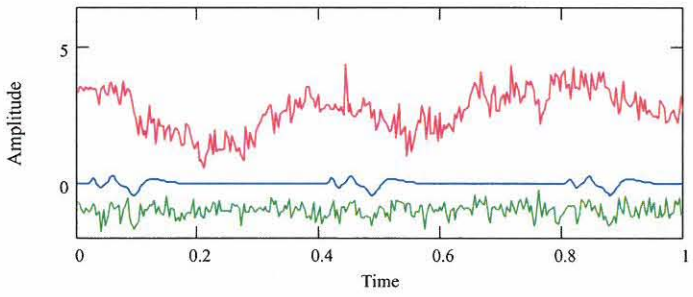
-9 dB	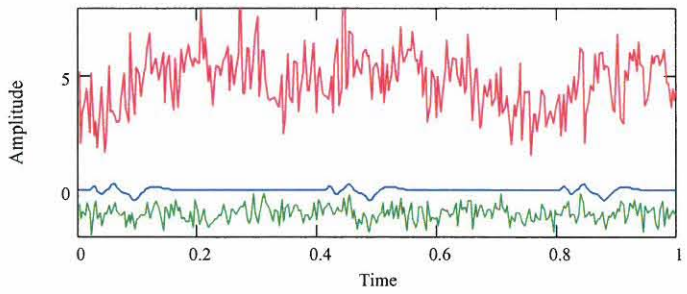

A further evaluation of the simulation of the autocorrelation method was done by taking different measured signals and using them as input for the system. These measured Doppler signals were divided into three groups:

- Group A consisted of signals with a high quality and is represented by the signal in Figure 7.2;
- Group B consists of signals where the influence of the noise is considerable but the presence of the heart beat can stil be detected with the use of autocorrelation. Group B is represented in Figure 7.3 and
- Group C consists of signals with a high noise level and is represented in Figure 7.4.

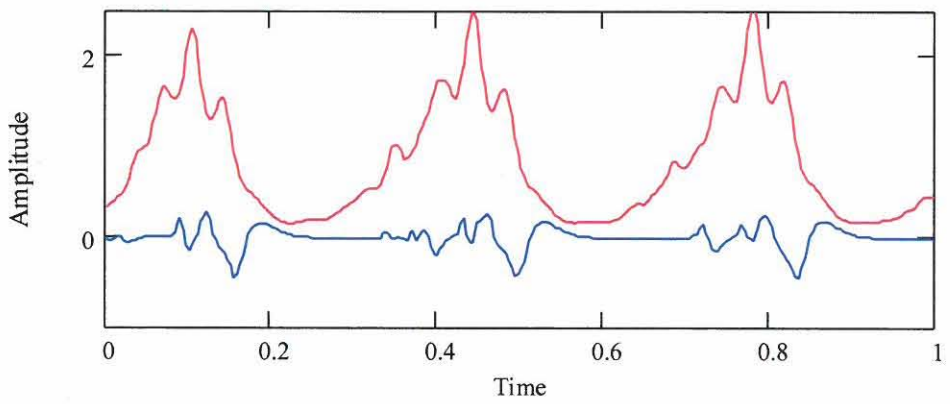

Figure 7.2: Typical signal in group A (bottom) and output of the autocorrelation method (top)

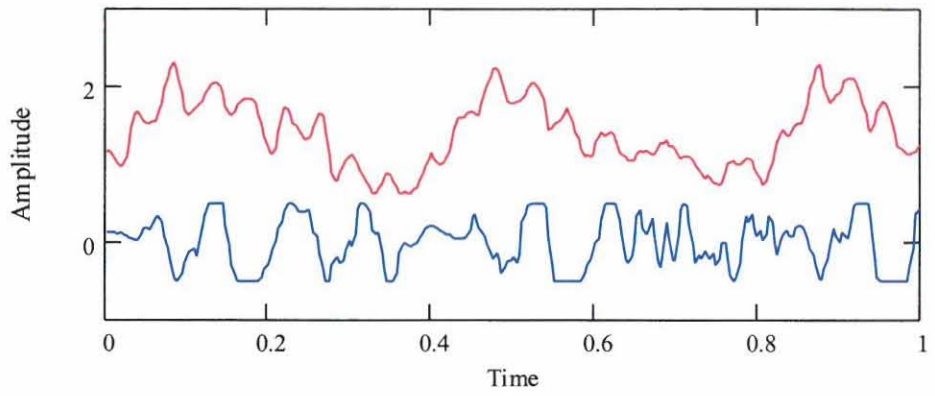

Figure 7.3: Typical signal in group B (bottom) and output of the autocorrelation method (top)

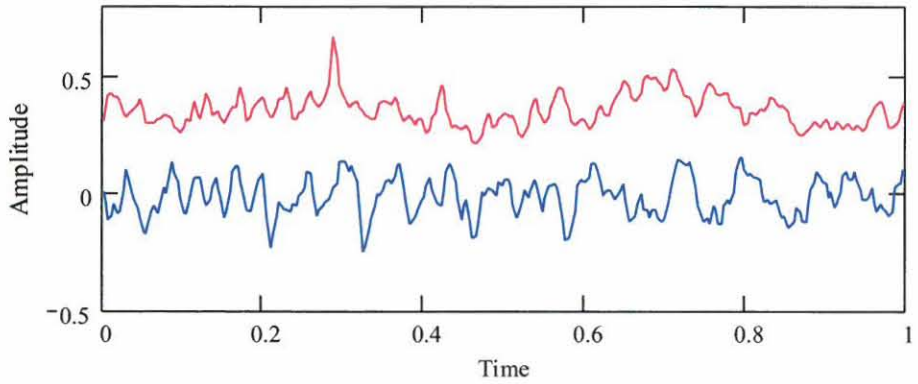

Figure 7.4: Typical signal in group C (bottom) and output of the autocorrelation method (top)

7.4 Evaluation of the simulation of the filter method

In order to evaluate the process of the simulation of the filter method, the ideal signal was used as input for the simulation. Different levels of noise were added to the signal in order to determine at which signal-to-noise levels the fetal heart beat could stil be recovered successfully.

Table 7.2: Output of filter method at different SNR's

SNR in dB	Output of filter method (top), ideal signal (middle) and ideal signal with noise (bottom)
No noise	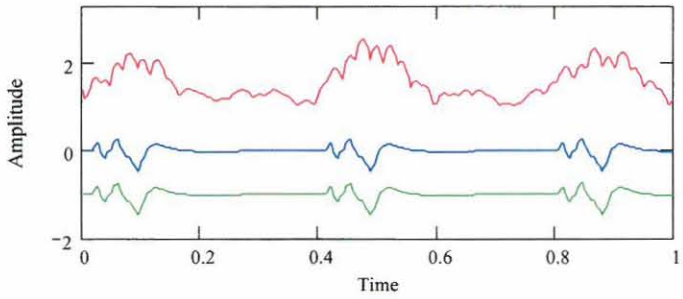
-3 dB	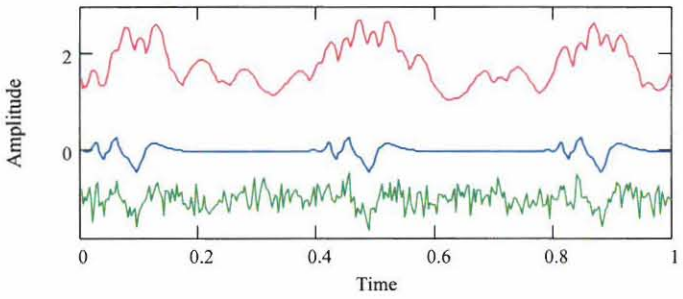
-6 dB	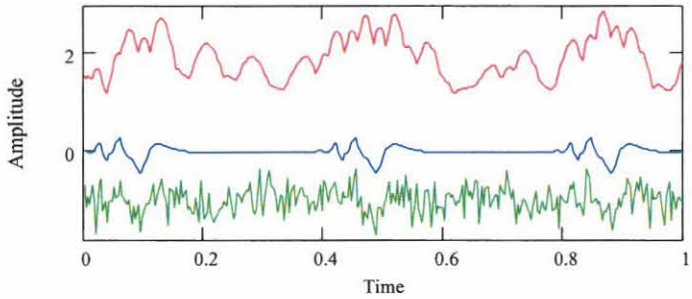
-9 dB	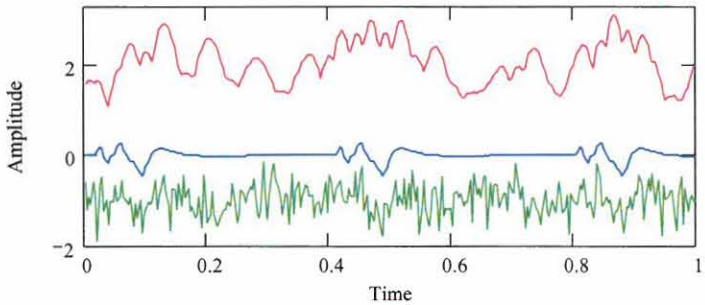

Similar to the autocorrelation method, a further evaluation of the simulation of the filter method was done by using the typical measured signals as input.

These typical Doppler signals were as follow:

- Group A consisted of signals of a high quality and are presented in Figure 7.5;
- Group B consists of signals where the influence of the noise is considerable but the presence of the heart beat can stil be detected with the use of the filter method. Group B is represented in Figure 7.6.
- Group C consists of signals with a large noise component and is represented in Figure 7.7.

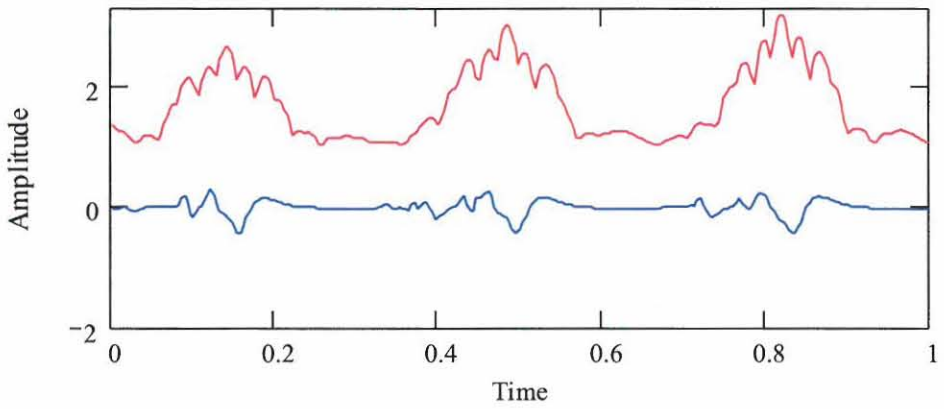

Figure 7.5: Typical signal in group A[26] (bottom) and output of the filter method (top)

[26] As defined in paragraph 7.3

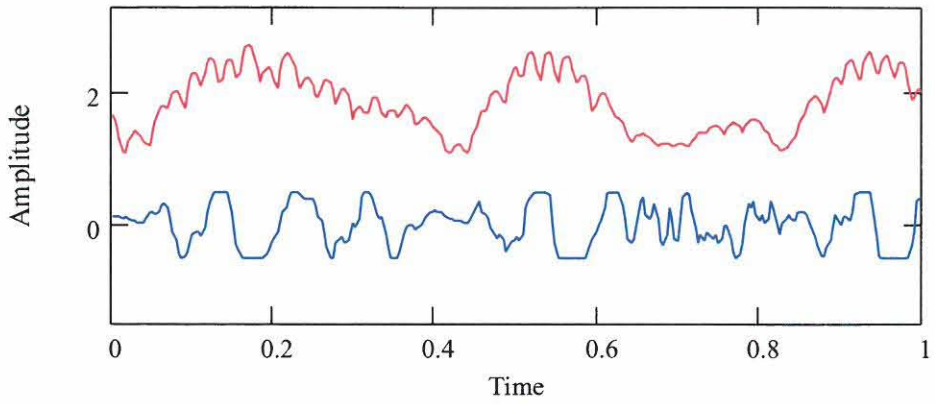

Figure 7.6: Typical signal in group B[27] (bottom) and output of the filter method (top)

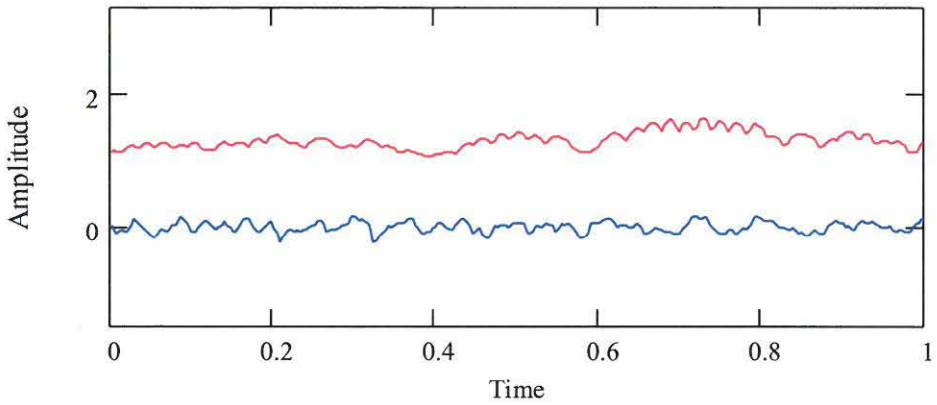

Figure 7.7: Typical signal in group C[28] (bottom) and output of the filter method (top)

7.5 Evaluation of the simulation of the Wavelet transformations

In order to have a better understanding of the frequency spectrum which is present in the Doppler signal and exactly at what time the different frequencies

[27] As defined in paragraph 7.3
[28] As defined in paragraph 7.3

are present, wavelet transformations were used. The signal in Figure 7.8 was used as input for the simulations and the output of the wavelet transform is indicated in Figure 7.9. Although wavelet transformations were not used in the final DSP implementation, insights gained, led to the development of the filter method.

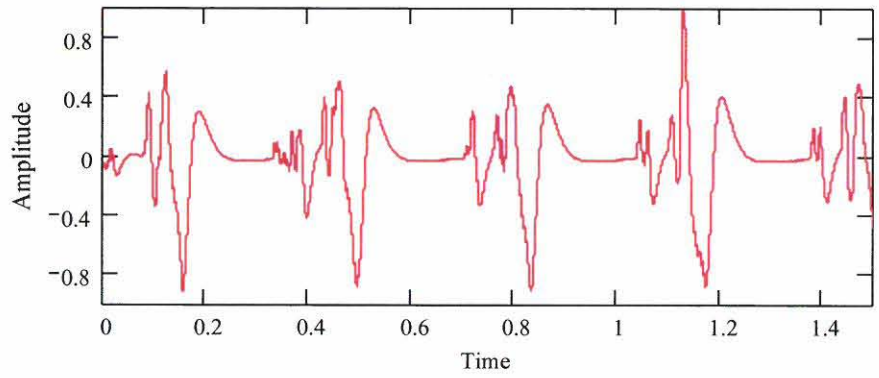

Figure 7.8: Measured Doppler signal of fetal heartbeat

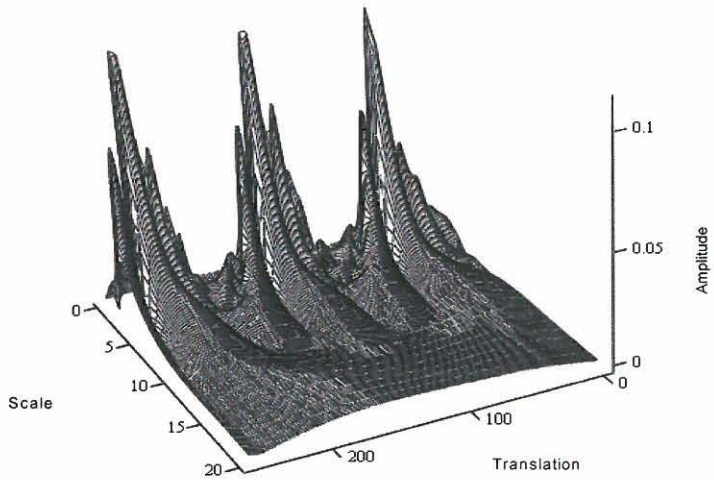

Figure 7.9: Output of simulation of wavelet transform with signal in Figure 7.8 as input

7.6 Evaluation of the systems as implemented in the DSP hardware

In order to evaluate the DSP implementation the perfect signal was used as input. Thereafter different levels of noise were added to the signal. The DSP implemented systems of the filter as well as the autocorrelation method had three output indications, namely:

- The first output was an indication that the relative amplitude of the signal was too low;
- The second output became active when the heartbeat was not present and
- The third output was active if the heartbeat was present.

The criteria on which these decisions were taken, are discussed in paragraph 5.2.1 for the filter method and in paragraph 6.3 for the autocorrelation method.

With a SNR of -8 dB the DSP implemented filter method could still indicate the fetal heartbeat. With the use of the autocorrelation method the presence of the signal could be identified up to a SNR of -6.5 dB.

8 Conclusion

8.1 Introduction

In this study the filter as well as the autocorrelation methods were chosen for implementation in DSP hardware. This chapter consists of the conclusions that were drawn during the analysis of the ultrasonic Doppler signal and the investigation of the different methods of implementation.

8.2 Ideal signal

In order to evaluate the system an ideal signal was generated. Figure 8.1 is part of the measured signal which was selected on grounds of correlation with a typical heartbeat signal. Figure 8.2 indicates a typical heartbeat signal. The P-part of the signal is formed because of the atrial de-polarisation, the Q-H-S part is present as result of the ventricular de-polarisation and the T-part is formed because of the ventricular re-polarisation. From the above-mentioned it can be concluded that the signal in Figure 8.1 is the fetal heartbeat. This conclusion is further supported by the fact that the frequency of the pulse, correlates with the expected frequency against which the fetal heartbeat appears, namely 2 to 3 Hz. This frequency is considerably higher than the heartbeat of the mother which appears at approximately 1 Hz.

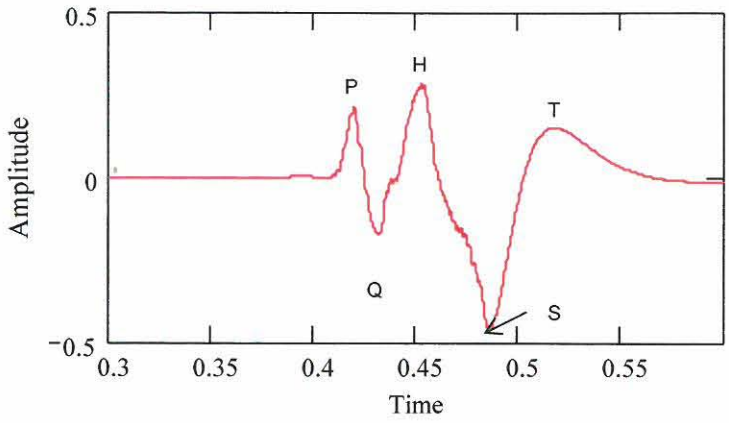

Figure 8.1: Part of measured signal that was chosen to form the ideal signal

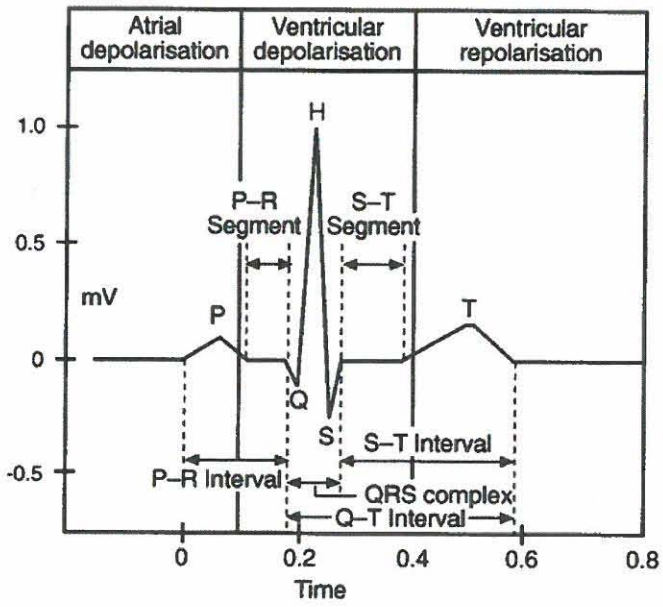

Figure 8.2: Theoretical form of a typical heartbeat signal [14, p. 34]

8.3 Filter and autocorrelation methods

In Figure 8.3 the performance of the simulations of the filter and the autocorrelation methods are compared. From the first set of outputs, which had the noiseless ideal signal as input, the presence of the fetal heartbeat could be clearly observed on the filter as well as in the autocorrelation method. At the next

two sets of outputs, respectively at -3 and -6 dB the influence of the increasing noise can be observed. It was still possible in both methods, to identify the fetal heartbeat. The last sets of outputs in Figure 8.3 are the outputs of the simulations at the SNR of -9 dB. Although the presence of the fetal heartbeat in the filter method is identifiable, uncertainty exists.

In the output of the autocorrelation method the presence of the fetal heartbeat, against a SNR of -9 dB could not be observed. With a SNR of -8.5 dB for the simulation of the filter method and with a SNR of -7 dB for the simulation of the autocorrelation method the heartbeat could be identified. From the above-mentioned results of the simulations of the filter and the autocorrelation methods it can be concluded that both methods are suitable for DSP implementation and the successful identification of fetal heart beat.

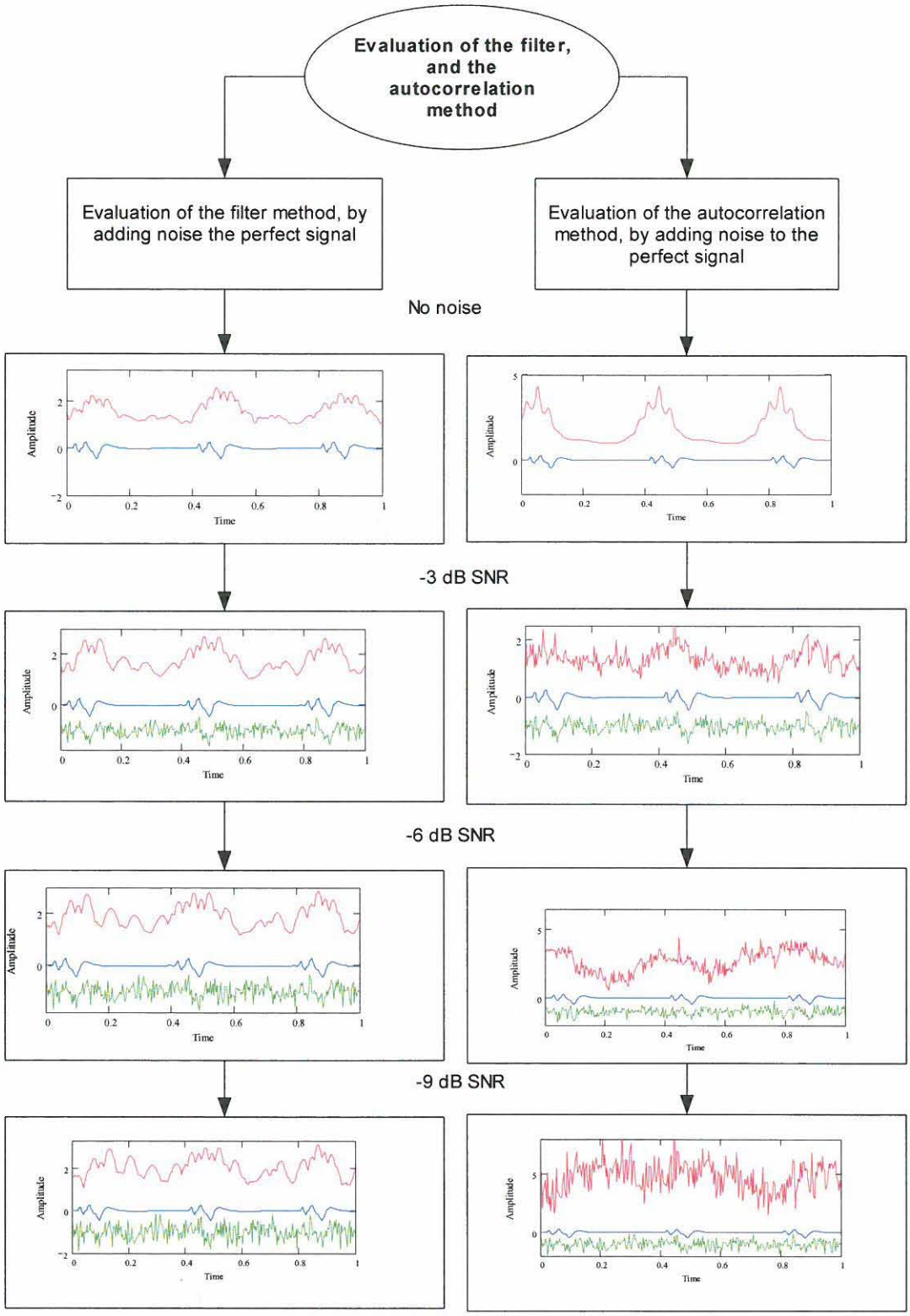

Figure 8.3: Results of simulations of the filter and the autocorrelation methods, against different SNR's

A further method of evaluation was to take typical measured signals as input for the simulations. Three groups[29] of signals were identified and used as inputs for the simulations of both methods. Figure 8.4 gives an indication of the output of the simulations with different typical signals as input. From Figure 8.4 it can be concluded that the simulations of the filter and the autocorrelation methods can successfully detect the presence of fetal heartbeat. In the case of signals from group C in Figure 8.4 the SNR was too high for any of the systems to successfully identify the presence of the fetal heartbeat.

In the DSP implementation of the autocorrelation method measured signals with a SNR of -6.5 dB was successfully identified and with the filter method the fetal heartbeat with a SNR of -8 dB was identified successfully. It can thus be concluded that both the filter and the autocorrelation method can be used successfully for the detection of the fetal heartbeat in noisy Doppler signals.

[29] As defined in paragraph 7.3

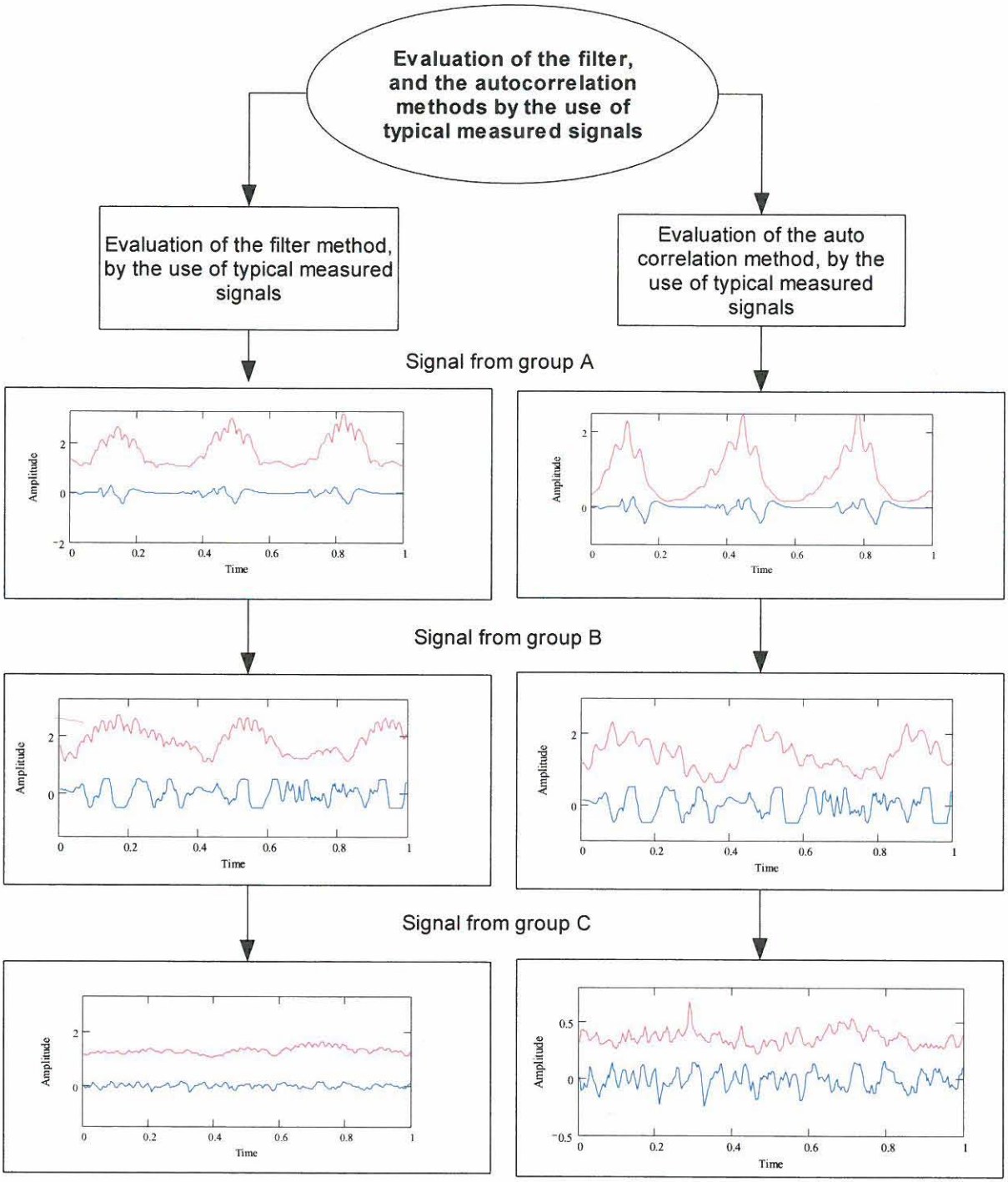

Figure 8.4: Simulation results with typical Doppler signals as input to the simulations of the filter and autocorrelation methods

8.4 Summary

The following conclusions were drawn:

- On grounds of a comparison between a part of a measured signal[30], that was used to construct the ideal signal and the theoretical[31] signal form of the fetal heart beat, it can be concluded that the concerned signal is coming from the fetal heart.

- The identification of the fetal heartbeat with typical measured signals as input to the simulations for both methods is an indication of the correct functioning of the simulations.

- With a SNR of -8.5 dB for the simulation of the filter method and with a SNR of -7 dB for the simulation of the autocorrelation method the fetal heartbeat could be identified. It can thus be concluded that both methods are suitable for DSP implementation and the successful identification of fetal heart beat.

- In the DSP implementation of the autocorrelation method ideal signals with a SNR of -6.5 dB was successfully identified and with the filter method the fetal heartbeat with a SNR of -8 dB was also identified successfully. It can thus be concluded that both the filter and the autocorrelation method can be used successfully for the detection of the fetal heartbeat in noisy ultrasonic Doppler signals.

[30] The measured signal is indicated in Figure 8.1
[31] The theoretical signal is indicated in Figure 8.2

8.5 The way forward

In this study, filter and autocorrelation methods were investigated and specific methods of implementation were developed. The knowledge gained can now be used for the development of a portable commercial unit capable of identification of pregnancy in sheep.

Appendix A

Simulation of filter method

$J := 32838$ last sample $\qquad 2^{14} = 1.638 \times 10^{4}$

$c := 0..J - 71$ sample range

signall := READPRN("c:/data/dop text files/012 s 5000.txt") signal

$signal_c := signall_c \cdot 2$ $\qquad M := 20$

$var := \frac{M}{1000}$ $\qquad no := rnorm(J, 0, \sqrt{var})$ noise

$signalnoise_c := signal_c + no_c$ noise + signal

$t_c := \frac{c}{5000}$

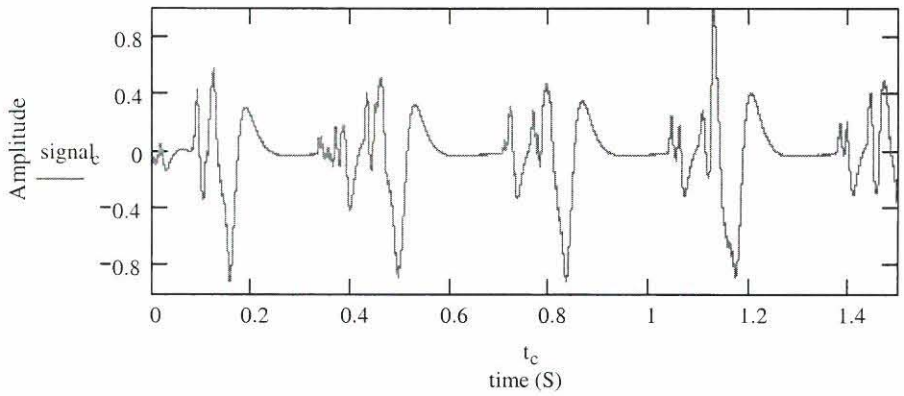

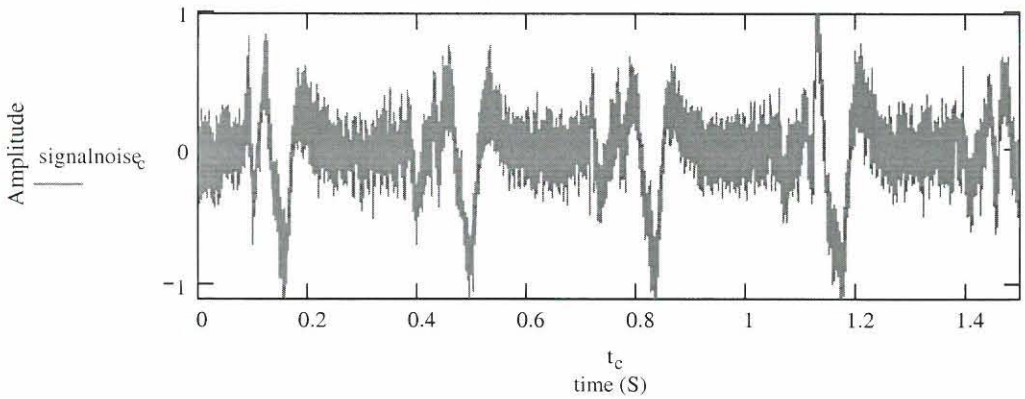

$$ensignal := \left| \sum_c |signal_c| \right| \qquad ennoise := \sum_c |no_c|$$

$$ensignal = 2.571 \times 10^3 \qquad ennoise = 3.692 \times 10^3$$

$$i := 0..M$$

$$signaltonoise_M := 10 \cdot \log\left(\frac{ensignal^2}{ennoise^2}\right)$$

$$signaltonoise_M = -3.142 \ dB$$

fft on the signal

$$a := fft(signalnoise)$$

$$N := last(a) \qquad N = 1.638 \times 10^4$$

$$j := 0..N$$

$$f_j := \frac{j}{J} \cdot 5000 \qquad t_i := \frac{i}{5000}$$

applying a FIR filter

$$filt_j := \left(if\left(6 < f_j < 14, a_j, 0\right)\right) \cdot \left(if\left(|a_j| < .1, 0, 1\right)\right)$$

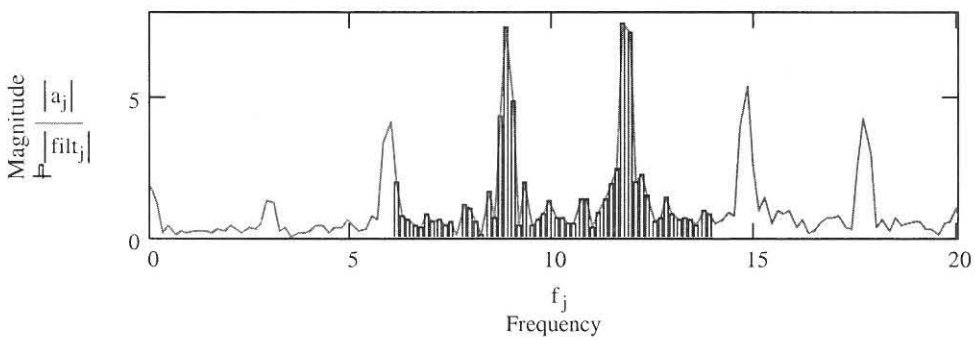

$C := ifft(filt)$

$N2 := last(C)$ $N2 = 3.277 \times 10^4$

$k := 0 .. N2$

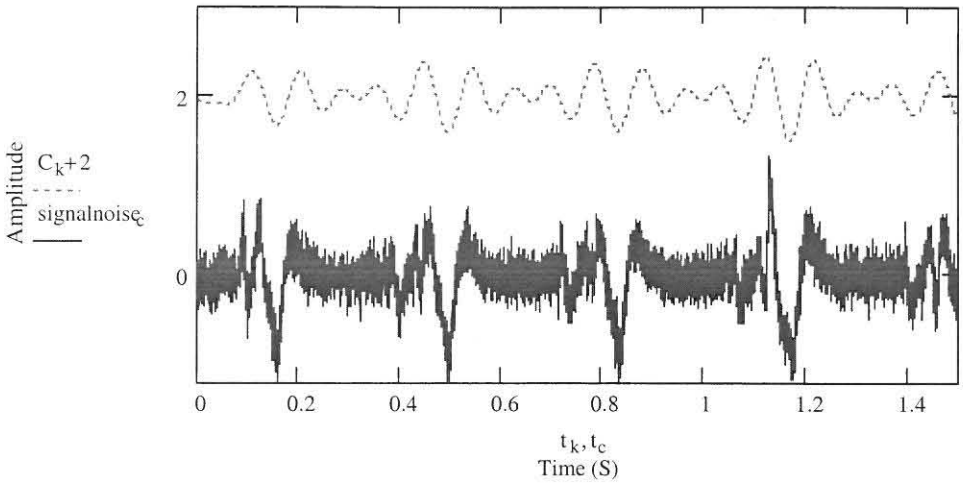

$l := 0 .. \left(2^{14} - 1\right)$ $m := 120$

$$d_l := \frac{\left(\left|C_l\right| + \left|C_{l+m}\right|\right)}{2}$$

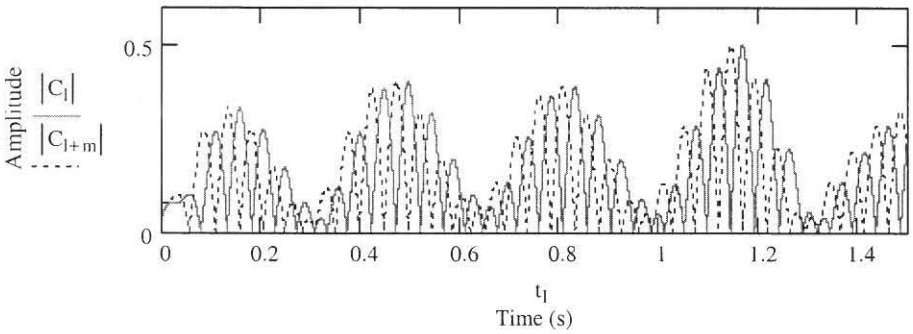

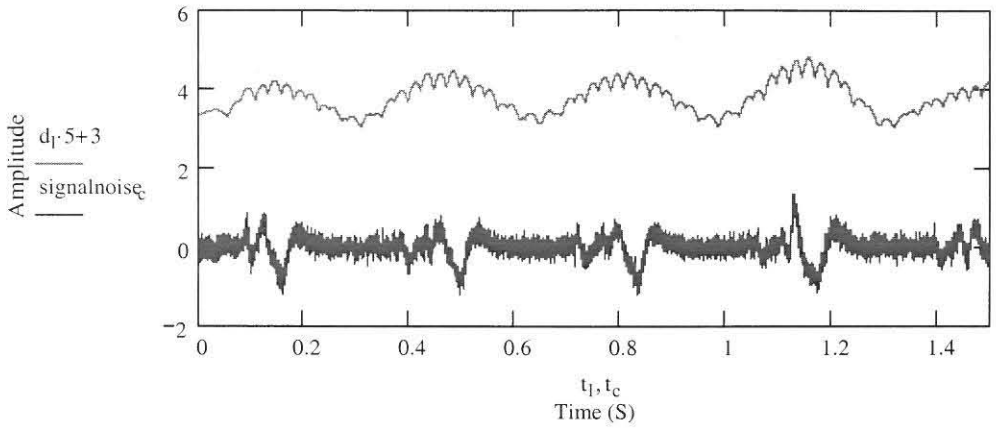

$A := \mathrm{fft}(d)$

$N := \mathrm{last}(A)$ $\quad N = 8.192 \times 10^3$

$j := 0 .. N$

$$f_j := \frac{j}{\left(2^{14} - 1\right)} \cdot 5000$$

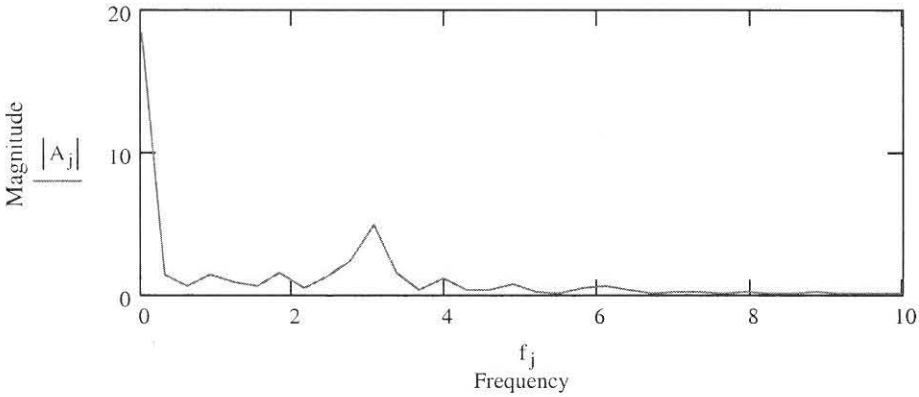

$g := 2 .. 8$ $\qquad h := 8 .. 82$

$$\frac{5}{5000} \cdot J = 32.838$$

$$Z := \frac{\left(\sum_g |A_g|\right)}{6} \qquad G := \frac{\left(\sum_h |A_h|\right)}{74} \qquad ff$$

Z = 1.073 G = 0.27

$e := if(Z > G, 1, 0)$

$e = 1$ if e=1 there is a hart beat if e=0 no beat

$filt2_j := if(0.5 < f_j < 4, A_j, 0)$

$filt2ab_j := |filt2_j|$

$filt3_j := if[filt2ab_j < (max(filt2ab)) \cdot 0.4, 0, filt2_j]$ 75%

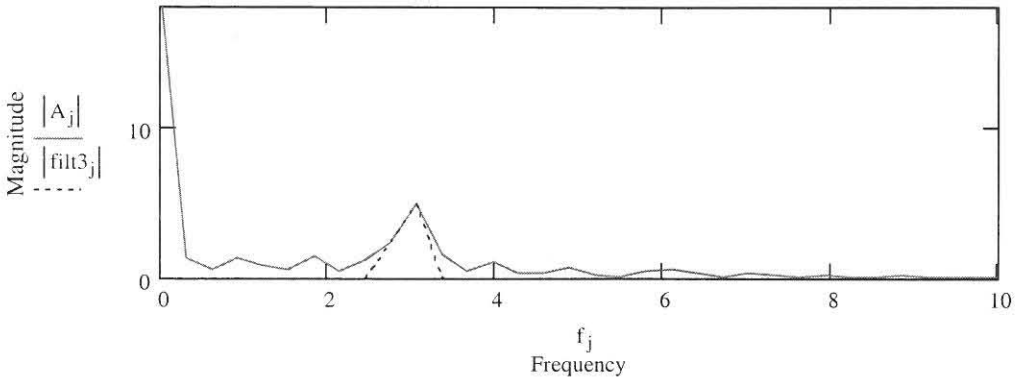

$g := ifft(filt3)$

$N2 := last(g)$ $N2 = 1.638 \times 10^4$

$k := 0..N2$

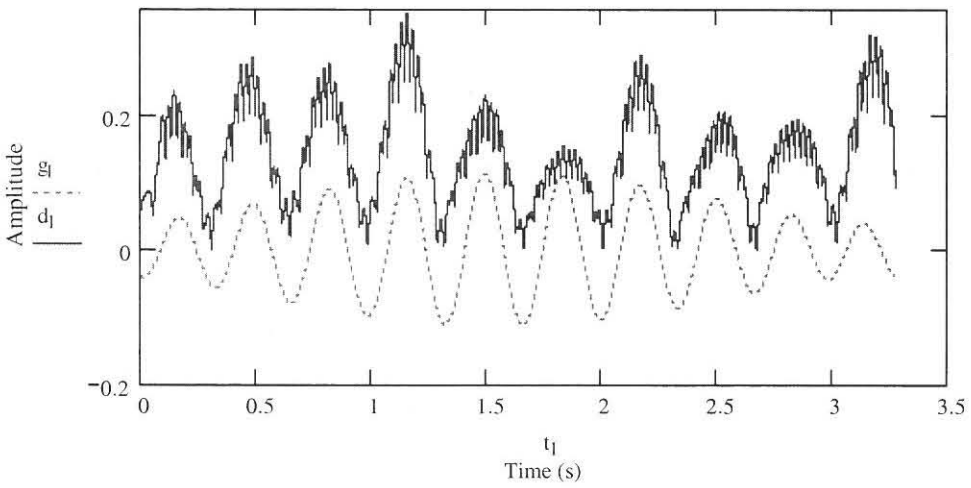

$\min(g) = -0.113$

$\text{mean}(g) = 0$

$h_l := \text{if}\left(\text{mean}(g)\cdot 0.8 < g_l, 1, 0\right)$

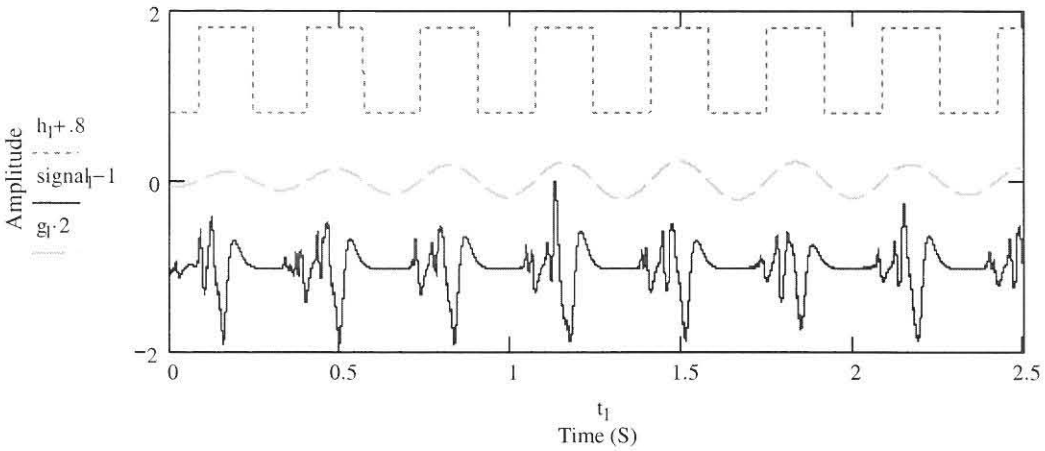

Simulation of correlation

$c := 0..35000$

$a := 95..120$

$w := 0..55$

$b := READPRN("c:data/dop\ text\ files/012\ s\ 10000.txt")$

$e(c) := b_{c \cdot 18}$ $\quad bl_w := e(w + 85)$

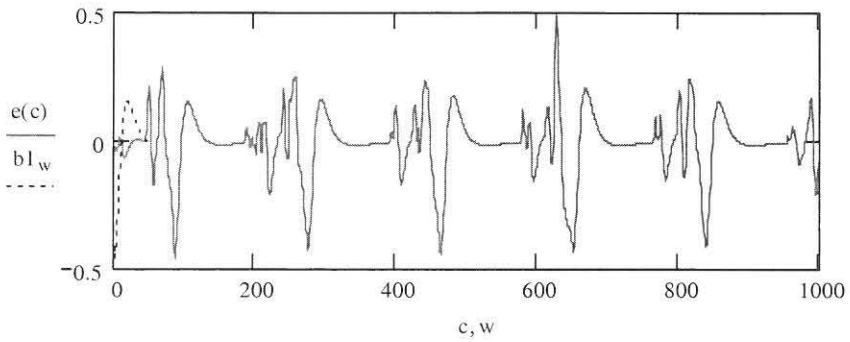

$$d_c := \sum_w bl_w \cdot e(c + w)$$

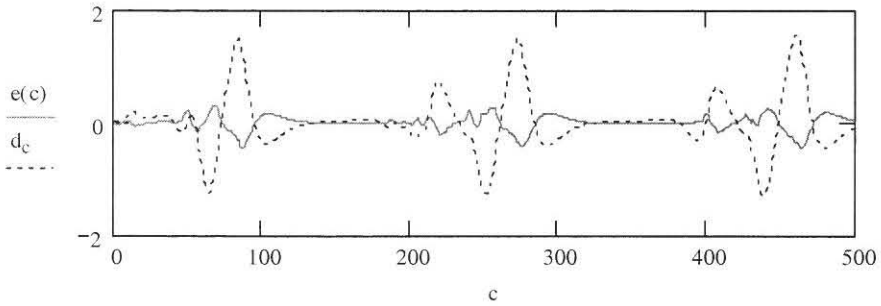

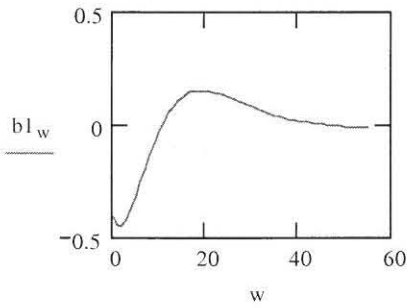

Simulation of autocorrelation

$J := 350$ $F := 127$

$c := 0..J - 71$ $w := 0..29$

signal := READPRN("H:/shared/hartklop/data/dop text files/012 perf.txt")

$M := 1$

$var := \frac{M}{1000}$ $no := rnorm(J, 0, \sqrt{var})$

$signalnoise(c) := signal_{c \cdot 18} + no_c$

$t_c := \frac{c \cdot 18}{5000}$

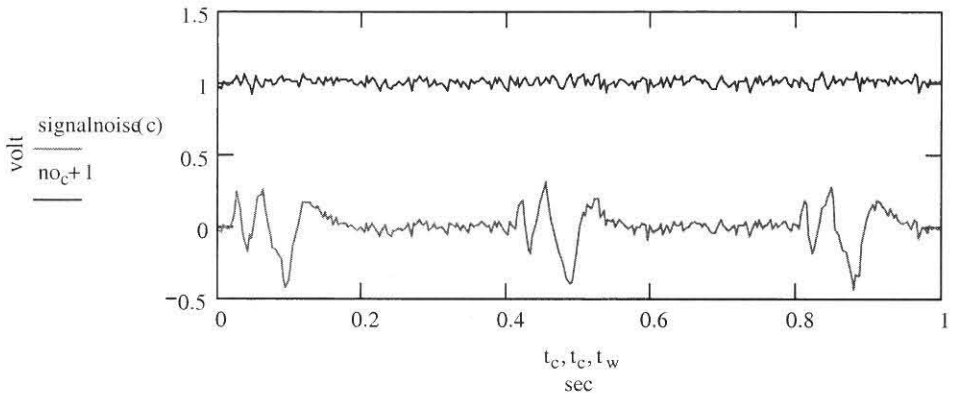

$ensignal := \left| \sum_c \left| signal_{c \cdot 18} \right| \right|$ $ennoise := \sum_c \left| no_c \right|$

ensignal = 17.604

ennoise = 6.742

$i := 0..100$

$signaltonoise_M := 10 \cdot \log\left(\frac{ensignal^2}{ennoise^2} \right)$

$signaltonoise_M = 7.8$ dB

b1(F, w) := signalnoise (w + F)

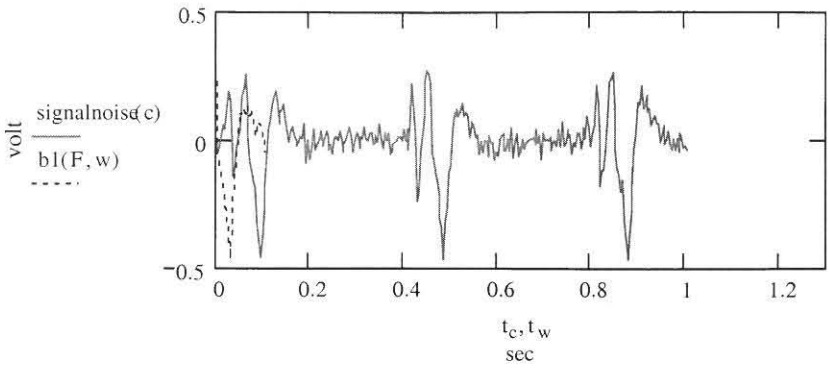

g := 256

a := 0.. g − 1

$$d(F, a) := \sum_{w} \left| b1(w, F) \right| \cdot \left| signalnoise\,(a + w) \right|$$

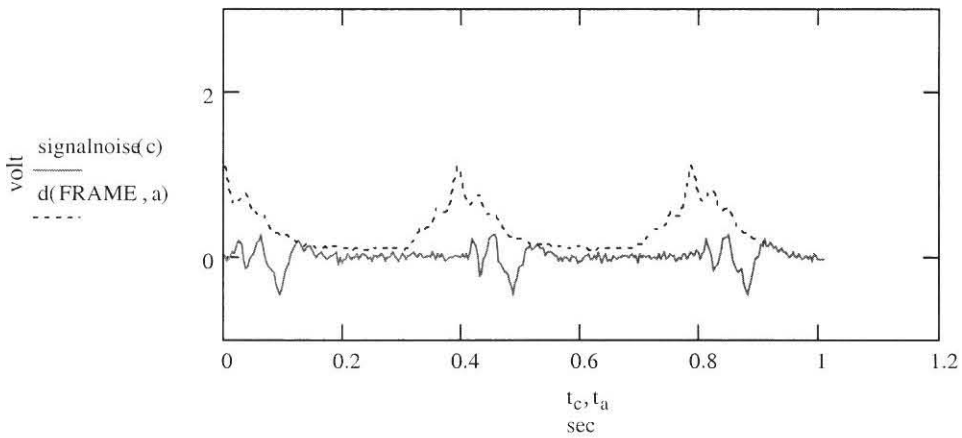

Best sample calculation

$D := 0 .. F$

$S_D := \sum_a d(D, a)$

$G_a := \sum_D d(D, a)$

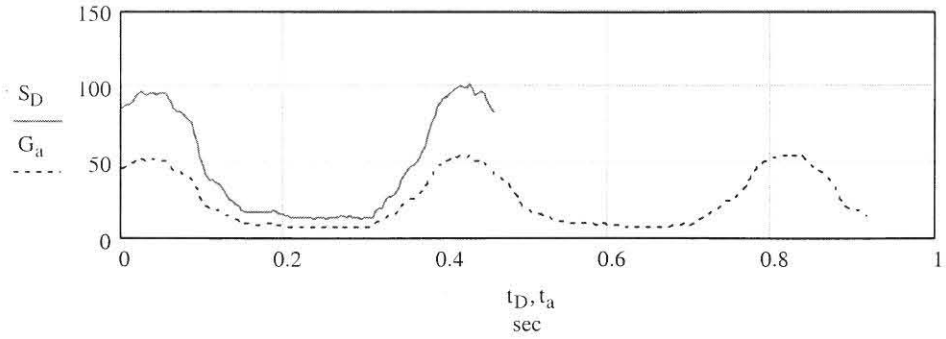

$V := \max(S)$

$L_D := \text{if}(S_D \geq V, D, 0)$

$P := \sum_D L_D$

$P = 119$ $\max(M) = 1$

calculating the correlation of the best sample

$a := 0 .. g - 1$

absolute value

$O_a := \sum_w b1(w, P) \cdot signalnoise(a + w)$ $A_a := \sum_w |b1(w, P)| \cdot |signalnoise(a + w)|$

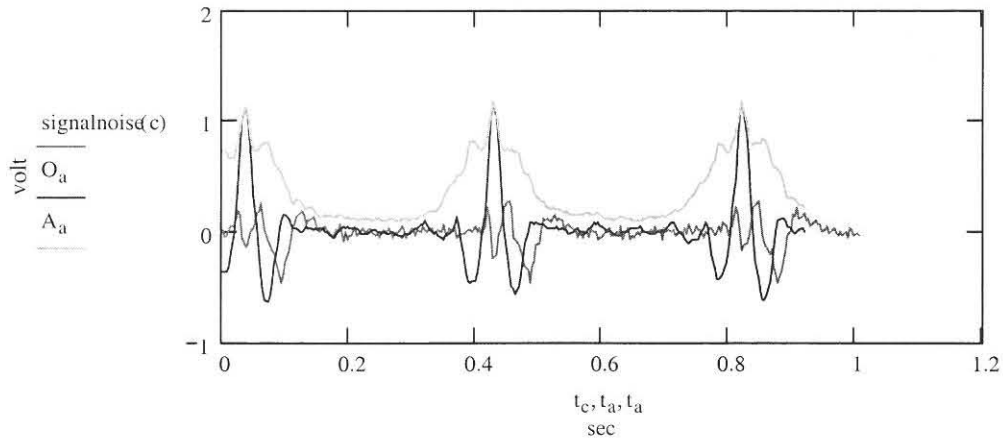

Central University of Technology, Free State

Best sample calculation

$D := 0..F$

$S_D := \sum_a d(D,a)$ $\qquad$ $G_a := \sum_D d(D,a)$

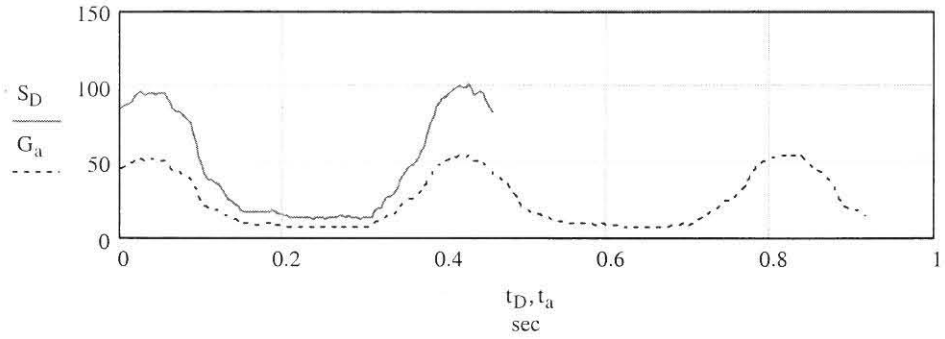

$V := \max(S)$

$L_D := \text{if}(S_D \geq V, D, 0)$

$P := \sum_D L_D$

$P = 119$ $\qquad$ $\max(M) = 1$

calculating the correlation of the best sample

$a := 0..g - 1$ $\qquad$ absolute value

$O_a := \sum_w b1(w,P) \cdot signalnoise(a + w)$ $\qquad$ $A_a := \sum_w |b1(w,P)| \cdot |signalnoise(a + w)|$

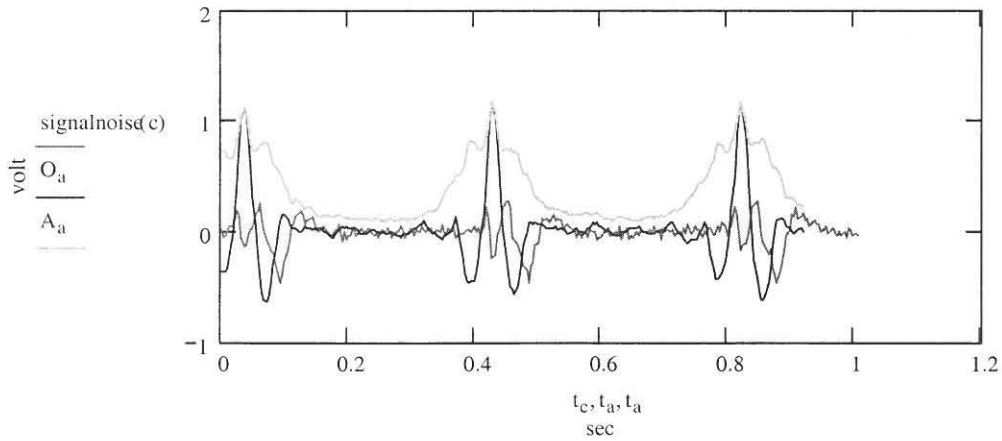

Simulation of WT and STFT

$N := 2^8$ $i := 0..N-1$ $x := 0..2^{14}-1$

$b_x := READ("c:/data/no1.txt")$

$y(x) := b_{x,1}$

Time domain signal

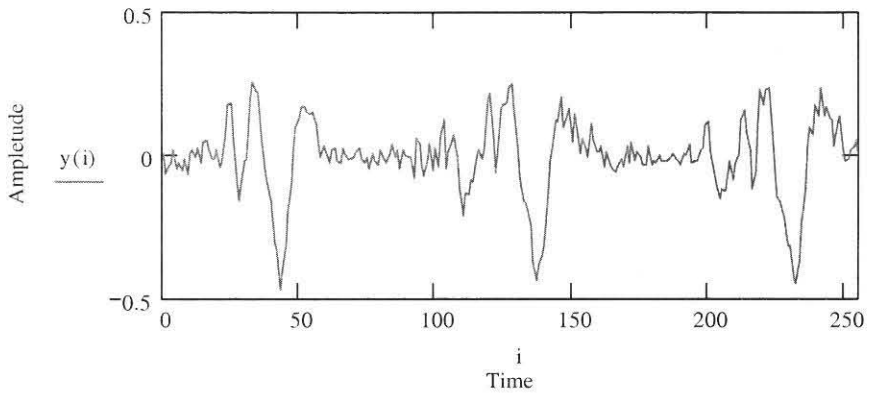

$j := 0..\left(\frac{N-1}{2}\right)$

$K := 50$ window size

$o := 0..K$

$z := 0, K..N-K$ steps

$Y_{o,z} := y(o+z)$ $j := 0..\frac{N-1}{2}$

$t := -10..10$ $s := 1..20$

$$c_{j,z} := \frac{1}{N-1} \cdot \sum_{o} y(o+z) \cdot e^{-\left(\sqrt{-1}\right) \cdot \left(\frac{2\pi j}{N-1}\right) \cdot o}$$ FFT

$\sigma := 4$ $\tau := i$

$$\psi(t) := \frac{1}{\sqrt{2\pi\sigma^3}} \cdot \left[e^{\frac{-t^2}{2\sigma^2}} \cdot \left(\frac{t^2}{\sigma^2} - 1 \right) \right]$$ Mexican Hat

$C_{j,z} := \left| c_{j,z} \right|$

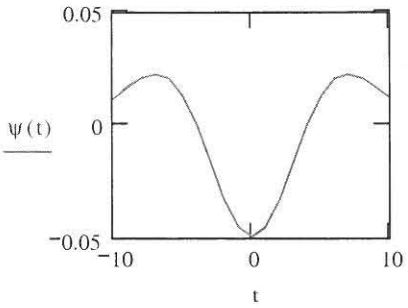

$$w_{\tau,s} := \frac{1}{\sqrt{|s|}} \cdot \sum_{i} y(i) \cdot \psi\left(\frac{i-\tau}{s} \right)$$

$W_{\tau,s} := \left| w_{\tau,s} \right|$

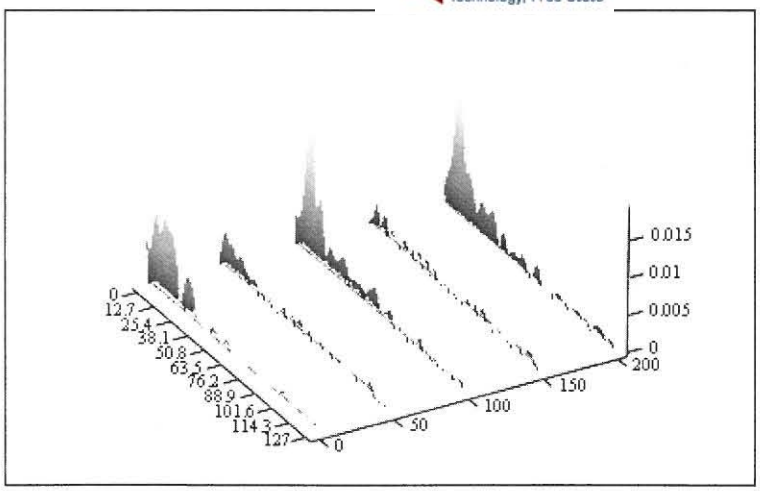

C

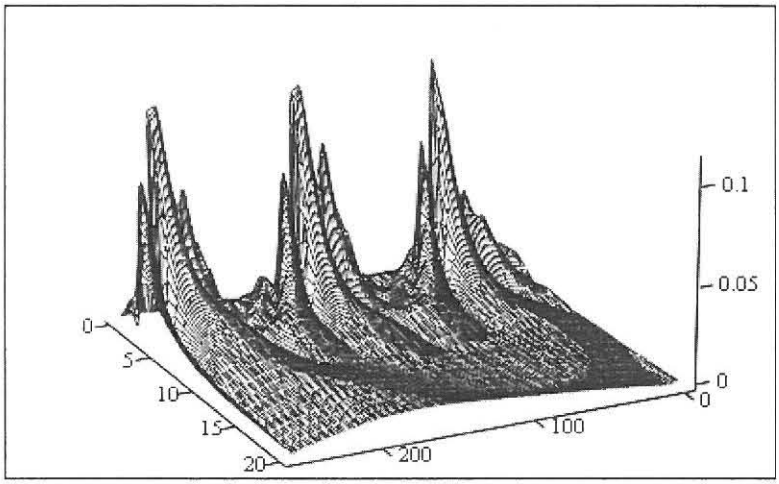

W

Appendix B

Simulation results WT and STFT at a SNR of 10.8 dB

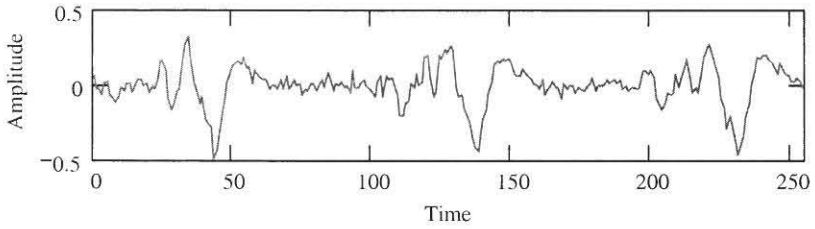

Figure B.1: Time domain signal with a SNR of 10.8 dB

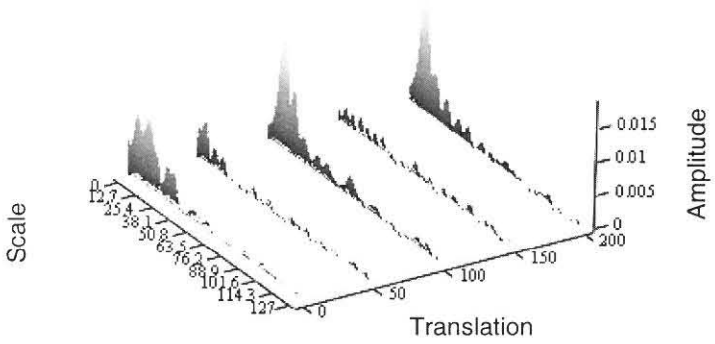

Figure B.2: Short time Fourier transform of signal with a SNR of 10.8 dB

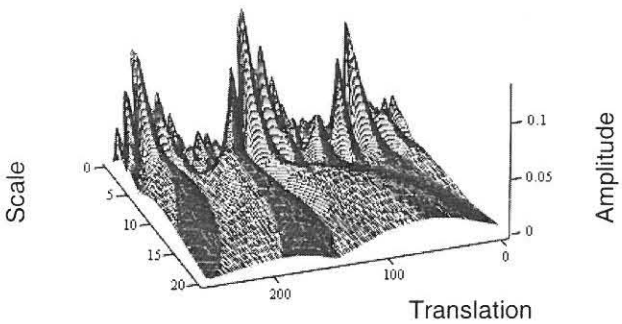

Figure B.3: Wavelet transform of signal with a SNR of 10.8 dB

Simulation results of WT and STFT at a SNR of 0 dB

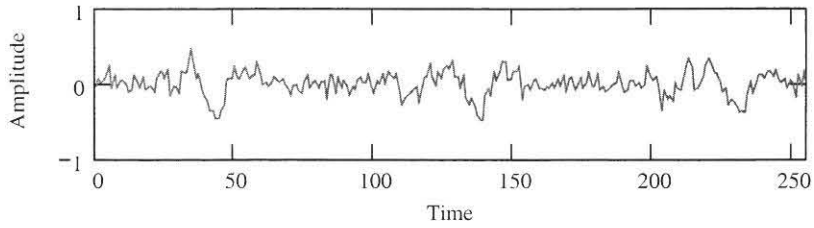

Figure B.4: Time domain signal with a SNR of 0 dB

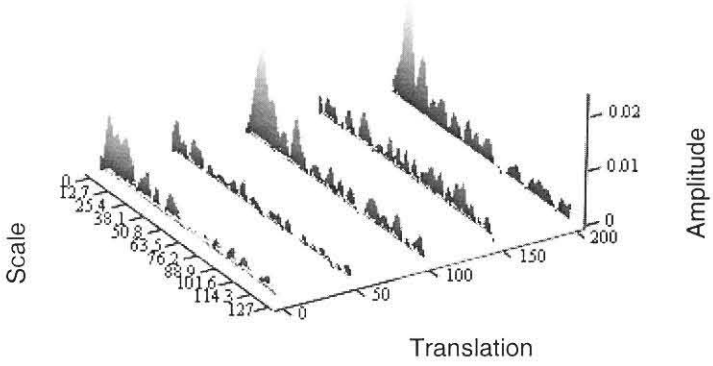

Figure B.5: Short time Fourier transform of signal with a SNR of 0 dB

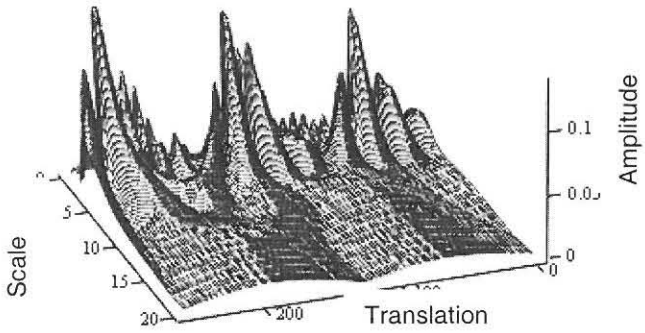

Figure B.6: Wavelet transform of signal with a SNR of 0 dB

Simulation results of WT and STFT at a SNR of -3 dB

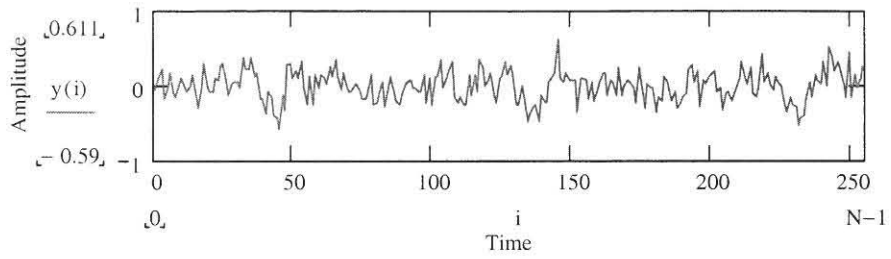

Figure B.7: Time domain signal with a SNR of -3 dB

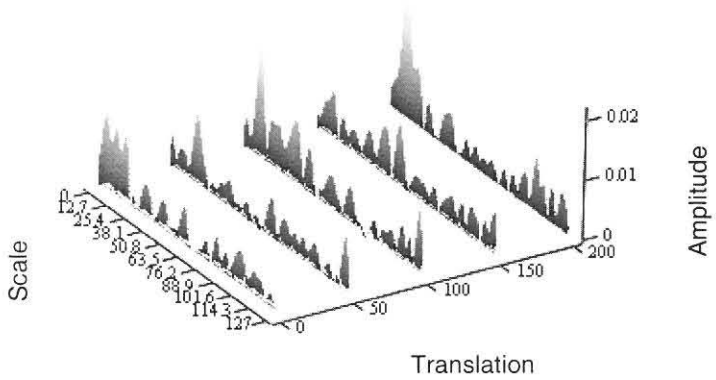

Figure B.8: Short time Fourier transform of signal with a SNR of -3 dB

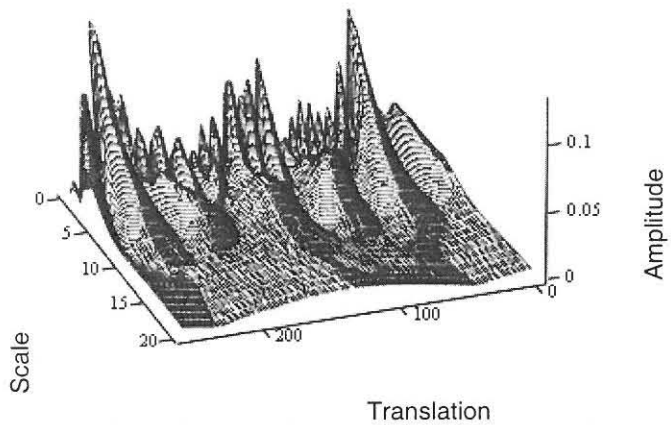

Figure B.9: Wavelet transform of signal with a SNR of -3 dB

Simulation results of WT and STFT at a SNR of -6 dB

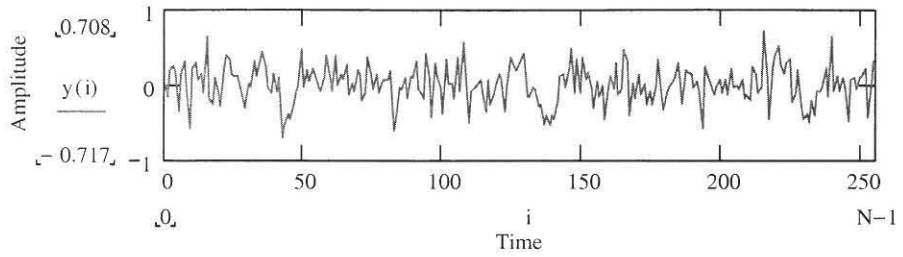

Figure B.10: Time domain signal with a SNR of -6 dB

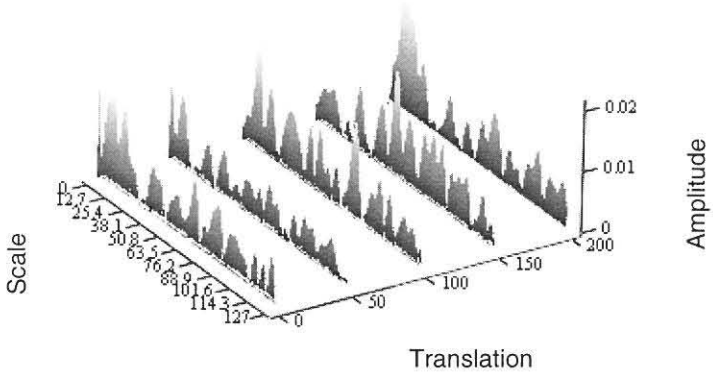

Figure B.11: Short time Fourier transform of signal with a SNR of -6 dB

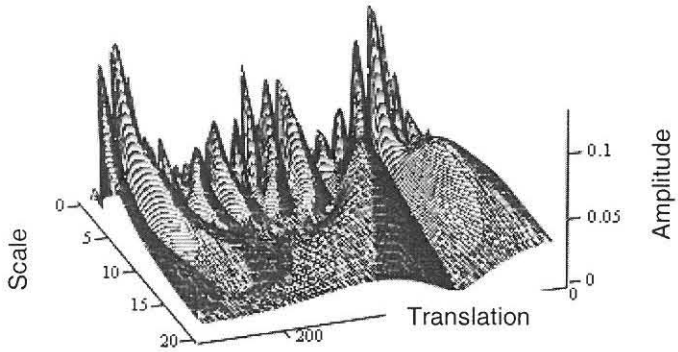

Figure B.12: Wavelet transform of signal with a SNR of -6 dB

Simulation results of filter method

In Table B.1 the output of the filter method is shown for different frequency ranges of the band pass filter in block six of the block diagram in Figure 5.12.

Table B.1: Influence of different band pass filters on the simulation results of the filter method

Band pass filter between the following frequency's as part of filter method	Output of filter method; Original signal (bottom), isolated frequency (middle) and square wave (top)
0.1-2.8 Hz	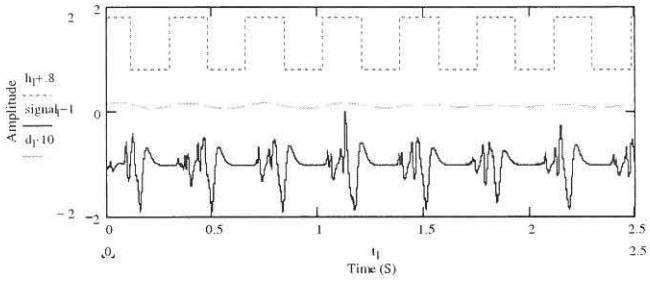
0.1-2.5 Hz	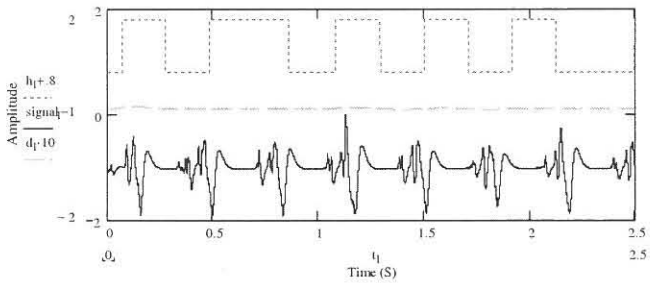

Table B.1: Influence of different band pass filters on the simulation results of the filter method (Continued)

3-6 Hz	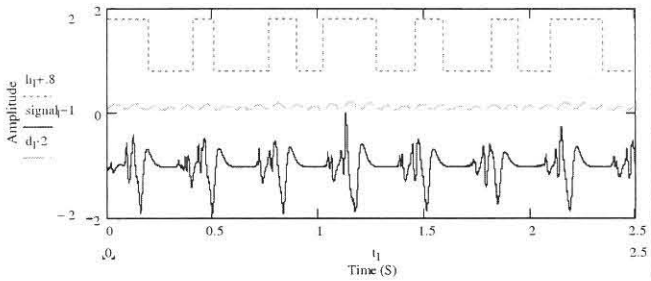
4-6 Hz	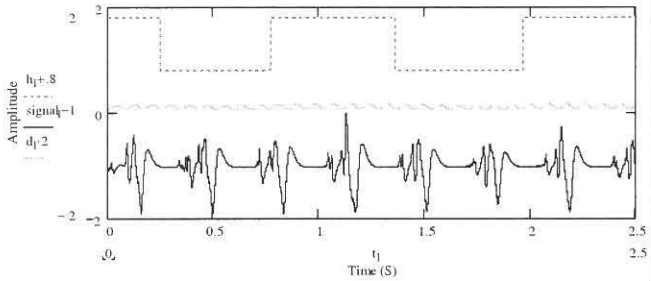
3.5-6 Hz	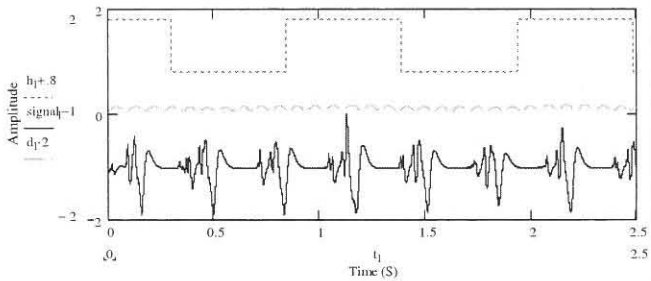
3.1-6 Hz	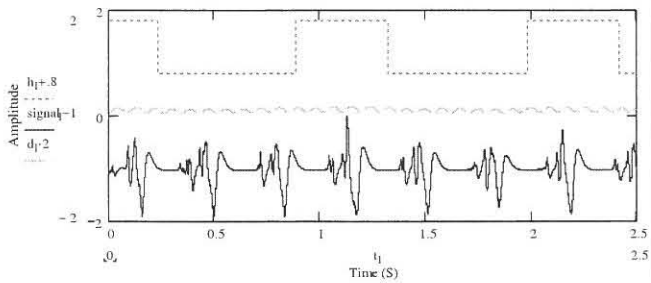

Table B.1: Influence of different band pass filters on the simulation results of the filter method (Continued)

2.9-6 Hz	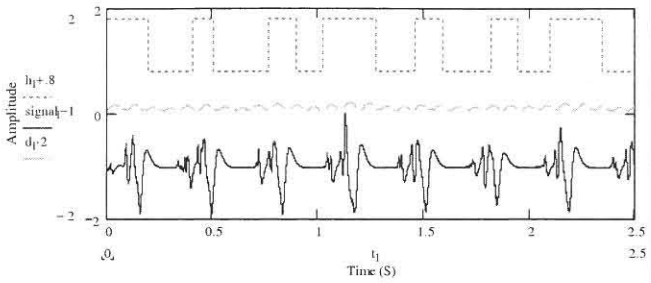
2.9-6.2 Hz	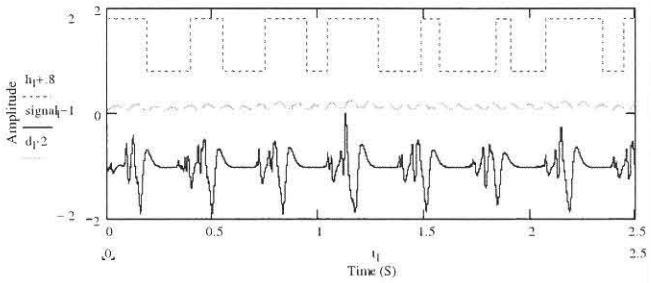
6-9 Hz	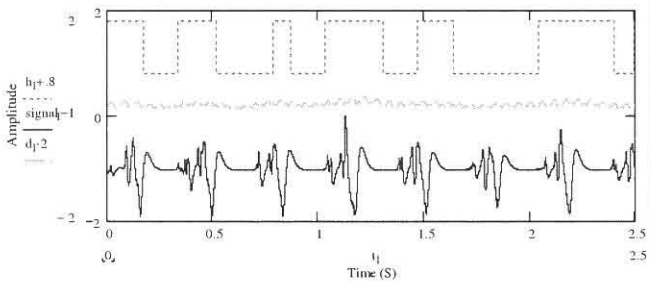
6-10 Hz	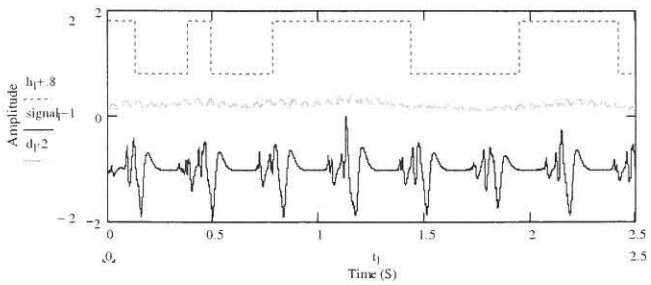

Table B.1: Influence of different band pass filters on the simulation results of the filter method (Continued)

6-14 Hz	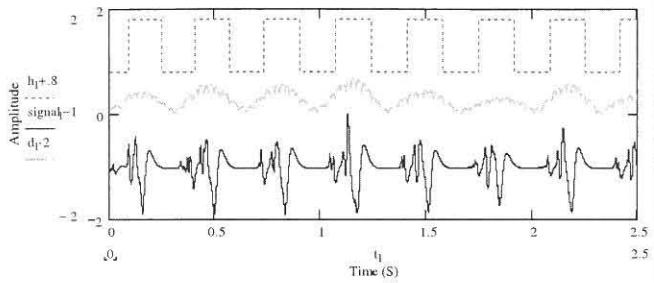
6-13 Hz	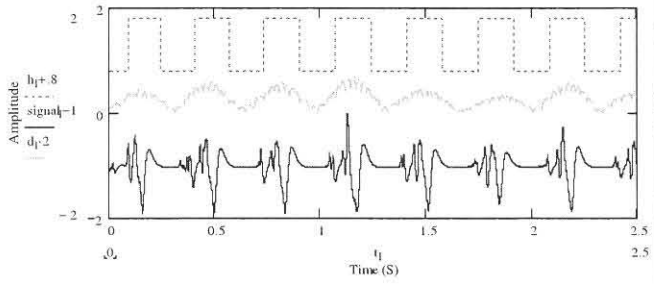
6-12 Hz	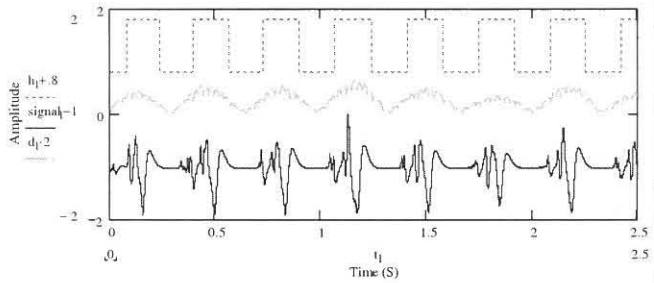
6-11 Hz	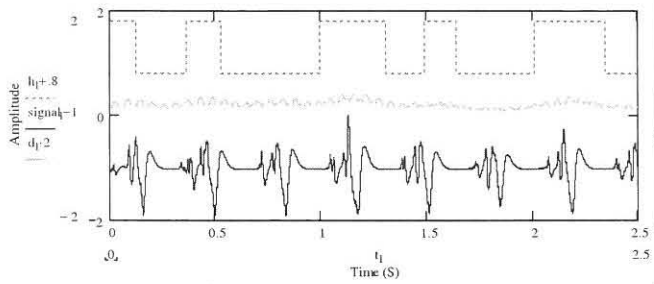

Table B.1: Influence of different band pass filters on the simulation results of the filter method (Continued)

7-12 Hz	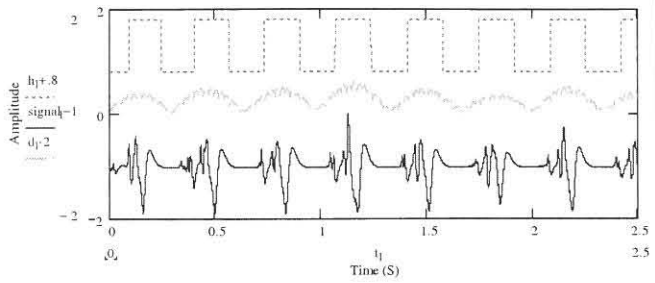
8-12 Hz	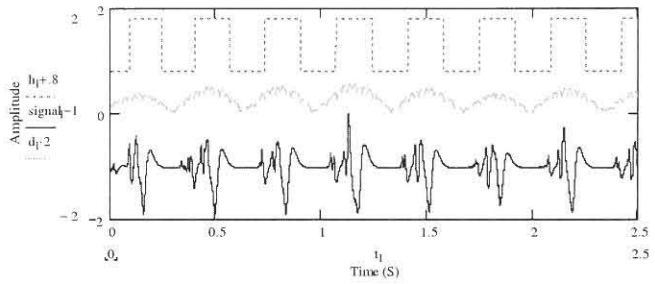
9-12 Hz	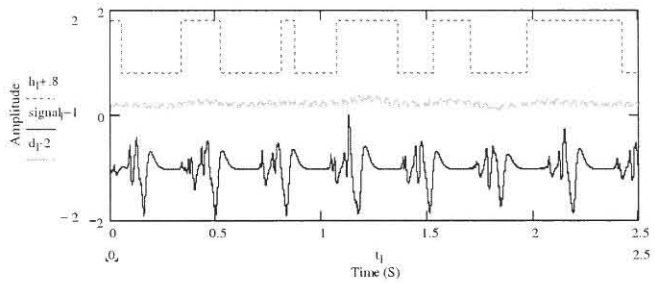
8.5-12 Hz	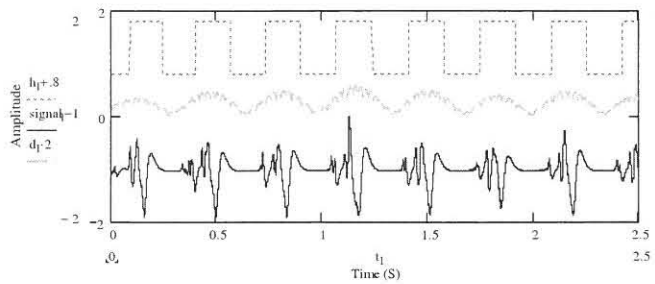

Table B.1: Influence of different band pass filters on the simulation results of the filter method (Continued)

8.5-11.5 Hz	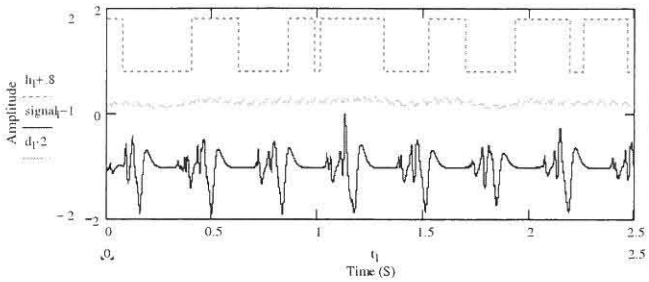
11.5-15 Hz	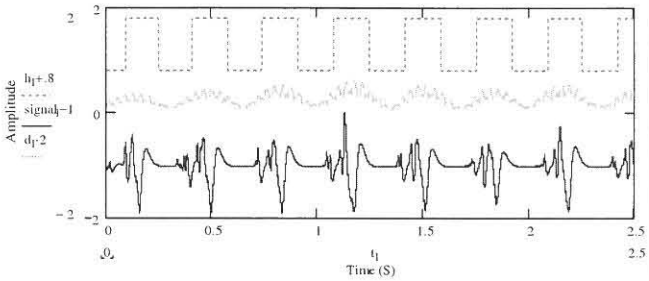
11.5-14 Hz	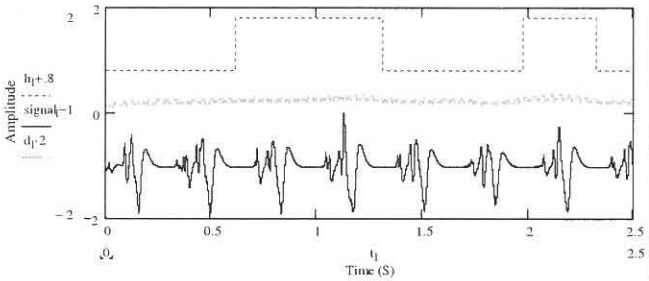
11.5-14.5 Hz	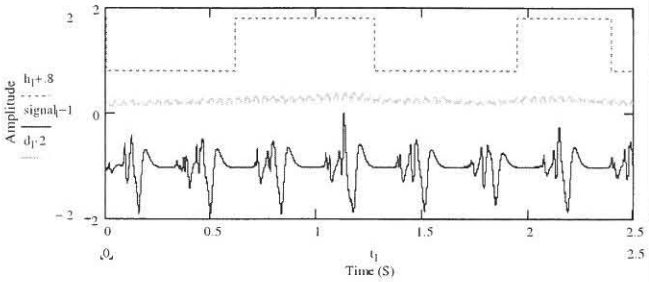

Table B.1: Influence of different band pass filters on the simulation results of the filter method (Continued)

15-18 Hz	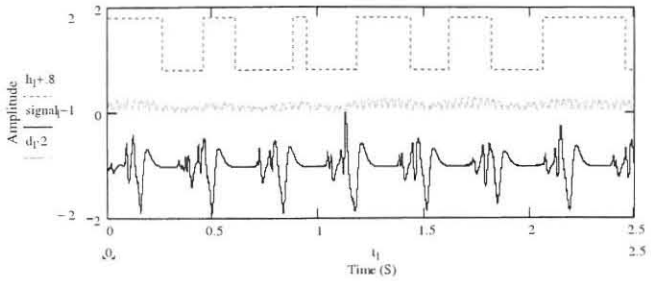
14.5-18 Hz	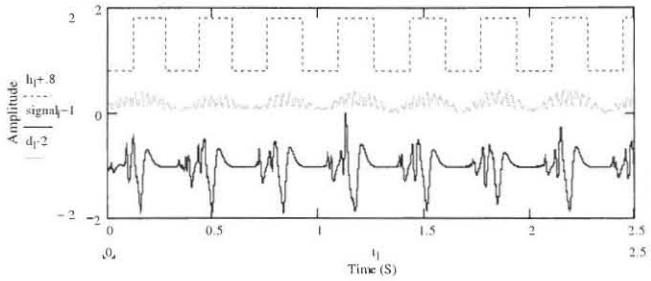
14.5-17.5 Hz	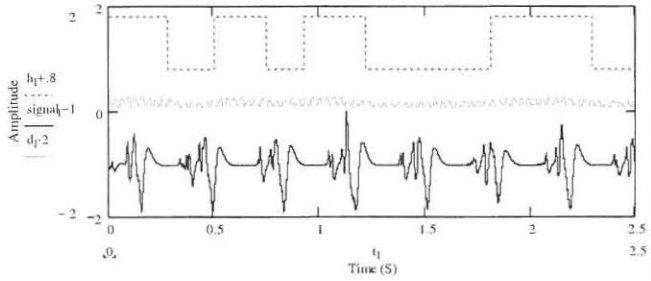

LIST OF REFERENCES

1 Bollwein, H., Meyer, H.H.D., Maierl, J., Weber, F., Baumgartner, U. and Stolla, R. 2000. Transrectal Doppler sonography of uterine blood flow in cows during the estrous cycle, Theriogenology. Vol. 53, pp.1541-1552.

2 Brands, P.J., Willigers, J.M., Ledoux, L.A.F., Reneman, R.S. and Hoeks, A.P.G. 1998. A noninvasive method to estimate pulse wave velocity in arteries locally by means of ultrasound, Ultrasound in Med. & Biol. Vol. 24 no 9, pp.1325-1335.

3 Calliada, F., Campani, R., Bottinelli, O., Bozzini, A. and Sommaruga, M.G. 1998. Ultrasound contrast agents Basic principles, European Journal of radiology. Vol. 27, pp.S157-S160.

4 Chiu, C.C. and Yen S.J. 2001. Assessment of cerebral auto regulation using time-domain cross-correlation analysis, Computers in Biology and Medicine. Vol. 31, pp.471-480.

5 Doherthy, A., James, I.R. and Newman J.P. 2002. Estimation of the Doppler ultrasound maximal umbilical waveform envelope:. Estimation method, Ultrasound in med. & Biol. Vol. 28, pp.1251-1259.

6 Dtearns, S.D. Hush, D.R. Digital signal analysis. Prentice-Hall, Englewood Cliffs, 1990.

7 Gonzàlez, J.S., Vàzquez, K.R. and Nocetti, D.F.G. 2000. Model-base spectral estimation of Doppler signal using parallel genetic algorithms, Artificial Intelligence in Medicine, Vol. 19, pp.75-89.

8 González, J.S., Nocetti, D.R.G. and Ruano, M.G. 1999. High performance parallel-DSP computing in model-based spectral estimation, Microprocessors and Microsystems. Vol. 23, pp.337-344.

9 Guidi, G., Corti, L. and Tortoli, P. 2000. Application of autoregressive methods to mitigate spectral analysis, Ultrasound in Med & Biol, Vol.26, pp.585-592.

10 Güler, I., Hardalac, F. and Kaymaz, M. 2002. Comparison of FFT and adaptive ARMA methods in transcranial Doppler signals recorded from the cerebral vessels, Computers in Biology and Medicine. Vol. 32, pp.445-453.

11 Güler, I., Hardalac, F. and Übeyli, E.D. 2002. Determination of Behcet disease with the application of FFT and AR methods, Computer in Biology and Medicine. Vol. 32, pp.419-434.

12 Güler, I., Hardalac, F. and Barisci, N. 2002. Application of FFT analysed cardiac Doppler signals of fuzzy algorithm, Computer in Biology and Medicine. Vol. 32, pp.435-444.

13 Güler, I., Hardalac, F. and Müldür, S. 2001. Determination of aorta failure with the application of FFT, AR and wavelets methods to Doppler technique, Computers in Biology and Medicine. Vol. 31, pp.229-238.

14 Jennings, D. Flint, A. Turton, B.C.H. Nokes, L.D.M. Introduction to medical electronics applications. Edward Arnold, London, 1995.

15 Jervis, B.W. Ifeachor, E.C. Digital Signal Processing. Harlow, Addison Wesley, 2002.

16 Jurkovic, D. Jauniaux, E. Ultrasound and Early Pregnancy Parthenon Publishing Group, New York, 1996.

17 Keeton, P.I.J. and Schlindwein, F.S. 1998. Spectral broadening of clinical Doppler Signals using FFT and autoregressive modeling, European Journal of Ultrasound. Vol.7, pp.209-218.

18 Karelsson, B., Berson, M., Helgason, T., Geirsson, R.T. and Pourcelot, L. 2000. Effects of fatal and maternal breathing on the ultrasonic Doppler signal due to fetal heart movement, European Journal of Ultrasound. Vol. 11, pp.47-52.

19 Kulkarni, A.A., Joshi, J.B., Kumar, V.R. and Kulkarni, B.D. 2001. Wavelets transform of velocity-time data for the analysis of turbulent structures in a bubble column, Chemical Engineering Science. Vol. 56, pp.5305-5315.

20 Livingstone, C. Obstetric Ultrasound. Harcourt Publishers, London, 1999.

21 Ludu, A., O'Connell, R.F. and Draayer, J.P. 2003. Nonlinear equation and wavelets, Mathematics an Computers in Simulation. Vol. 62, pp.91-99.

22 Ménigault, E., Berson, M., Vieyres, P., Lepoivre, B., Pourcelot, D. and Pourcelot, L. 1998. Feto-maternal circulation: mathematical model and comparison with Doppler measurements, European Journal of Ultrasound. Vol. 7, pp.129-143.

23 Operators manual Sonicaid 421 OXFORD Medical Limited 1998.

24 Pela, G., Bruschi, G., Cavalotta, A., Manca, C., Cabassi, A. and Borghetti, A. 2001. Doppler Tissue Echocardiography: Myocardial Wall Motion Velocities in Essential Hypertension, Eur J Echocardiography. Vol. 2, pp.108-117.

25 Polikar, R. Rowan University, The wavelet tutorial, 2001, http://engineering.rowan.edu.

26 Powis, R.L. Schwartz, R.A. Practical Doppler ultrasound Williams & Wilkins, Baltimore, 1991.

27 Shanmugan, K.S. Breipohl, A.M. Random Signals detection, estimation and data analyses. Wiley, New York, 1988.

28 Texas Instruments (TI) http: //focus .ti.com /docs /prod /productfolder .jhtml ?generic PartNumber = TMS320C6711C&pfsection=desc.

29 Turkoglu, I., Arslan, A. and Ilkay, E. 2002. An expert system of diagnosis of the heart valve diseases, Expert Systems with Applications. Vol. 23, pp.229-236.

30 Verlinde, D., Beckers, F., Ramaekers, D. and Aubert, A.E. 2001. Wavelet decomposition analysis of heart rate variability in aerobic athletes, Autonomic Neuroscience: Basic and Clinical. Vol. 90, pp.138-141.

31 Wavelets extension pack, MathCAD.

32 Wells. P.N.T. 1998. Doppler studies of the vascular system, European Journal of Ultrasound. Vol. 7, pp.3-8.